COMPOSITION AND CHARACTERISTICS OF PARTICLES

IN THE OCEAN:

EVIDENCE FOR PRESENT DAY RESUSPENSION

by

MARY JOSEPHINE RICHARDSON

A.B., Smith College
(1975)

SUBMITTED IN PARTIAL FULFILLMENT
OF THE REQUIREMENTS FOR THE
DEGREE OF

DOCTOR OF PHILOSOPHY

at the

MASSACHUSETTS INSTITUTE OF TECHNOLOGY

and the

WOODS HOLE OCEANOGRAPHIC INSTITUTION

May 1980

Signature of Author: _____
Joint Program in Oceanography
Massachusetts Institute of Technology – Woods
Hole Oceanographic Institution, May 1980

Certified by: _____
Thesis Supervisor

Accepted by: _____
Chairman, Joint Oceanography Committee in the
Earth Sciences, Massachusetts Institute of
Technology – Woods Hole Oceanographic Institution

COMPOSITION AND CHARACTERISTICS OF PARTICLES IN THE OCEAN:

EVIDENCE FOR PRESENT-DAY RESUSPENSION

by

MARY JOSEPHINE RICHARDSON

ABSTRACT

This study of particulate matter in the water column and the
underlying surface sediments verifies the occurrence of local,
present-day resuspension in the deep sea. The location of the major
portion of this work was the South Iceland Rise, a region influenced
by the flow of Norwegian Sea Overflow Water. Measured current
velocities exceeded 20 cm/sec in the axis of the bottom current for
the duration of the deployments, approximately two weeks.
Particulate matter was sampled with Niskin bottles, to obtain the
standing crop of suspended matter and with sediment traps, to obtain
the material in flux through the water column. Box cores were taken
to obtain surface sediment samples for comparison with the trap
samples.

Suspended particulate matter (SPM) and light-scattering studies
demonstrate that in the Iceland Rise area the correlation of the
L-DGO nephelometer to concentration of SPM differs between clear
water and the nepheloid layer. Correlations of light scattering to
SPM concentration also differ regionally, but for predicting
concentration from light scattering, regression lines at two
locations are indistinguishable. Particle size distributions have
lower variance in the nepheloid layer than those in clear water
which have roughly equal volumes of material in logarithmically
increasing size grades from 1-20 μm. Apparent density differences
between SPM in clear water and the nepheloid layer are not
distinguishable in the Iceland Rise study; apparent densities
increase in the nepheloid layer in the western North Atlantic. An
apparent density of 1.1 g/cm^3 adequately separates clear water
from nepheloid layer samples in this region. Compositional
variations seen between clear water and the nepheloid layer include
a decrease in small coccoliths and an increase in clays and mineral
matter. These compositional variations are more dramatic in the
western North Atlantic region, due to dissolution of carbonate at
the seafloor, later resuspended into the nepheloid layer.

Sedimentological evidence of resuspension and redistribution of
material are: 1) presence of sediment drifts throughout the Iceland
Basin; 2) occurrence of coarse, glacial age sediments beneath the
axis of the bottom current; and 3) differences in mineralogy,
carbonate and organic carbon contents between surface sediments
beneath the bottom current and those in a channel.

A comparison of the vertical flux of material measured by
sediment traps at 500 meters above bottom (mab) with the
accumulation rate in cores, shows that the present-day surface input
is an order of magnitude smaller than the accumulation rate. This
observation suggests transport of material into some sections of the
region by bottom currents or by turbidity currents.

The horizontal flux of particulate matter into and out of the
region by the bottom current is 100 kg/sec. This material may
contribute to the formation of Gardar sediment drift downstream.
The trends in % $CaCO_3$ and % organic carbon through the water
column and in the surface sediments suggest that dissolution of
carbonate and decomposition and consumption of organic carbon occurs
primarily at the seafloor. These data also suggest preferential
preservation at channel stations and/or preferential erosion beneath
the bottom current.

A comparison of sediment-trap samples with box-core surface
samples further supports present-day resuspension. Benthic
foraminifera, iron-oxide coated planktonic foraminifera and the
glacial, subpolar planktonic foraminifera (Neogloboquadrina
pachyderma (sinistral)) in traps at 10, 100 and a few specimens at
500 mab, provide conclusive evidence for local resuspension. The
coarse fraction (>125 μm) of the sediment trap material collected at
10 mab comprises 21-34% of the samples. Calculations indicate that
this material is locally derived (few kilometers) resuspended
material.

Thesis Supervisor: Dr. Charles D. Hollister

Title: Senior Scientist

TO MY PARENTS

ACKNOWLEDGEMENTS

TABLE OF CONTENTS

Page

-10-

Page

LIST OF FIGURES

LIST OF PLATES

LIST OF TABLES

-16-

CHAPTER 1

INTRODUCTION

Voluminous sediment drifts in the northern North Atlantic (e.g.,

Feni, Gardar, and Hatton sediment drifts; Jones et al., 1970;

Hollister et al., 1978; McCave et al., 1980) are evidence for the

transport and redistribution of massive quantities of deep-sea

sediments through geologic time. The working hypothesis of this

thesis is that resuspension of deep-sea sediments continues to occur

in the northern North Atlantic, specifically in the Iceland Rise

region, and is measurable on time scales of days to months.

This investigation, to study present-day resuspension and its

influence on the characteristics of suspended particulate matter,

was principally conducted on the south Iceland Rise. This region is

particularly suitable for three reasons: 1) Norwegian Sea Overflow

Water flows roughly parallel to contours through the region at

velocities in excess of 20 cm/sec (Steele et al., 1962; Shor,

1978). Laboratory experiments indicate that these speeds are

capable of eroding cohesive shelf sediments and abyssal clays

(Lonsdale and Southard, 1974; Young and Southard, 1978), and so they

are probably capable of eroding the local sediments. 2) Near-bottom

nepheloid layers are present with high concentrations of suspended

particulate matter. The existence of these features is indicative

of an ongoing process keeping material in suspension near the

seafloor. 3) Geologic evidence indicates a continuation of sediment

erosion and redistribution through the Recent. For example, beneath the axis of the bottom current, the small amount of Recent sediment present is coarse-grained, winnowed of its fines. Also, the Katla Ridges (Malmberg, 1974), which are sedimentary features in the study area, have been constructed and shaped by both bottom currents and turbidity currents through geologic time (Shor, 1979). In addition, farther downstream lies the Gardar sediment drift, a huge pile of sediment formed by deposition from bottom currents (Hollister et al., 1978; McCave et al., 1980).

A large portion of this work focuses on the transport and properties of suspended particulate matter. Particulate matter in the water column was collected with both water bottles and sediment traps in two regions, the Iceland Rise and the continental rise southeast of New York. The suspended particulate matter was examined to determine and interpret the changes in particles that occur from mid-water depths through the near-bottom nepheloid layer. Surface sediments recovered in box cores were compared with trapped material to estimate the fraction of resuspended material and to assess the changes occurring to particles from transit through the water column to residence on the seafloor. Current-meter measurements and CTD lowerings were used to determine the spatial extent and magnitude of the bottom current, and together with measurements of the suspended particulate matter concentrations, to estimate the horizontal transport of particulate matter.

Specific questions addressed in this thesis are:

(1) Where are the present bottom-current velocities sufficient
to erode the local surface sediments?

(2) What are the composition and characteristics of material
settling from the surface waters, and how do they differ from
those of material being transported in the near-bottom
nepheloid layer?

(3) What processes are responsible for the observed changes in
suspended particulate matter in the water column?

(4) What fraction of nepheloid-layer particles are resuspended?

(5) How far can particles travel in single episodes of
resuspension?

The structure of the thesis in answering these questions is as
follows. Chapter II details the regional settings, summarizes the
hydrography, and explains the rationale for the sampling schemes
selected. Chapter III discusses the horizontal and vertical spatial
variability in characteristics of suspended particulate matter in
the Iceland Rise region and along the continental rise in the
western North Atlantic. It emphasizes the existence and
interpretations of the differences between near-bottom nepheloid
waters and the overlying clear water. Chapter IV deals with
resuspension and advection by bottom currents as inferred from a
comparison between the composition of the contents of sediment traps
in the lower portion of the water column and that of the surface
sediments. Chapter V is a summary of the conclusions of the thesis.

CHAPTER II

REGIONAL SETTINGS, HYDROGRAPHY AND SAMPLING SCHEMES

The principal study region for this thesis work is the Iceland

Rise. To broaden the scope of the work beyond a regional study, a

comparison of the Iceland Rise results of suspended particulate

matter is made with the results of a similar study in the western

North Atlantic across the continental rise southeast of New York.

This comparison allows the site-specific results to be

differentiated from those perhaps more generally applicable. A

detailed description of the Iceland Rise region and a summary of the

applicable regional and hydrographic differences in the western

North Atlantic continental rise region follows.

REGIONAL SETTING: ICELAND RISE

Previous investigations have shown that Norwegian Sea Overflow

Water dominates the abyssal circulation of the northern and western

North Atlantic (Figure 2.1; Lee and Ellett, 1965; Worthington, 1969;

Worthington, 1976). In the Arctic basins and shelves north of

Iceland, surface water is cooled and mixed downward by convective

overturning in the winter (Peterson and Rooth, 1976). This cold,

dense water mixes with warmer, more saline North Atlantic water as

it cascades over sills in the ridge from Greenland to Scotland

(Steele et al., 1962; Crease, 1965; Lee and Ellett, 1965;

Worthington and Volkmann, 1965; Dietrich, 1967; Worthington, 1969;

Figure 2.1   Generalized western boundary, bottom-water circulation
              in the North Atlantic. Study areas south of Iceland
              and southeast of New York, denoted by the box and
              triangle respectively, are located in the path of a
              bottom current.
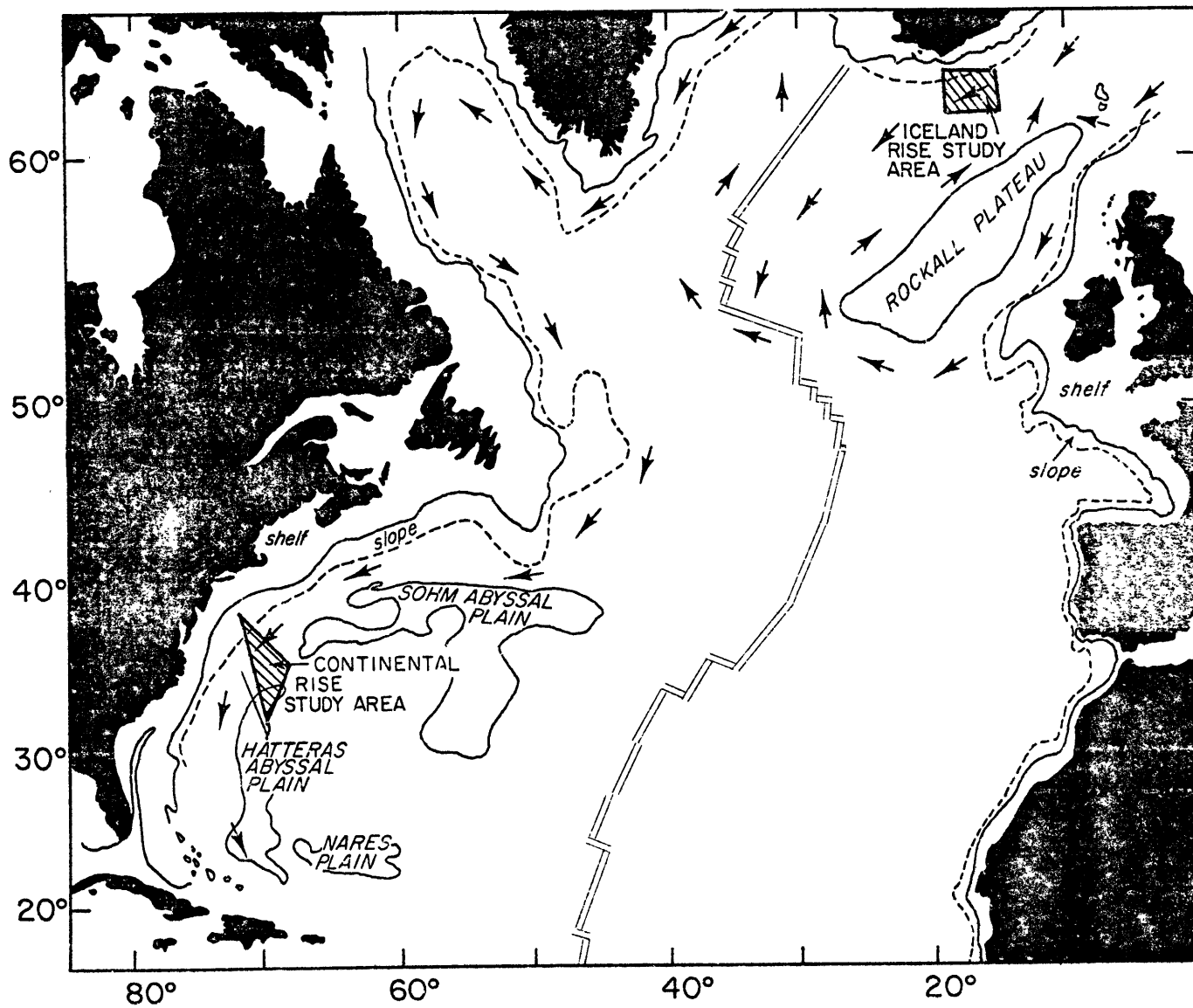
Swift et al., 1980). Water flows southward along the eastern flank

of the Reykjanes Ridge, and westward through the Charlie-Gibbs

Fracture Zone at approximately 53°N (Worthington and Volkmann,

1965; Garner, 1972; Schmitz and Hogg, 1978; Shor et al., 1980).

From this latitude southward, the overflow water is mainly

restricted to the western basin of the North Atlantic and flows

along the western boundary.

The south Iceland Rise, the study area for this work (Figure

2.1), is directly in the path of the Norwegian Sea Overflow Water.

This water flows southwestward through the region directed upslope

from the contours of the East Katla Ridge by 30° to 45° (Figure

2.2; Steele et al., 1962; Worthington, 1970; Shor et al., 1977).

Significant transport of Norwegian Sea Overflow Water, with current

velocities on the order of 20-30 cm/sec (Shor, 1979), has been

documented through this region.

Geologic effects of the Norwegian Sea Overflow Water are seen in

abundance in the Iceland Basin region (Figure 2.3). Gardar Drift on

the western side of the Iceland Basin, Feni Drift in Rockall Trough,

and Hatton Drift on the western flank of Rockall Plateau are all

thought to be formed and molded by deposition and redistribution of

sediments from the overflow water (Johnson and Schneider, 1969;

Jones et al., 1970; Davies and Laughton, 1972; Ellett and Roberts,

1973; Lonsdale and Hollister, 1979; McCave et al., 1980).

The detailed study region, the Katla Ridge province (Figure 2.2;

Malmberg, 1974) in the south Iceland Rise, consists of two

Figure 2.2   Bathymetry of the Iceland Rise study area. Contours
              are in corrected meters. Current measurements were
              made along the northern transect across the eastern
              flank of the East Katla Ridge. Current velocities
              show westward to southwestward flow with an upslope
              component. The southern transect of stations extends
              from the nose of the West Katla Ridge into the Iceland
              Basin.
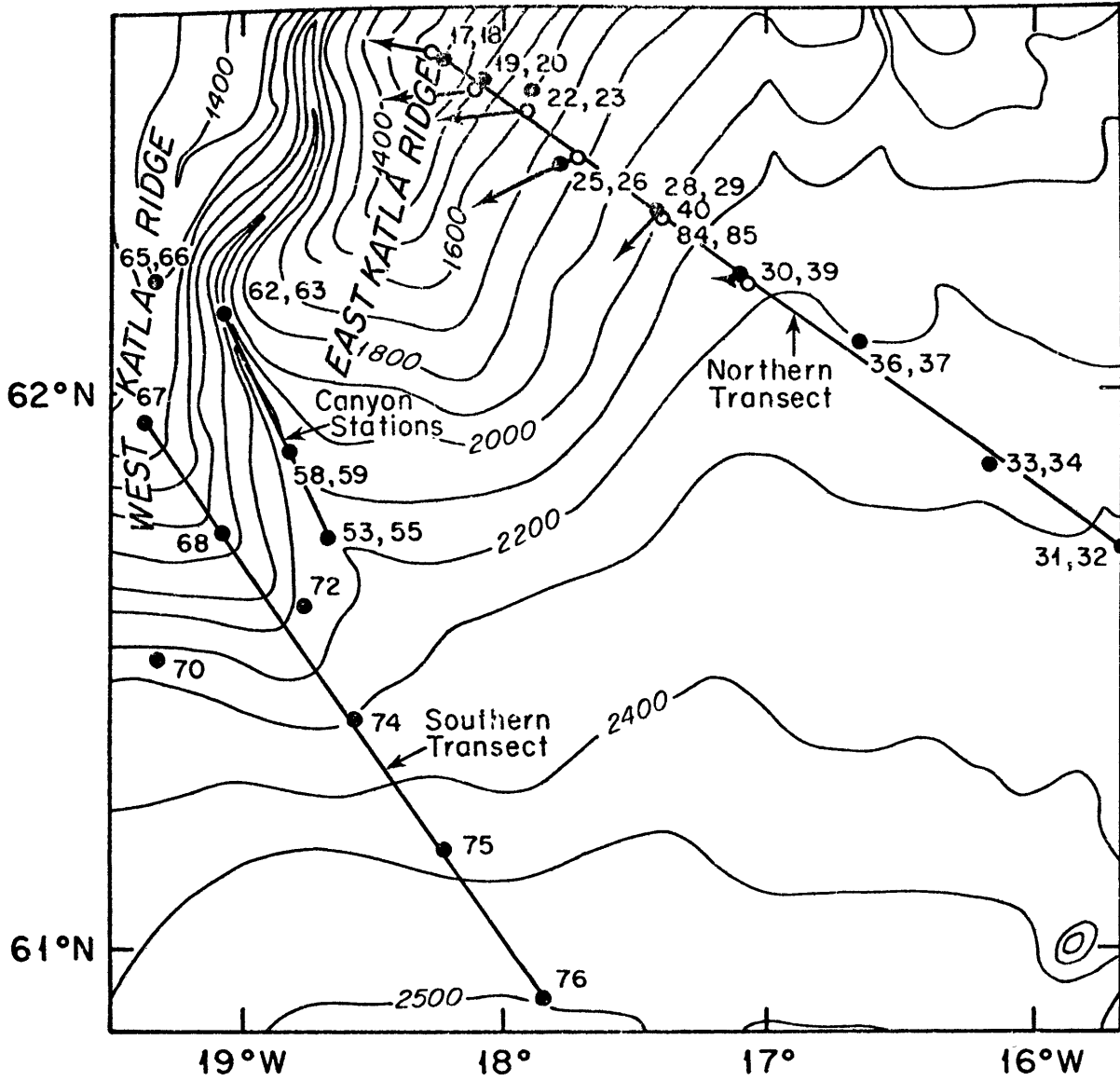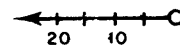
Figure 2.3   Location of the major sediment drifts in the
              northeastern North Atlantic. Arrows trace the flow of
              bottom water through the region. From McCave et al.
              (1980).

28°W 24°W 20°W 16°W 12°W

ICELAND

SNORRI DRIFT

Reykjanes Ridge

BJORN DRIFT

GARDAR DRIFT

ICELAND RISE

STUDY AREA

Iceland-Faeroe Ridge

1000

200

62°N

60°N

58°N

56°N

54°N

HATTON DRIFT

2000

3000

Maury Channel

Rockall Plateau

Rockall Bank

Rockall Trough

FENI DRIFT

Irish Margin

4000

SEDIMENT DRIFT
BOTTOM CURRENT AXIS
TURBIDITE CHANNEL

0   100   200
KILOMETERS

ISOBATHS IN METERS
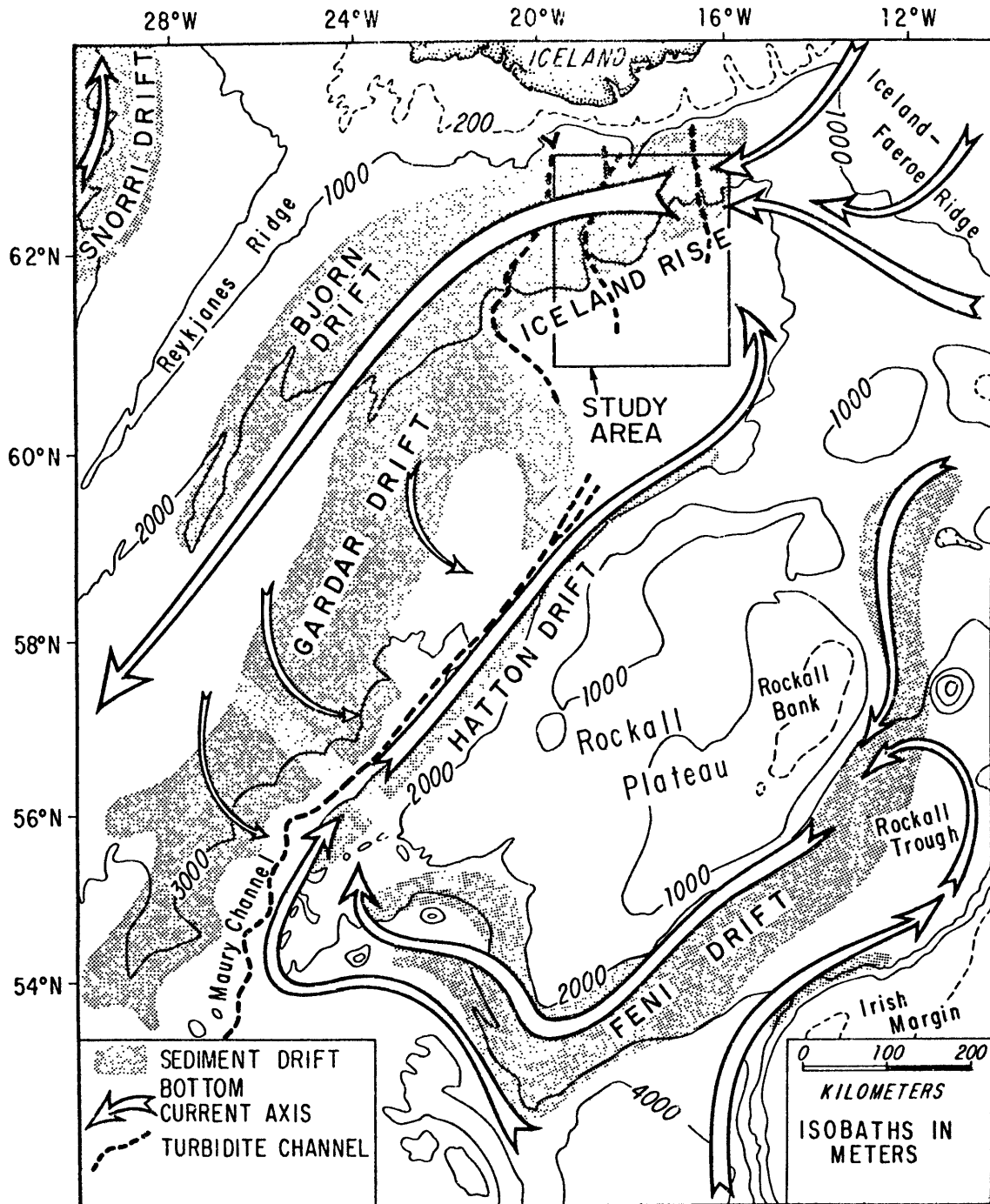
sedimentary ridges, the East and West Katla Ridges (Shor et al.,
1977). The East Katla Ridge, striking NNE, has smooth parallel
contours along its eastern flank from 1200-2100 m. Along this
flank, the overflow water flows as a geostrophic current, roughly
parallel to the regional contours (Steele et al., 1962). East Katla
Ridge is separated from West Katla Ridge by a narrow turbidity-
current canyon. The West Katla Ridge, oriented approximately N-S,
has a wide, blunt nose and is separated from Gardar Drift to the
southwest by a second turbidity-current canyon (Figures 2.2 and 2.3).

The south Iceland Rise is a region where both a strong surface
source and a resuspended input of particulate matter are to be
expected. Biogenic material in the surface waters and terrigenous
material from volcanic and glaciofluvial sources are probable
components of the flux of primary particulates (i.e. those of
surface origin) through the water column. These sources are likely
to have peak inputs during the spring and summer months, during the
period of sampling for this study. The input of resuspended
material is likely to be high due to the strong flow of Norwegian
Sea Overflow Water through the region. The bottom current may be
sporadic (Steele et al., 1962), but it has been observed in both
winter and summer (Crease, 1965; Lee and Ellett, 1965; Shor, 1979).
A mean velocity in the current core greater than 20 cm/sec was
recorded during this study (Shor, 1979).

REGIONAL SETTING: WESTERN NORTH ATLANTIC

The area chosen for comparative study of the characteristics of particulate matter was the continental rise southeast of New York in the western North Atlantic (Figure 2.1). Hydrographically, this region is influenced by the deep northeastward-flowing Gulf Stream Gyre System (Worthington, 1976; Luyten, 1977; Laine and Hollister, 1980), and the southwestward-flowing Western Boundary Undercurrent (Figure 2.4; Hollister, 1967; Zimmerman, 1971; Richardson, 1977). Through geologic time, deep contour-following currents have shaped and developed the continental rise of eastern North America (Heezen et al., 1966; Field and Pilkey, 1971; Eittreim and Ewing, 1972; Hollister and Heezen, 1972). This continental boundary is dissected by many canyons which may have disgorged vast amounts of terrigenous debris into the deep sea during lower stands of sea level; presently, however, most of the sediment transported by rivers is trapped in estuaries and does not escape the continental shelf (Meade, 1972). Some terrigenous material may be supplied at mid-water depths by horizontal transport from the continental slope (Drake et al., 1972; Pierce, 1976). The introduction of biogenic material from the surface waters decreases rapidly from the highly productive, nutrient-rich slope waters to the unproductive Sargasso Sea. Particle input to the water column from the seafloor by resuspension and advection of sediments in this region, is possible from either the Gulf Stream Gyre System or the Western Boundary Undercurrent.

Figure 2.4   Locations of hydrographic stations in the western
North Atlantic. Stations were taken from the base of
the continental slope to the lower continental rise.
Arrows indicate the abyssal flow of the Western
Boundary Undercurrent and the Gulf Stream Gyre.

shelf

CONTINENTAL RISE

SOHM ABYSSAL PLAIN

slope

D58

*KN58

710 *715

*718

*730

*734

BLAKE PLATEAU

HATTERAS ABYSSAL PLAIN

BERMUDA RISE

45°

40°

35°

30°

25°

80° 75° 70° 65° 60° 55° 50°

-30-
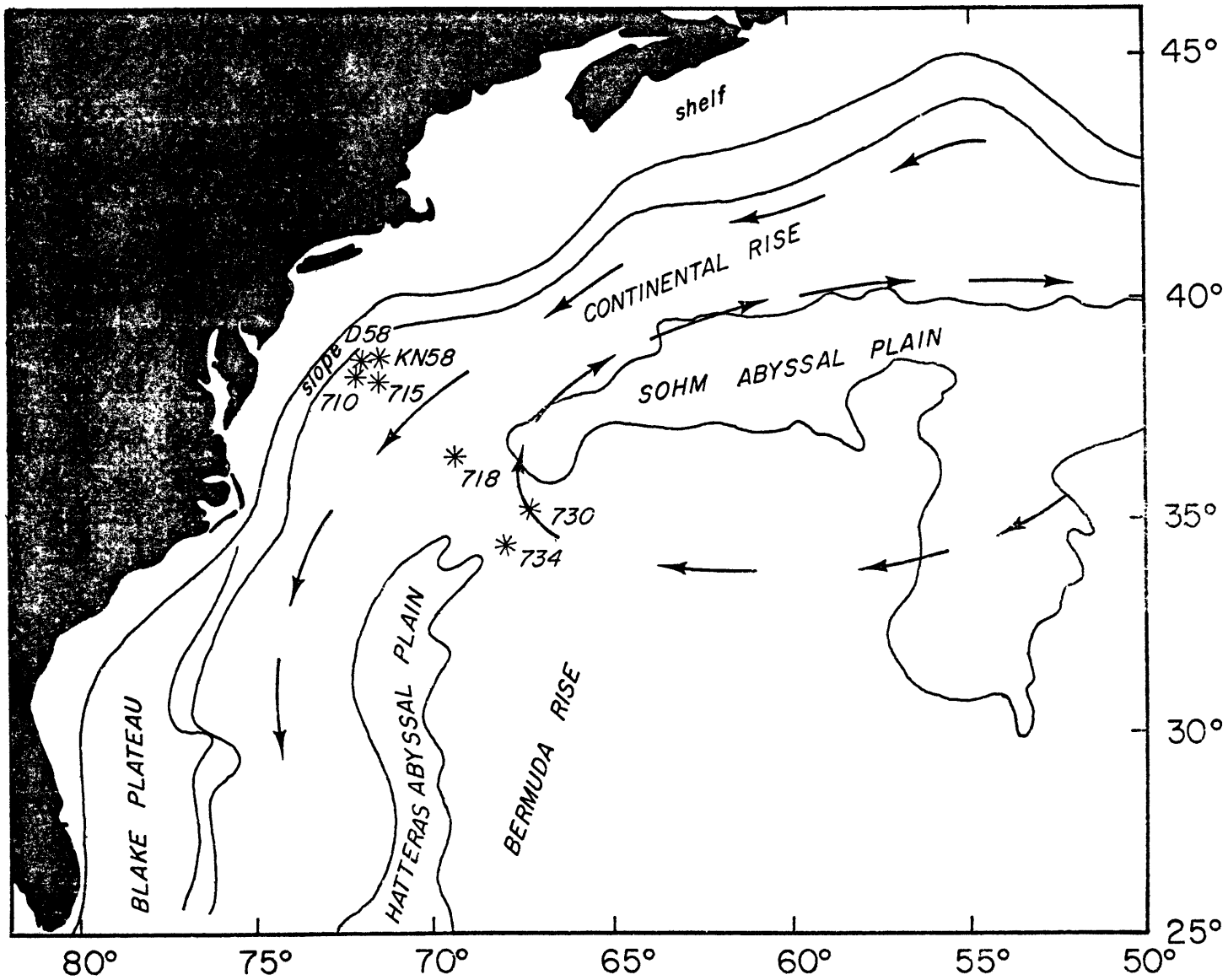
HYDROGRAPHY

The Iceland Rise study, of which this thesis work is a part, was a multidisciplinary, cooperative effort. As part of a comprehensive study of bottom currents and abyssal sedimentation south of Iceland, Shor (1979) described the hydrography of the region. The specifics of the instruments and methods used and calculations made for his work are contained in Shor (1979). A summary of his results which are pertinent to this study follows.

Six current meters were deployed for approximately one week, each during a two week period, at 10 m above bottom (mab) down the eastern flank of the East Katla Ridge from 1200 to 2171 m at 200 m isobath intervals (Figure 2.2). The meters between 1393 and 1796 m recorded velocities in excess of 20 cm/sec for the duration of the experiment (Table 2.1). The direction of flow was predominantly to the west-southwest, tending approximatly 30° upslope with a maximum speed of 29 cm/sec (Figure 2.2). To the northwest and southeast of this inferred core of the overflow current, the mean current speed was 10 cm/sec or less, and flow directions were more variable. At the 2000 m mooring, the current record indicates velocities below threshold (<2 cm/sec) for two days. Prior to and following this event, currents exceeded 20 cm/sec (Figure 2.5).

Current meter data are restricted to a single transect of stations across the region, referred to as the northern transect (see Figure 2.2). Photographic evidence of currents agrees well

TABLE 2.1: Current meter data. (from Shor, 1979)

	HT ABOVE BOTTOM (meters)	DURATION (hours)	VECTOR MEAN speed	VECTOR MEAN direction	MEAN SPEED (cm/sec)	VELOCITY @ 217° (cm/sec)
CM 1	10	162	10.6 cm/sec	227°T	14.0	10.4
CM 2	10	151	20.9 cm/sec	226°T	21.0	13.7
CM 3	10	144	13.3 cm/sec	282°T	14.5	5.4
CM 4	10	156	5.8 cm/sec	273°T	8.8	3.2
CM 5	10	152	20.0 cm/sec	247°T	20.4	17.3
CM 6	10	132	18.7 cm/sec	265°T	21.5	12.5

	LATITUDE	LONGITUDE	WATER DEPTH	GMT
CM 1	62°17.4'N	17°24.6'W	2000 (meters)	2300/26 June-1900/03 July
CM 2	62°28.3'N	17°53.5'W	1600	0400/27 June-1330/03 July
CM 3	62°34.9'N	18°15.0'W	1177	0820/27 June-1000/03 July
CM 4	62°10.8'N	17°03.6'W	2171	0300/04 July-1800/10 July
CM 5	62°23.2'N	17°42.4'W	1796	0825/04 July-1200/10 July
CM 6	62°30.8'N	18°04.8'W	1393	1930/04 July-0800/10 July

Figure 2.5   Current velocity vectors plotted against time.   Current
meter locations are shown in Figure 2.2.   Measurements
are 30-minute averages.   Tidal components have not
been removed.   Note the consistency of velocities in
the three meters at 1393, 1600 and 1796 m, located in
the core of the overflow water.   From Shor (1979).

SPEED
(cm sec⁻¹)

0   30

CM 4   2171 m.

CM 5   1756 m.

CM 6   1393 m.

CM 1   2000 m.

CM 2   1600 m.

CM 3   1177 m.

10·VII·77   9   8   7   6   5   4   3   2   1·VII   30   29   28   27·VI
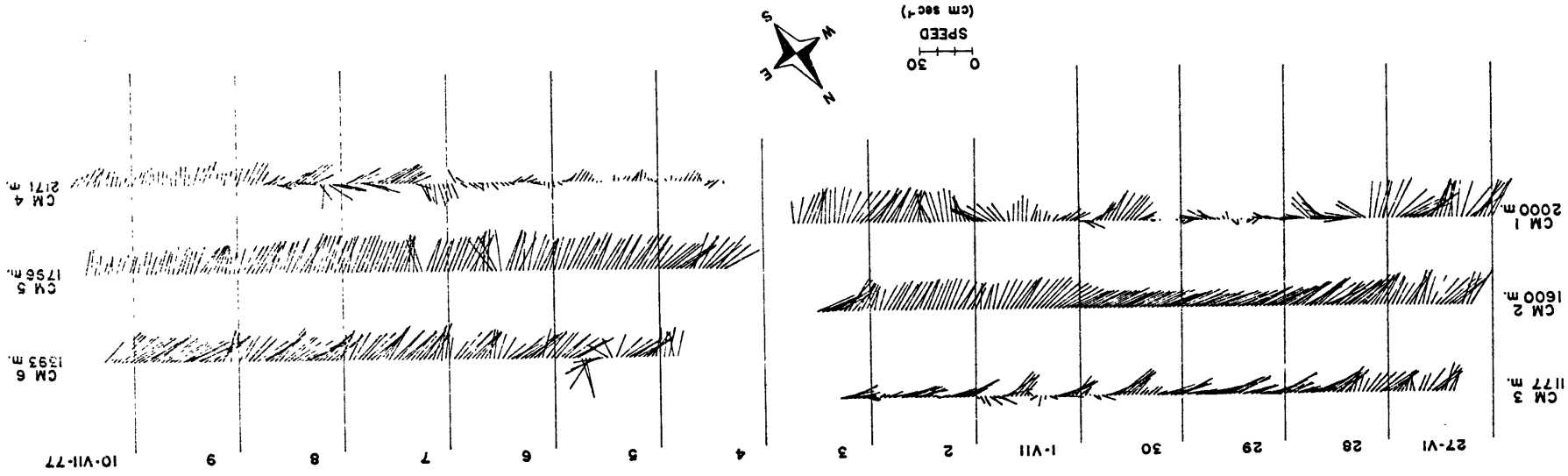
with actual measurements for this northern transect of stations.
Bottom photographs indicate that currents are westward along the
West Katla Ridge, and oscillating northerly and southerly flow, is
indicated for canyon stations.

Geostrophic calculations made from hydrographic sections
generally show southwestward velocities increasing with depth for
individual pairs of stations. Calculated velocities are highest
between 1600 and 1800 m for the northern transect and between 1800
to 2100 m for the southern transect, which corresponds with the
minima in potential temperature (see Shor, 1979; Figures 2.5 and
2.6). Volume transport through the northern transect is calculated
to be 5.0 x 10^6 m^3/sec; and through the southern line, is
4.2 x 10^6 m^3/sec. A small eastward flow, 0.8 x 10^6 m^3/sec,
was indicated between stations 31 and 76.

Isothermal bottom mixed layers along the northern transect of
stations were observed to be 30-50 m thick in the axis of the bottom
current; off-axis and along the southern line, the layers were
10-20 m thick. These layers are thought to form by turbulent mixing
at boundaries (Armi, 1978). In this study, the thickest mixed
layers occur in conjunction with the highest velocities or in the
canyon. Mixed layers are absent where current velocities are
inferred from direct measurements and geostrophic calculations, to
be low (see Shor, 1979; Figure 2.8).

SAMPLING SCHEMES AND APPROACHES

A primary purpose of this thesis is to determine whether resuspension is presently occurring and to examine the influence of resuspension on the composition and characteristics of suspended particulate matter. Approaches to this problem and the rationale for using particular sampling schemes are discussed in this section.

CURRENT COMPETENCE

Resuspension is generally acknowledged to be responsible for the existence of nepheloid layers in the deep sea (Heezen et al., 1966; Betzer and Pilson, 1971; Eittreim and Ewing, 1974; Biscaye and Eittreim, 1977). However, it is difficult to predict the conditions under which a deep-sea current is competent to actively resuspend seafloor sediments. Laboratory flume experiments have estimated critical erosion velocities for deep-sea clays and oozes to be in the range of 15-35 cm/sec (Southard et al., 1971; Lonsdale and Southard, 1974; Young and Southard, 1978). Within the axis of the overflow current, from 1400-1800 m along the flank of the East Katla Ridge, velocities were within this range for the duration of the experiment. Upslope and downslope of the axis, velocities are usually less than 15 cm/sec (Figure 2.5). This observation suggests that resuspension may be occurring during the entire time of the experiment in the current core, and occasionally when velocities exceed those critical for erosion, at the stations further removed.

Since the laboratory experiments of Southard and co-workers represent idealized circumstances and were not performed with sediment or biota from this particular study area, a comparison of the field and laboratory measurements alone cannot be used to conclusively establish that resuspension is actively occurring. Instead, it simply indicates that resuspension is likely. Suspended particulate matter in the study area was examined to determine whether changes in the composition and characteristics of the particles in the lower portion of the water column were indicative of resuspension.

SUSPENDED MATTER

Suspended particles are usually measured by filtration of water samples collected with Niskin bottles (Brewer et al., 1976). This method gives only an instantaneous point measurement of concentration, and with the small volume of water collected (5-30 liters), does not provide a representative sample of the rare larger particles in suspension (Bishop, 1977). Large particles may be major contributors to the mass flux of material through the water column (McCave, 1975). The two principal means of collecting these large particles are large-volume filtration systems and sediment traps (Bishop, 1977; Gardner, 1977a; Honjo, 1978; Spencer et al., 1978). Large-volume filtration has been restricted to shallow depths (<1500 m), precluding sampling in the deep-sea near-bottom nepheloid layer. Sediment traps can be used at all water depths.

Niskin bottles were used to collect the standing crop of small particles. Based on SEM photomicrographs of filtered samples and particle size distributions measured with a Coulter counter, most material collected in Niskin bottles below the surface water in the study region is less than 20 μm. Based on the assumption of Stokes-law settling, the vertical fall velocities of particles in this size range, (5×10^{-5} to 1.3×10^{-2} cm/sec), are more than three orders of magnitude less than the horizontal velocities in the core of the bottom current south of Iceland. This suggests that the material collected by the Niskin bottles in the high current areas of this study is a quasi-conservative property of the water.

Sediment traps were used to collect time-integrated samples of the suspended material in flux. The size of material caught by the sediment traps ranged up to a few millimeters, indicating that there are large particles in flux through the water column which are not collected by water bottles. However, sediment traps are not only large particle collectors: 5-42% of the trap samples are composed of particles less than 20 μm. One problem with sediment traps is that the state of aggregation of particulate matter when it enters the traps is unknown. Loose aggregates may break up and with the high concentration of material on the floor of the sediment traps, aggregates may form. Size fractionation by sieving reveals small particles, particularly volcanic glass, adhered to large pteropods, foraminifera, diatoms, and organic matter. This agglomeration may have occurred in the sediment trap. The presence of intact and

collapsed fecal pellets on filters from the sieved fractions

indicates that these aggregates maintain their integrity through

wet-sieving, but filtration and drying of the samples may cause

pellets to collapse.

Measurement of concentrations of suspended particulate matter

from water bottles is limited by the number of bottles per cast.

Nephelometers provide nearly continuous measurements of light

scattering through the water column. To give a more detailed view

of the distribution of suspended particulate matter, light-

scattering observations were made during this study and correlated

with concentrations of suspended matter from samples obtained at the

same time.

These three instruments, Niskin bottles, sediment traps, and the

nephelometer, were used to obtain information on suspended

particulate matter during this study. The results are discussed in

the following chapters.

CHAPTER III

CHARACTERISTICS OF SUSPENDED PARTICULATE

MATTER FROM NISKIN BOTTLES

INTRODUCTION

The distribution and redistribution of marine particulate matter

is of great importance in interpreting the biological, chemical and

geological processes acting in the deep sea. Particulate matter

from the productive surface layer descends through the water column

slowly by individual particle settling and rapidly by fecal-pellet

transport, providing organic-rich food to the benthic communities.

Adsorption of dissolved species and scavenging of chemical elements

by the particulate matter may affect the distribution of chemical

tracers and radioisotopes throughout the water column.

Geologically, the suspended material in flux to the seafloor may

ultimately become part of the sedimentary record.

Presently, a primary source of particulate matter to the deep

ocean is the surface waters. Rivers, and off Iceland, glaciers,

deliver high suspended loads of terrigenous material as well as

dissolved nutrients necessary for the proliferation of plankton.

Phytoplankton and zooplankton dominate the particles present in the

surface waters. Their skeletons and pellets sink, comprising a

large fraction of the material in transit through the water column.

Other components, such as volcanic and wind-blown detritus, are

regionally important constituents of the suspended matter.

Particles settling from the surface waters are constantly
subjected to the physical, biological and chemical processes of
aggregation, disaggregation, decomposition and dissolution. These
processes are responsible for changing the characteristics of the
particulate matter during descent through the water column to the
seafloor.

Suspended material is also derived from the seafloor. Only
infrequently does freshly deposited material become permanently
incorporated into the sedimentary record at its first place of
deposition. More commonly, animals living in and on the seafloor
reprocess and transport the sediments through feeding and
bioturbation. Deep-sea currents can also resuspend and transport
the surface sediments. Both these mechanisms, animals and currents,
re-introduce previously deposited material into the water column.
This recurrent resuspension can result in vast redistribution of
material (Ewing and Hollister, 1972).

Suspended matter originating from the surface waters may differ
in its characteristics of particles from that originating at the sea
floor. Assessing and interpreting the differences in particles
settling from the surface waters versus those resuspended from the
seafloor is the purpose of this chapter.

NEPHELOID LAYERS

In many areas of the oceans, after a decrease in concentration
of suspended particulate matter (SPM) with depth due to dissolution,

decomposition, and consumption in the water column, there is an

increase in the concentration of SPM near the seafloor. This layer

of increased concentration of SPM (the near-bottom nepheloid layer)

is thought to be due to resuspension of sediment from the seafloor

(Heezen et al., 1966; Betzer and Pilson, 1971; Feely 1975; Brewer

et al., 1977; Biscaye and Eittreim, 1977). The depth of minimum

concentration of SPM above the near-bottom nepheloid layer is termed

the "clear-water minimum" (Biscaye and Eittreim, 1977; Figure 3.1).

Below this level, there is an increase in the resuspended component

of the SPM. By sampling in clear water and the nepheloid layer

below, the increasing influence of resuspended sediment can be

examined.

HISTORICAL PERSPECTIVE

The characteristics of marine particulate matter have been

studied extensively only in the past decade. With the initiation of

the GEOSECS program, a detailed examination of the geochemistry of

abyssal ocean water and SPM was begun. The GEOSECS program

collected SPM for chemical, mineralogic, and microscopic analyses

(Brewer et al., 1976). Since GEOSECS began, numerous techniques

have been employed to determine the properties of suspended

material. Compositional analyses have been performed with the

scanning electron microscope for morphologic identification (Honjo

et al., 1974; Honjo, 1976; Feely, 1976; Bishop et al., 1977), X-ray

diffraction for mineralogy (Feely, 1975), and neutron activation and

-43-

Figure 3.1   Idealized nephelometer profile. The unit Log E/E_D
              is a measure of scattering made by comparing the
              scattered light to a direct beam. Cross-hatched area
              represents the near-bottom nepheloid layer. Note the
              location of the clear water minimum.

LIGHT-SCATTERING

$LOG\ E/E_D$
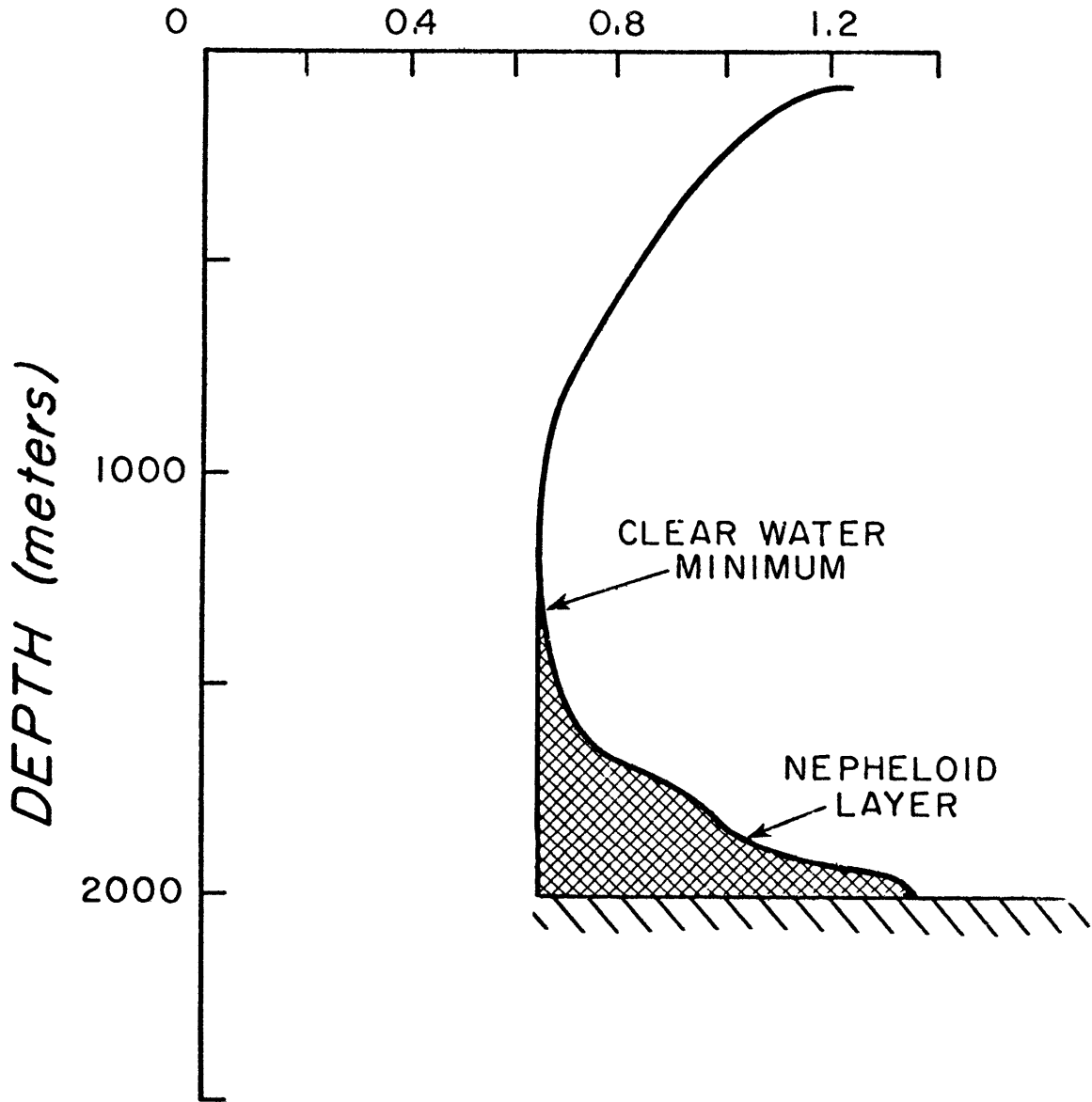
atomic absorption for elemental determination (Spencer et al., 1972; Krishnaswami and Sarin, 1976; Bishop et al., 1977). Size distributions of suspended matter have been determined with instruments which count and discriminate particles by volume, e.g., a Coulter counter (Carder et al., 1971; Plank et al., 1972; Sheldon et al., 1972; Brun-Cottan, 1976). Optical devices, nephelometers and transmissometers, have been widely used to indirectly measure the concentration of SPM. Nephelometers, which measure scattered light, have been used to document the existence of near-bottom nepheloid layers in many areas of the world's oceans (Ewing and Thorndike, 1965; Eittreim et al., 1972; Eittreim and Ewing, 1972; Biscaye and Eittreim, 1974; Kolla et al., 1976; Biscaye and Eittreim, 1977). Transmissometers, which measure transmitted light (a function of both absorption and scattering by SPM and water), have been used to monitor variations in the quantity of SPM, particularly in surface waters (Pak and Zaneveld, 1977; Bartz et al., 1978). Using data on SPM concentration and size, models have been formulated for the vertical flux of particles in the ocean (McCave, 1975; Bishop, 1977).

These techniques have been used to gain a global perspective of the distribution of SPM, gross compositional information, and preliminary ideas about its dynamics. Now that this base-line information has been established, it is possible to examine in detail those characteristics of marine particulate matter that may yield insight into its behavior and provenance.

OBJECTIVES

Geological and physical-oceanographic data were obtained in the
North Atlantic along the Iceland Rise (cruise ATLANTIS II-94) and in
the western North Atlantic along the continental rise (cruises
DALLAS, KNORR-58, and OCEANUS-6) with the following objectives in
mind:

(1) to determine the differences between clear-water particles
and nepheloid-layer particles with respect to size distribution,
composition, density, and light-scattering characteristics in
limited study regions;

(2) to identify properties of particles which might be useful in
distinguishing their prior source;

(3) to determine whether differences observed between properties
of nepheloid-layer particles and clear-water particles are
regionally site-specific;

(4) to identify those processes which most strongly influence
particle characteristics, e.g., dissolution, decomposition,
deposition, and resuspension.

OBSERVATIONAL TECHNIQUES

This investigation is a comparison of the characteristics of the
SPM in two regions: the Iceland Rise and the continental rise
southeast of New York (Figure 2.1). A total of thirty-two
hydrographic stations and twenty-four nephelometer stations were

occupied on the Iceland Rise during June and July 1977 (Figure 2.2), and seven hydrographic stations were occupied in the western North Atlantic along a transect southeast of New York in the summer of 1976 (Figure 2.4). Each hydrographic station employed six to twelve 5 or 30 liter Niskin bottles for collection of SPM. Samples were collected from the lower portion of the water column from both clear water and the near-bottom nepheloid layer. Reversing thermometers were used to obtain accurate records of sample depth in mid-water; a pinger was used to determine the height of the bottom bottles above the sea floor. Simultaneous nephelometer profiles using an L-DGO-Thorndike deep-sea photographic nephelometer (Thorndike, 1975) were taken at most Iceland Rise stations to ensure that samples were from a known position relative to the nepheloid layer (if present).

CONCENTRATION OF SPM

A 250 ml aliquot was taken from the Niskin bottles immediately on retrieval for size distribution determination of SPM. The remaining water was filtered with an in-line vacuum filtration system through a preweighed 47 mm diameter, 0.4 μm Nuclepore filter. Filters were washed ten times with filtered distilled water to remove salt and reweighed upon return to the laboratory to determine the mass of particles. For the Iceland Rise, water beneath the spigot was filtered onto a separate filter to collect the "dregs" (Gardner, 1977b). For the western North Atlantic, the entire water bottle was filtered onto one filter by tilting the

bottle to remove all the water. Concentrations reported as "corrected" concentration include this "dregs" material. Combined errors in filter weighing and volume readings amount to $\pm 9\%$ for concentrations of 20 $\mu g/l$ and $\pm 5\%$ at 100 $\mu g/l$.

SIZE DISTRIBUTIONS

Size distribution of SPM was determined with a Model TA II Coulter counter. With this instrument, particles suspended in an electrolyte (seawater) are drawn through a small aperture. When a suspended particle passes through the aperture, it decreases the volume of electrolyte in the aperture, thereby increasing the resistance and decreasing the current in the circuit. The percent current change is proportional to the ratio of the particle volume to the aperture volume. This relationship is linear for particles having diameters between 2% and 40% of the aperture diameter (Sheldon and Parsons, 1967).

Coulter-counter data are recorded in terms of either total number or total volume of particles counted and are subdivided into logarithmically increasing size grades, each grade representing a doubling of volume. A 50 μm aperture and a 2.0 ml sample size were used in this study to measure the size distribution of particles having equivalent spherical diameters from 1-20 μm.

LIGHT SCATTERING

Light-scattering was measured with a L-DGO-Thorndike deep-sea photographic nephelometer (Thorndike, 1975), designed to measure relative forward light scattering from 8° to 24°. Although light scattering is dependent on all the optical properties of the particles (Jerlov, 1968), forward scattering is most sensitive to variations in concentration of SPM and least sensitive to variations in particle size and index of refraction (Thorndike, 1975).

The nephelometer is composed basically of a light source and a camera lens. An attenuator is situated between the source and lens to calibrate direct light. Scattered light as well as the attenuated direct light are measured by the nephelometer. A ratio is formed between the intensity of the scattered light, E, and that of the attenuated direct light, E_D, to form a scattering index, E/E_D. Forming this ratio circumvents problems involved in correcting the scattering values due to variation in the intensity of the source and direct beam attenuation losses. Nephelometer readings are most often reported in terms of $\log(E/E_D)$.

Nephelometers are optical instruments and cannot directly yield absolute concentrations of SPM. However, nephelometer readings in a few instances have been calibrated by sampling and filtering water for SPM from nephelometer lowerings (Beardsley et al., 1970; Baker et al., 1974; Carder et al., 1974; Sternberg et al., 1974). The L-DGO-Thorndike nephelometer has been calibrated by Biscaye and Eittreim (1974) through their work in a limited region of the

Blake-Bahama Outer Ridge and the Hatteras Abyssal Plain (BBOR-HAP).
A slightly different calibration for this instrument was obtained by
them from the eastern North American lower continental rise (LCR)
(Biscaye and Eittreim, 1977).

COMPOSITIONAL ANALYSES

Composition of the SPM collected from the near-bottom nepheloid
layer and overlying clear water was studied by photographing
sections of filters with a scanning electron microscope. Five
stations in the Iceland Rise area and two along the western North
Atlantic transect were selected for quantification of the
composition of SPM. A sample from the nepheloid layer and one from
clear water for each station were photographed for optical
identification of the SPM. Four or five random photographs were
taken in each of four sections of a filter to determine homogeneity
of the SPM on the filters.

Additionally, "dregs" filters from two of the Iceland Rise
samples were photographed and counted to allow a valid comparison
with the western North Atlantic samples, where the entire sample was
collected on one filter. A comparison of "dregs" composition to
that of the above-spigot sample was made for the Iceland Rise
samples to examine the differentiation of the SPM while settling in
the water samplers (Gardner, 1977b).

Twelve classes of particles were identified and counted: small
coccoliths (<4 µm), large coccoliths (>4 µm), centric diatoms,

pennate diatoms, dinoflagellates, organic matter, plankton fragments, fecal pellets, aggregates, clays, mineral matter, and unidentified particles (Plate 3.1). Particles smaller than two microns were not included in the counts since positive identification was impossible.

Chi-square analysis of the compositional data was performed: a) to determine whether the random photographs represented subsamples of a homogeneous population of material on the filters; b) to determine whether compositional differences between clear-water samples and nepheloid-layer samples for individual stations were statistically significant; c) to determine whether the clear-water samples from all stations were statistically different from each other and whether the nepheloid-layer samples from all stations were statistically different from each other; and d) if all the above are true, to determine whether collectively the clear-water samples statistically differ from the nepheloid-layer samples.

RESULTS

SPM CONCENTRATION

High concentrations of SPM in the lowest few hundred meters of the water column extend from the sill depths along the Greenland-Scotland ridge, at approximately 62°N, southward along the western side of the North Atlantic basin outlining the path of

Plate 3.1 SEM photographs of suspended particulate matter.
Samples (1a,1b) are taken from clear water (a) and the
nepheloid layer (b) from the western North Atlantic.
Note the decrease in percentage of small coccoliths
and increase in percentage of clays and mineral matter
between these two samples. Samples (2a,2b) are
"dregs" filters from the Iceland Rise. Note the
aggregates of coccoliths and diatoms and the large
mineral grains. Approximate scale is given below each
photograph. X 1100.

-53-

1a

1b

2a

2b
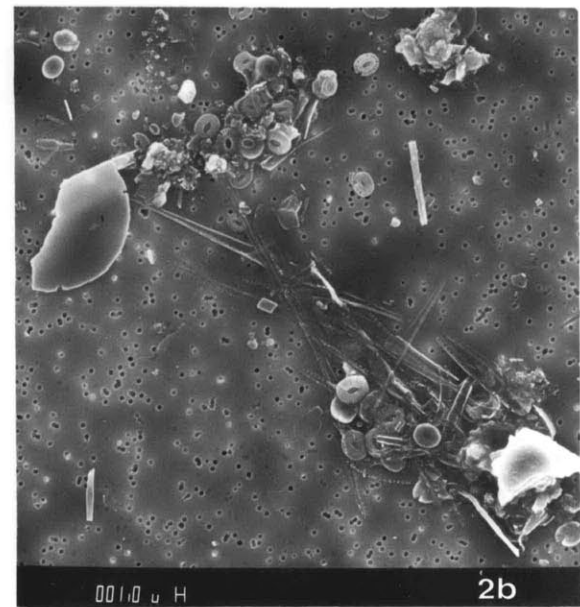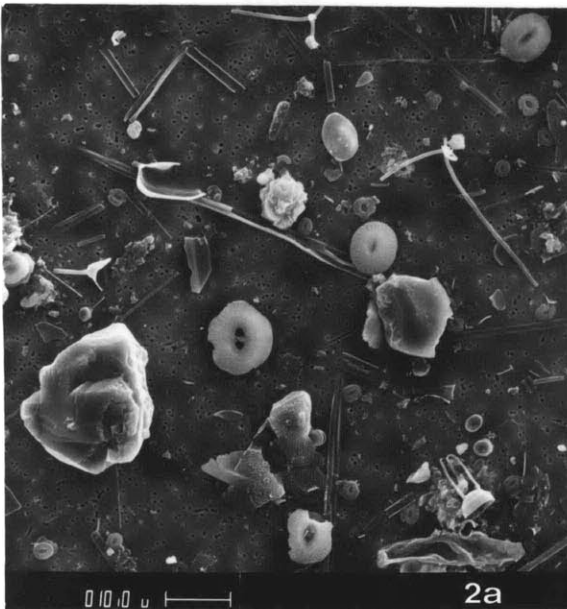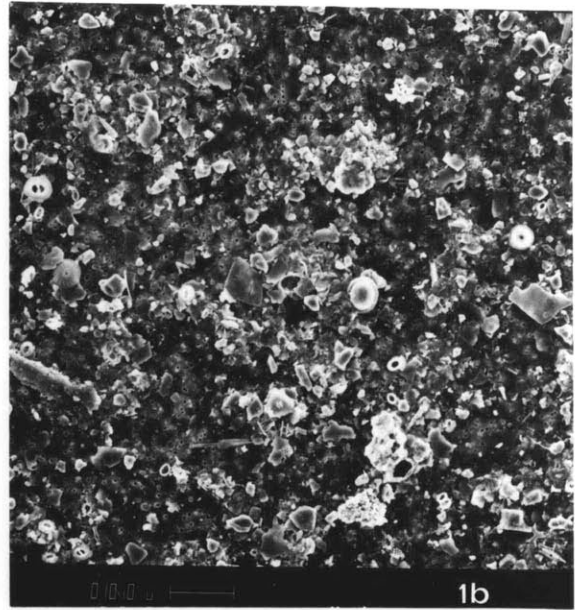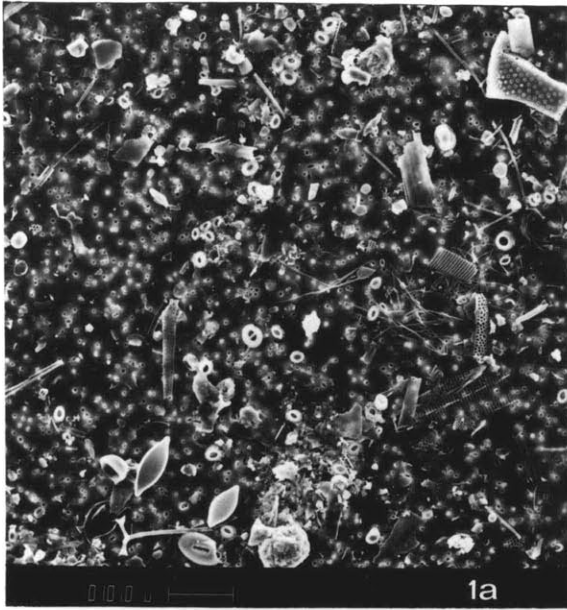
bottom-water flow (Figure 3.2; Brewer et al., 1976). This detailed

study of SPM across the bottom-current axis south of Iceland and

along a transect across the western North Atlantic margin is an

attempt to compare SPM characteristics from areas widely separated,

but perhaps influenced by the same bottom current.

Iceland Rise

Profiles of concentration of SPM were obtained in the lower

1000 m of the water column along two transects across the axis of

the bottom current from the crests of the East and West Katla Ridges

(1200 and 1500 m) into the Iceland Basin (2500 m)(Figure 2.2). In

water depths greater than 2000 m the profiles are characterized by

low concentrations (<30 µg/l, corrected concentration of ∿40 µg/l)

in mid-water depths with sharp increases in concentration in the

lowest hundred meters of the water column (Figure 3.3). Shallower

than 1800 m, concentrations in mid-water are higher (∿50 µg/l,

corrected concentration of ∿70 µg/l) with thicker nepheloid layers

(up to 300 m)(Figure 3.3).

Stations 29, 40, and 85 are reoccupations of a station at

approximately 2000 m. The character of the SPM profile changed

dramatically over a ten-day period (Figure 3.4), even at mid-water

depths. Station 29 showed a gradual increase in concentration

towards the seafloor to concentrations up to 120 µg/l (corrected

concentration >200 µg/l). Mid-water concentrations exceed 40 µg/l

(corrected concentration of ∿50 µg/l). Four days later, station 40

Figure 3.2   Distribution of suspended particulate matter in the
western Atlantic Ocean. High concentrations in the
nepheloid layer, seen from the Denmark Straits to
45°N, outlines the flow of the Norwegian Sea
Overflow water. From Brewer et al. (1976).

DEPTH (METERS)

1000 2000 3000 4000 5000 6000

GEOSECS
WESTERN ATLANTIC
PROFILE

1000:1 Vertical Exaggeration

SUSPENDED PARTICULATE
MATTER, μg/kg

< 12
12-20
20-25
25-50
50-100
100-200
> 200

GREENLAND SEA

DENMARK STRAITS

LABRADOR BASIN

NORTH AMERICAN BASIN

GUIANA BASIN

BRAZIL BASIN

VEMA CHANNEL

ARGENTINE BASIN

SCOTIA RIDGE

70° 60° 50° 40° 30° 20° 10°N 0° 10°S 20° 30° 40° 50°
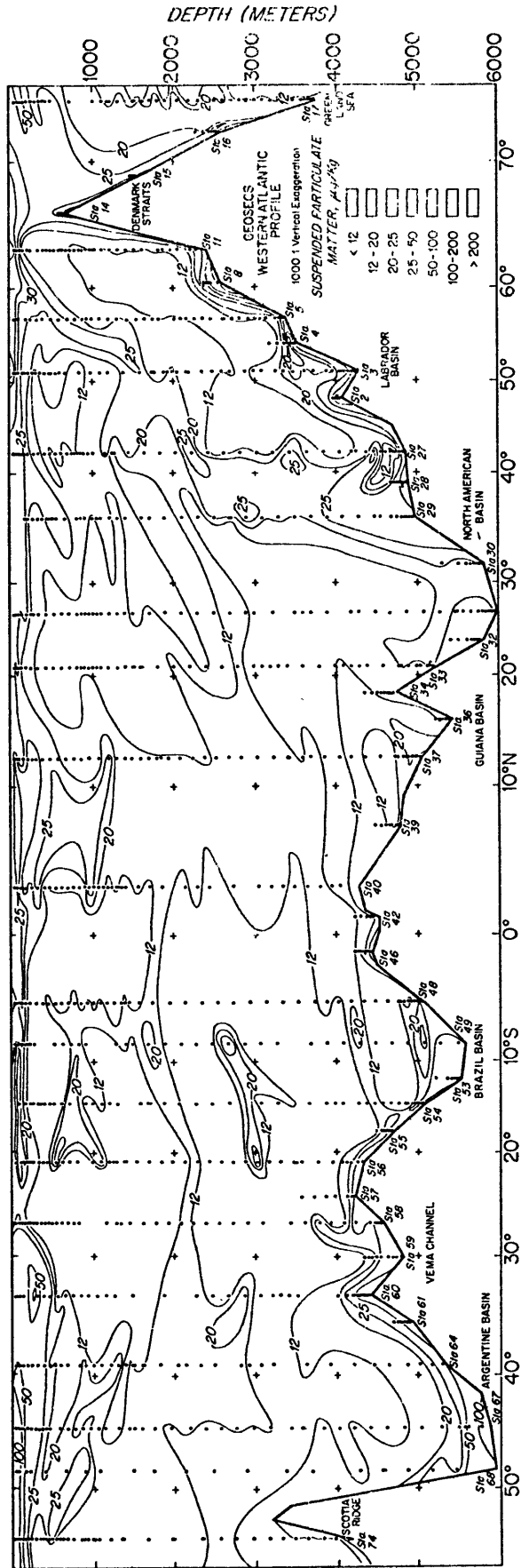
Figure 3.3   Profiles of suspended particulate matter from the
              Iceland Rise. Most profiles show nepheloid layers.
              a) Stations from the northern transect, both standard
              and corrected concentrations; b) stations from the
              southern line with standard and corrected
              concentrations.

a

NORTHERN LINE

CONCENTRATION (μg/l)

CORRECTED CONCENTRATION (μg/l)

b

SOUTHERN LINE

CONCENTRATION (µg/l)

CORRECTED CONCENTRATION (µg/l)
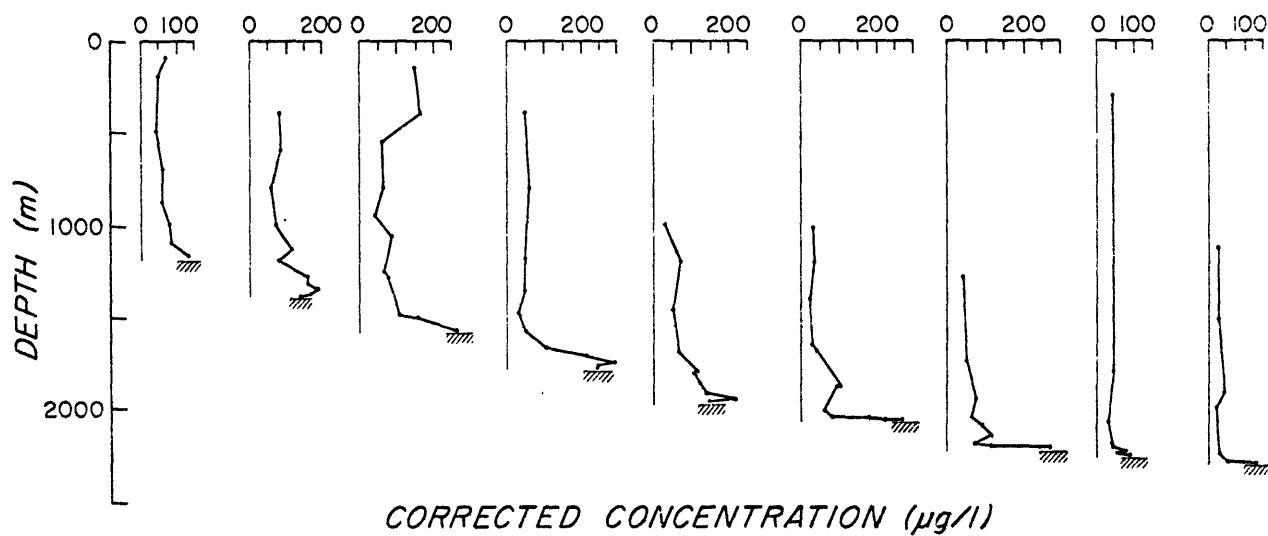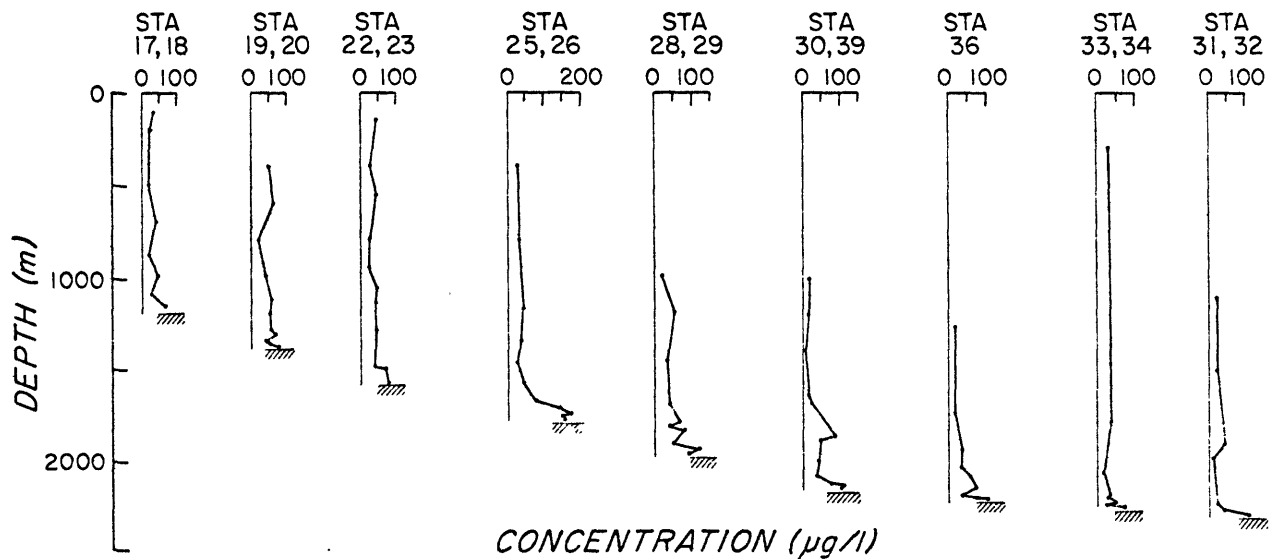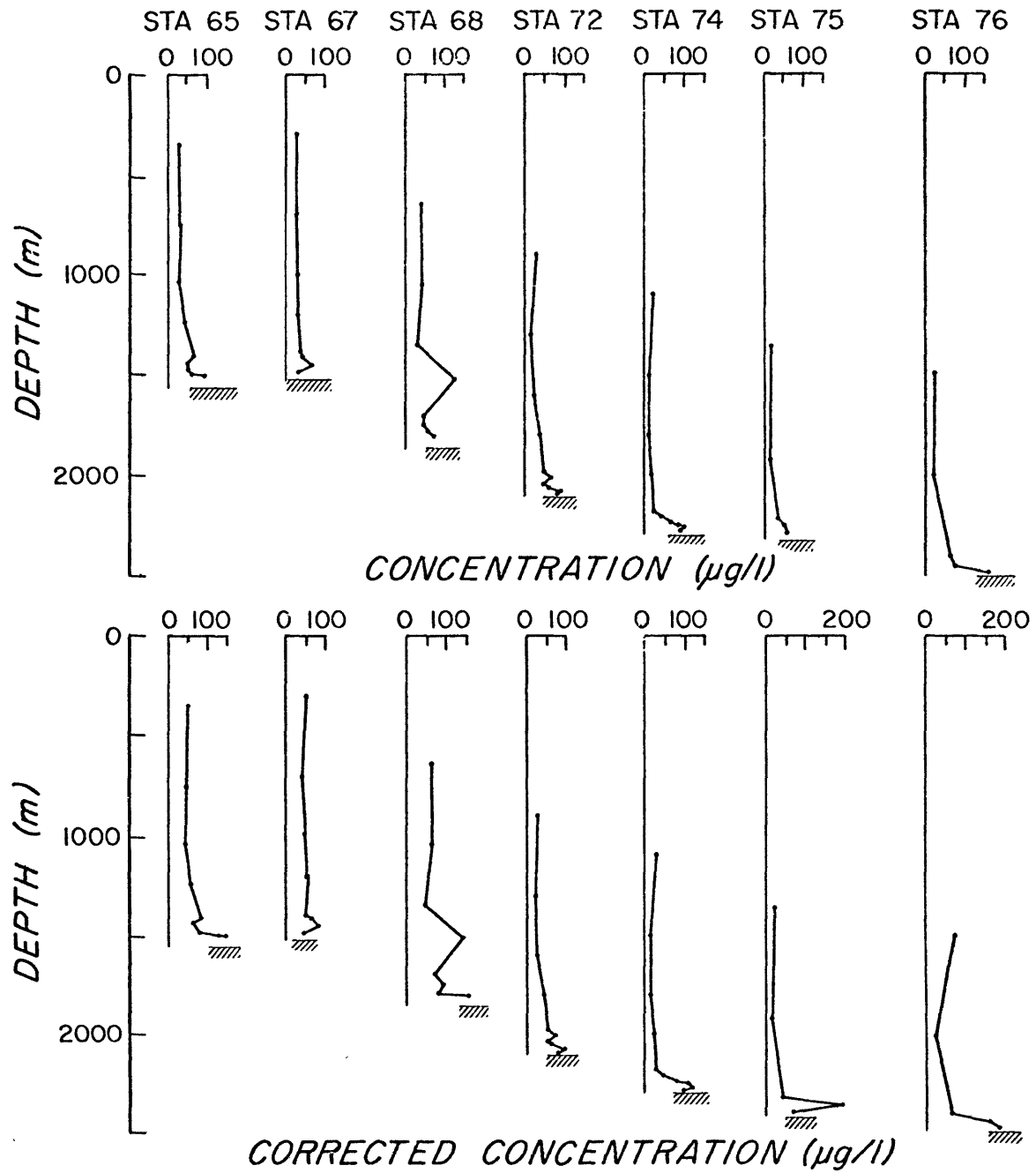
Figure 3.4   Profiles of suspended particulate matter from
              reoccupation of the station at 2000 m from the Iceland
              Rise. Note the temporal variability in both mid-water
              concentrations and nepheloid layer concentrations over
              a ten-day period.

REOCCUPATIONS OF THE 2000 m STATION

CONCENTRATION (µg/l)

CORRECTED CONCENTRATION (µg/l)
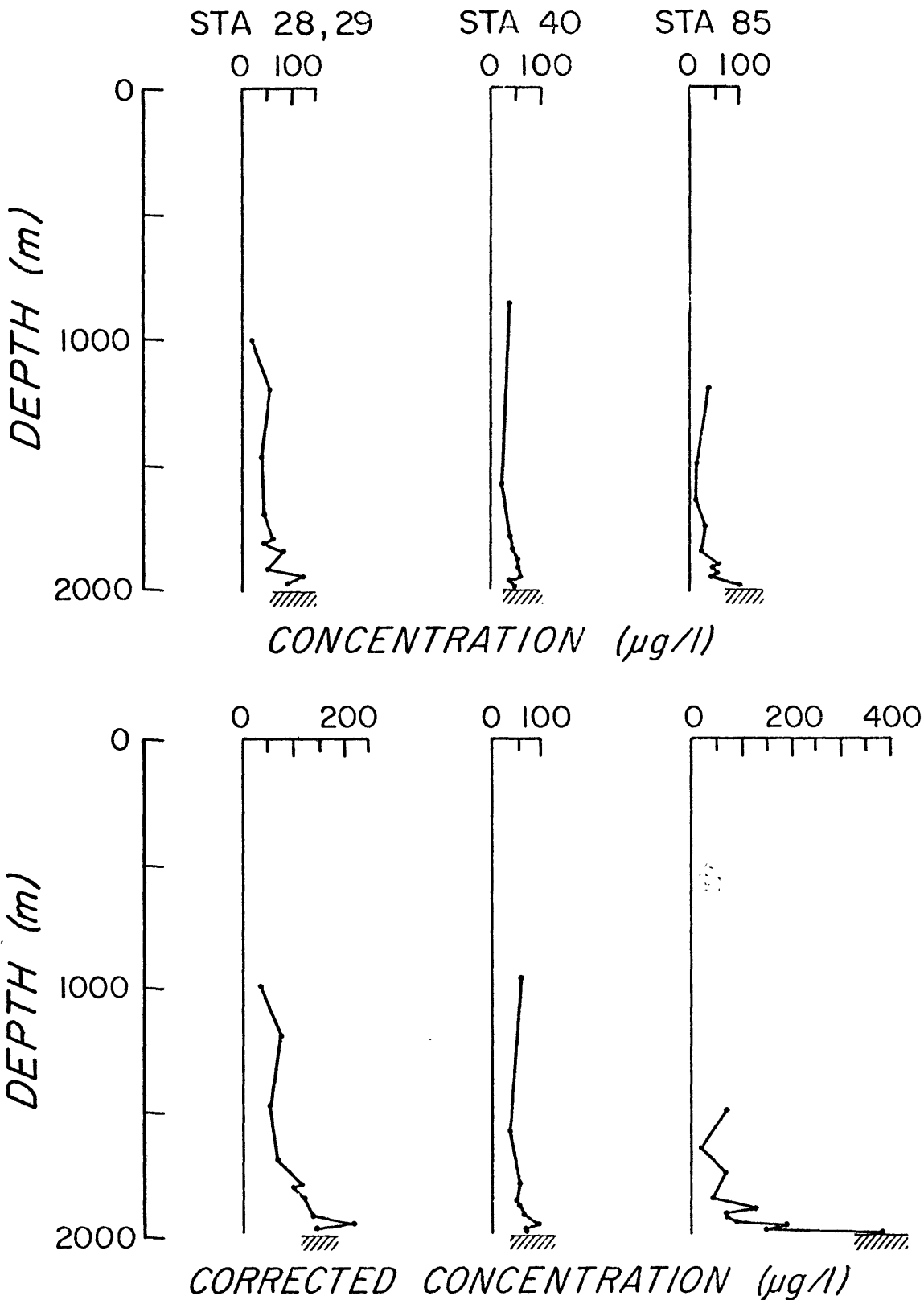
had both lower mid-water concentrations ($\sim$20 μg/l, corrected

concentration of $\sim$40 μg/l) and nepheloid-layer concentrations

(<60 μg/l, corrected concentration of $\sim$90 μg/l). For the final

reoccupation, mid-water values remained low (<20 μg/l, corrected

concentration of 20-70 μg/l), but nepheloid concentrations increase

to greater than 90 μg/l (corrected concentration > 300 μg/l).

Concentration maxima are seen in mid-water near the crest of the

Katla Ridges (Figure 3.5). These features are above the near-bottom

nepheloid layers and may be detached turbid waters laterally

advected from upstream (Armi, 1978).

Western North Atlantic

A single hydrographic section was made across the continental

rise southeast of New York (Gardner, 1977a). Nepheloid-layer

corrected concentrations on the slope and upper rise did not exceed

100 μg/l, while above the lower rise and abyssal plain, nepheloid-

layer corrected concentrations consistently exceeded 100 μg/l

(Figure 3.6). Mid-water maxima in particle concentrations in slope

and upper rise waters are interpreted as being caused by material

advected horizontally outward from the slope.

LIGHT-SCATTERING OBSERVATIONS

Information on SPM concentration from water bottles is limited

to a small number of discrete samples per station. In order to

obtain a continuous vertical profile of SPM, light-scattering

ICELAND RISE
NORTHERN SECTION

SUSPENDED PARTICULATE
CONCENTRATION (µg/l)
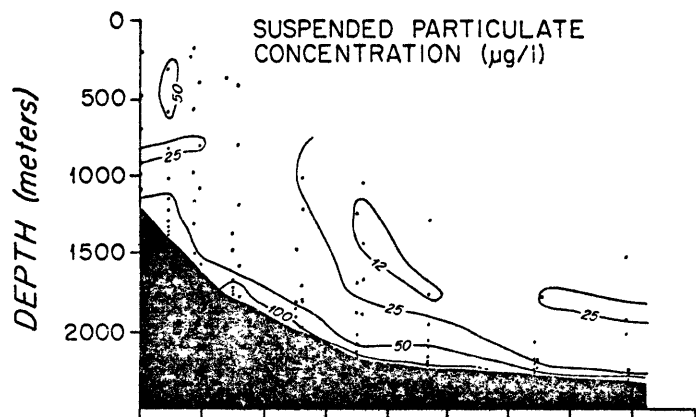
ICELAND RISE
SOUTHERN SECTION

SUSPENDED PARTICULATE
CONCENTRATION (µg/l)

SUSPENDED PARTICULATE
CORRECTED CONCENTRATION (µg/l)

SUSPENDED PARTICULATE
CORRECTED CONCENTRATION (µg/l)

DEPTH (meters)
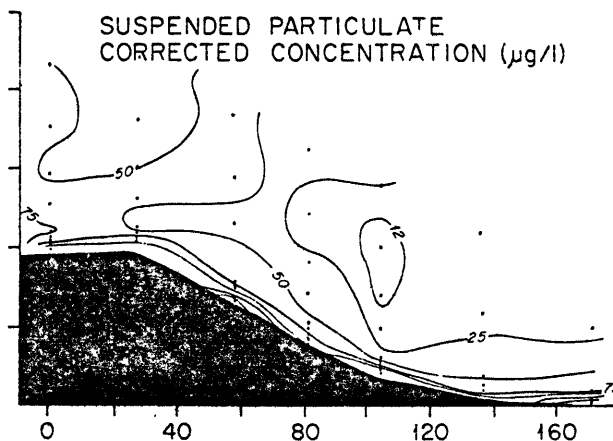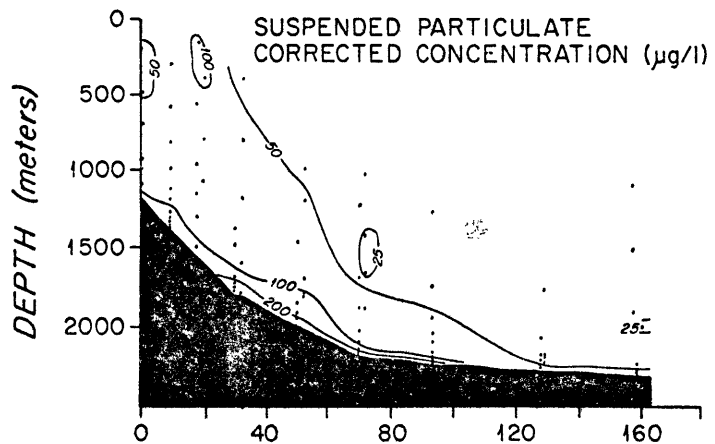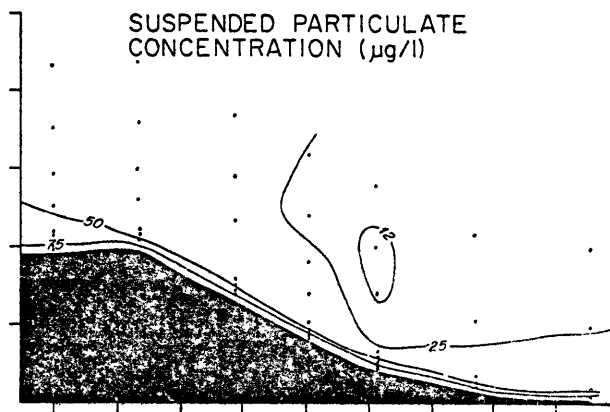
DISTANCE (kilometers)

Figure 3.6   Cross-section of suspended particulate matter along
              the continental rise southeast of New York.
              Concentrations are corrected for "dregs." Note the
              occurrence of some high concentrations in mid-water
              which may reflect advection of material from the
              slope. From Gardner (1977a).

STATION NUMBERS

SUSPENDED

PARTICULATE MATTER

$\mu g/\ell$
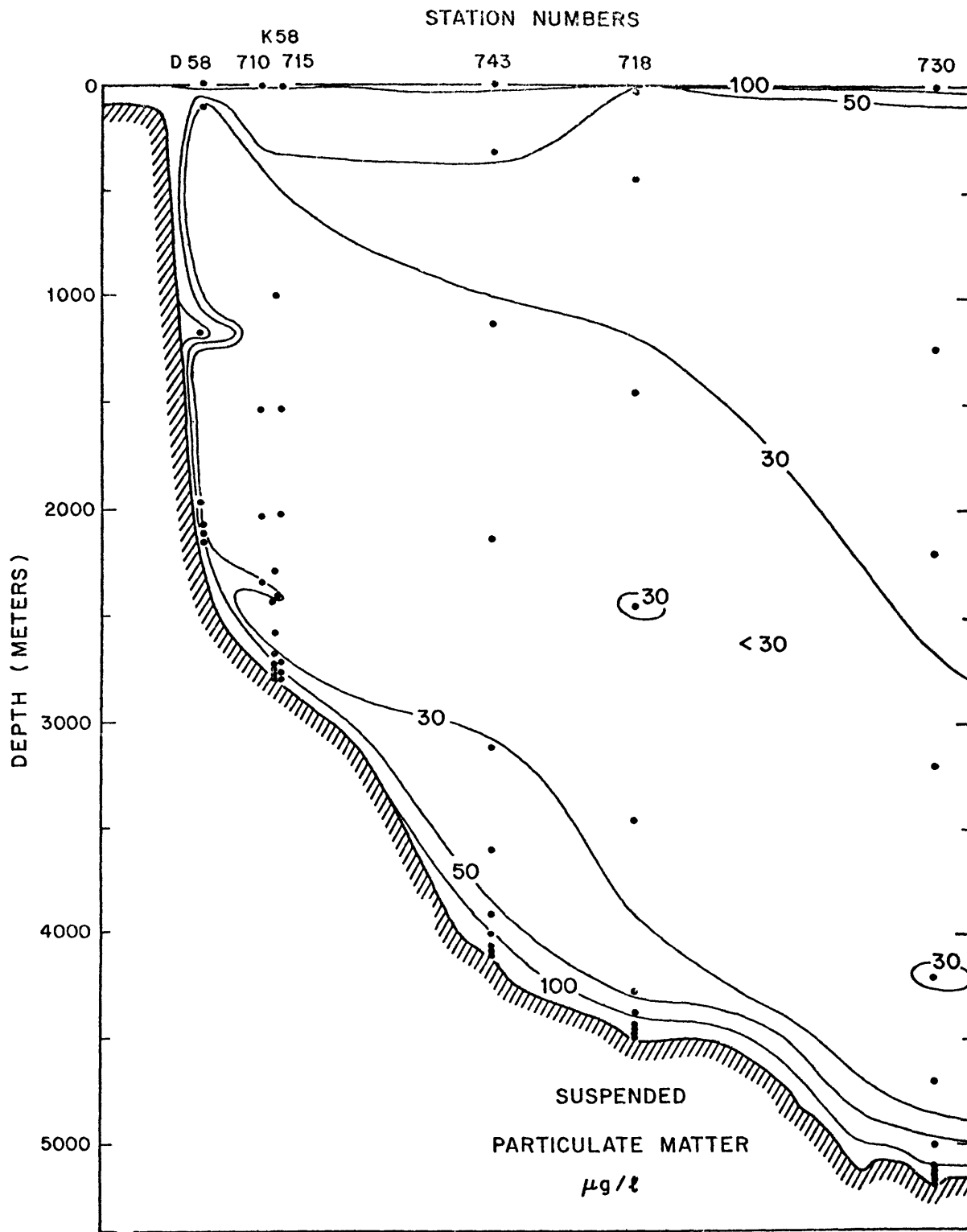
measurements, which can be calibrated in terms of SPM

concentrations, were made at most of the hydrographic stations in

the Iceland Rise region (Figure 3.7).

The nephelometer profiles exhibit features similar to those of

the SPM, but being more detailed, the nephelometer profiles allow

the vertical extent and structure of the nepheloid layer to be more

clearly defined. Lowest clear-water values (0.34 log E/E_D) are

found over the basin; highest near-bottom values (1.43-1.55

log E/E_D) occur along the ridge flank and over the basin in water

depths greater than 1800 m.

The character of the nephelometer profiles changes substantially

from the crest of the ridge eastward into the basin. The ridge-

crest profiles show variable light scattering throughout the water

column, generally in excess of 0.5 log E/E_D. At station 67, no

clearly defined nepheloid layer is observed. To the east, along the

ridge flank (1600-2200 m) nepheloid layers up to 700 m thick are

developed. Clear-water values decrease below those from the ridge

crest. The nepheloid layers for the last profile of each transect,

located over the basin, are thin (<100 m), but show a very sharp

gradient from clear water to the nepheloid layer.

Profiles taken within the canyon between the two ridges are

somewhat erratic. A general increase in light scattering from

mid-water to the seafloor is observed, but the nepheloid layer is

not as well-defined as it is along the ridge flanks (Figure 3.7).

Light scattering is fairly high (>0.6 log E/E_D) for these profiles

throughout the entire water column.

Figure 3.7   Nephelometer profiles from the Iceland Rise region.
              Nepheloid layers are sharper and thinner with
              increasing depth. Location of samples taken for
              suspended particle size analysis is indicated by (o)
              for clear water samples and (x) for nepheloid layer
              samples. a) Northern section; b) southern section; c)
              canyon stations.

NORTHERN LINE

STA 17   STA 19   STA 22   STA 25   STA 28

LIGHT-SCATTERING
(LOG E/E$_D$)

STA 30, 39   STA 37   STA 33   STA 32

LIGHT-SCATTERING
(LOG E/E$_D$)

SOUTHERN LINE

STA 65   STA 66   STA 67

LIGHT-SCATTERING
(LOG E/E_D)

STA 68   STA 72   STA 75   STA 76

LIGHT-SCATTERING
(LOG E/E_D)

CANYON STATIONS

C

STA 62　　　　STA 58　　　　STA 53

LIGHT-SCATTERING
(LOG E/E_D)
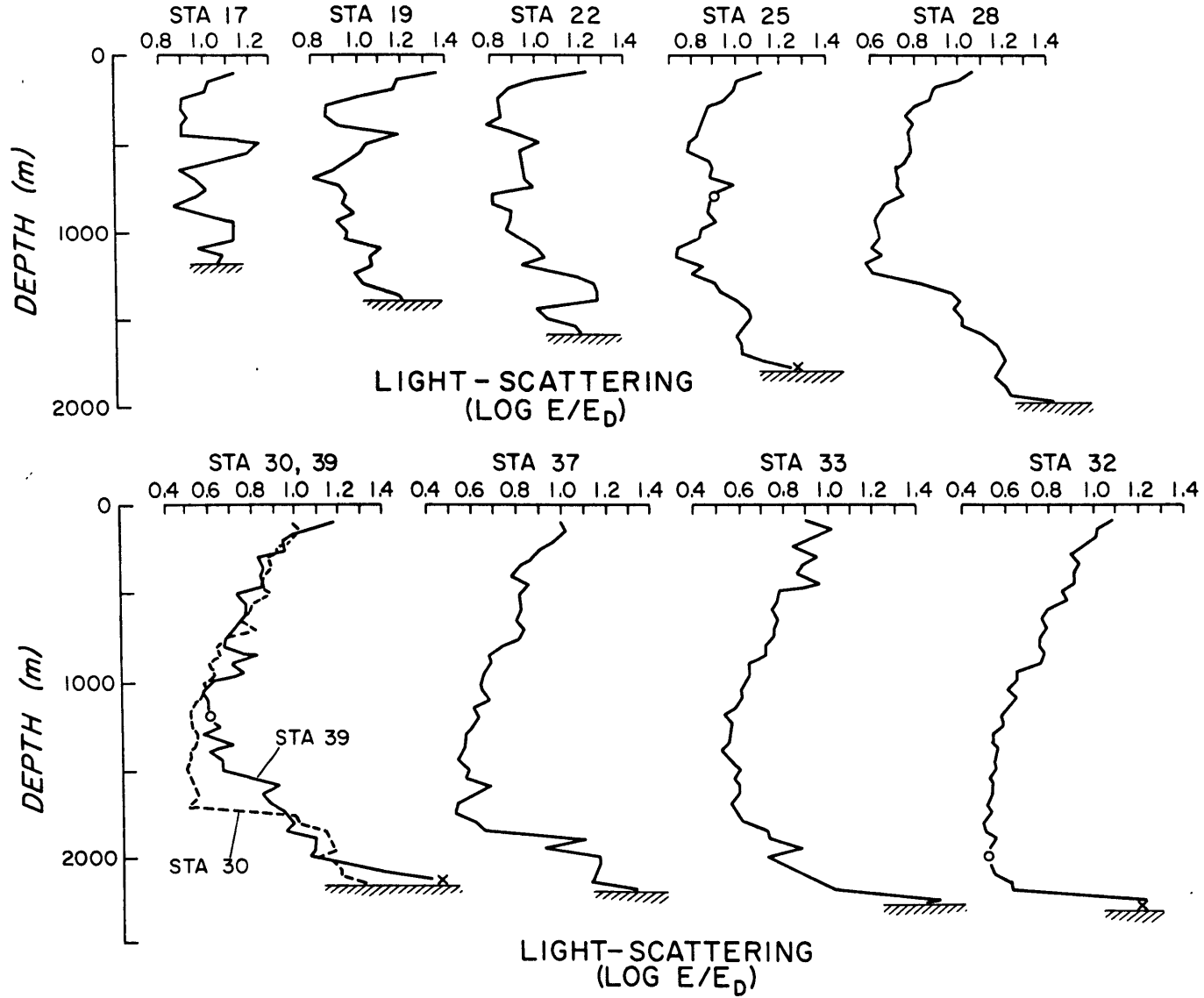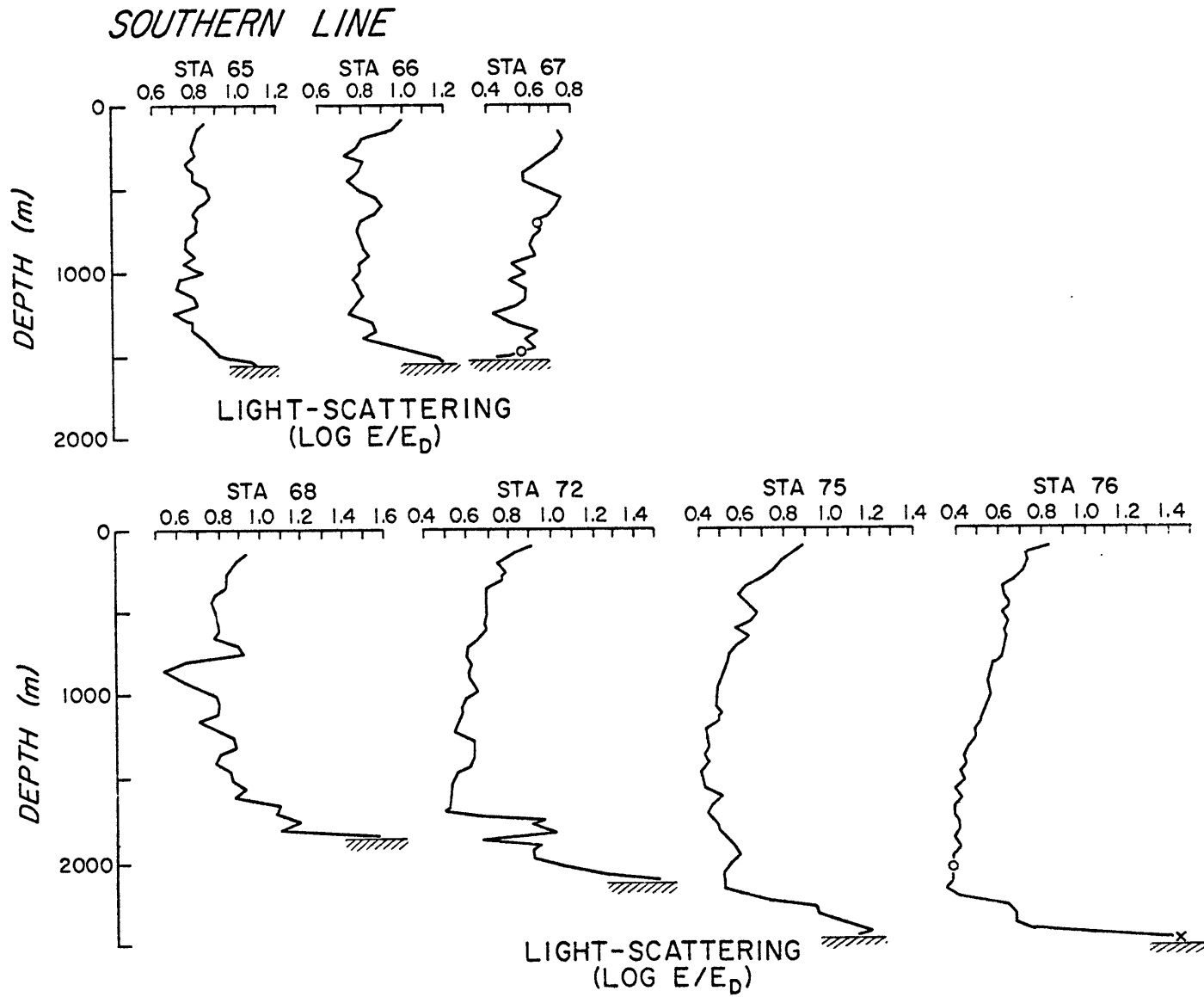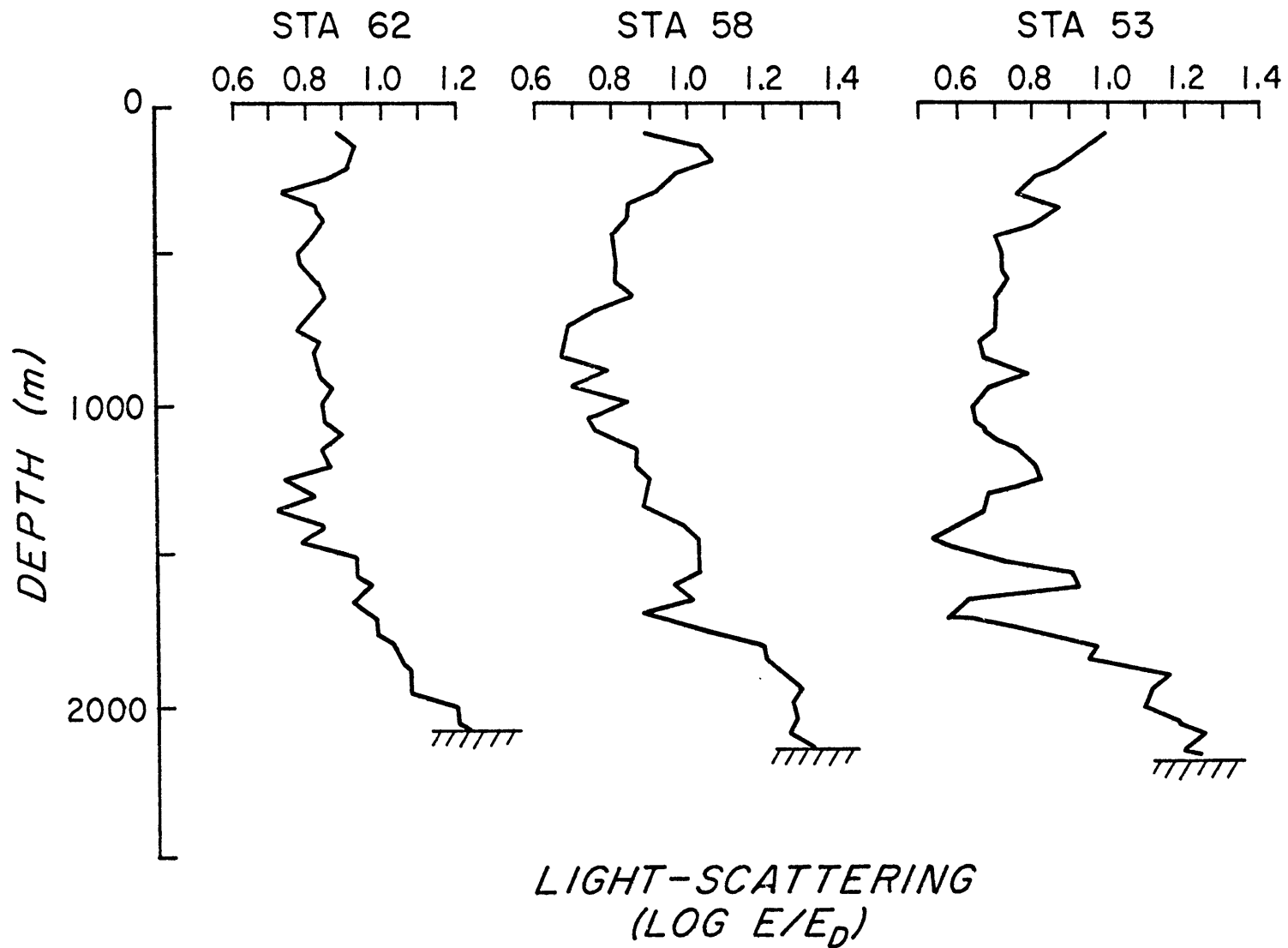
The two reoccupations of station 28 (2000 m) gives some idea of the temporal variability of the nepheloid-layer structure over 10 days (Figure 3.8). The first occupation shows a sharply defined nepheloid layer, 700 m thick, with a second increase in light scattering in the deepest 10 m of the water column. Station 40, taken 4 days later, has a much thinner (400 m) nepheloid layer. The nepheloid layer is characterized by a gradual increase with depth leveling off to a constant value for the final 150 m. The second reoccupation (Station 84) has a nepheloid layer 450 m thick with a sharp increase with depth in light scattering in the lowermost 30 m. These reoccupations demonstrate that light scattering in the region is highly variable over the time scale of ten days.

The nephelometer profiles have been compiled to give cross-section distributions of light-scattering values (Figure 3.9). These cross sections show the extent and influence of the bottom current in the region. In the axis of the current (1600-2000 m), the nepheloid layer is several hundred meters thick, but diffuse, suggesting mixing of material up into the water column. In the basin, the nepheloid layer is thin, perhaps reflecting the lesser influence of the bottom current.

High values of light scattering in the surface waters are probably caused by both high biological productivity and Icelandic terrigenous input. The general decrease in clear-water values from the ridge crests into the basin is a function of the distance from Iceland.

Figure 3.8   Nephelometer profiles from reoccupation of the station
              at 2000 m from the Iceland Rise, showing the temporal
              variability in the thickness and structure of the
              nepheloid layer over a ten-day period.

REOCCUPATION OF THE 2000 m STATION

STA 28   **STA 40**   **STA 84**

DEPTH (m)

*LIGHT—SCATTERING
(LOG E/E_D)*
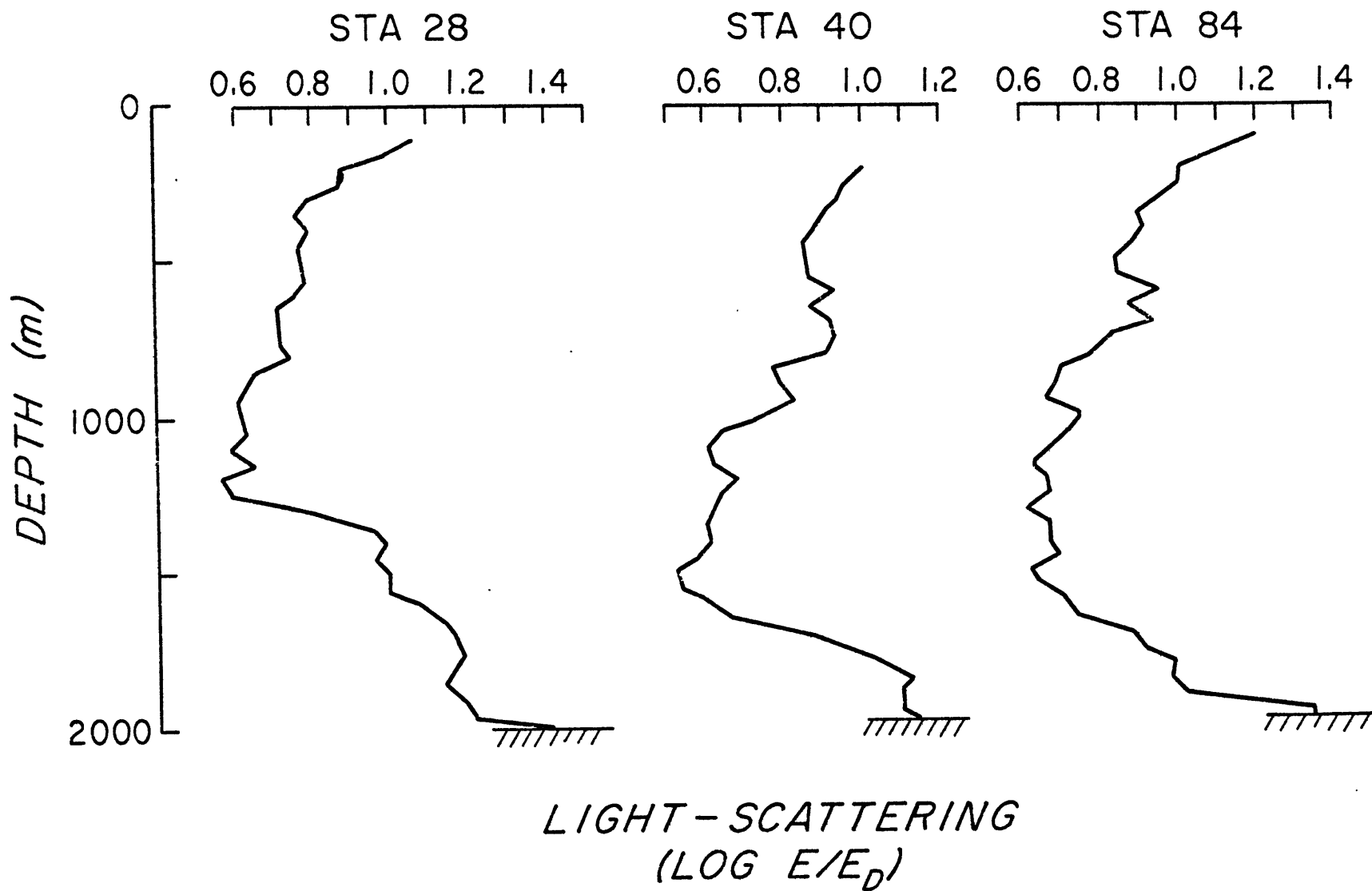
Figure 3.9   Cross-sections of light-scattering for the northern
              and southern lines on the Iceland Rise. Vertical
              lines indicate station control. Light-scattering
              readings were made at 25 m intervals.

LIGHT SCATTERING (LOG E/E$_D$)
ICELAND RISE
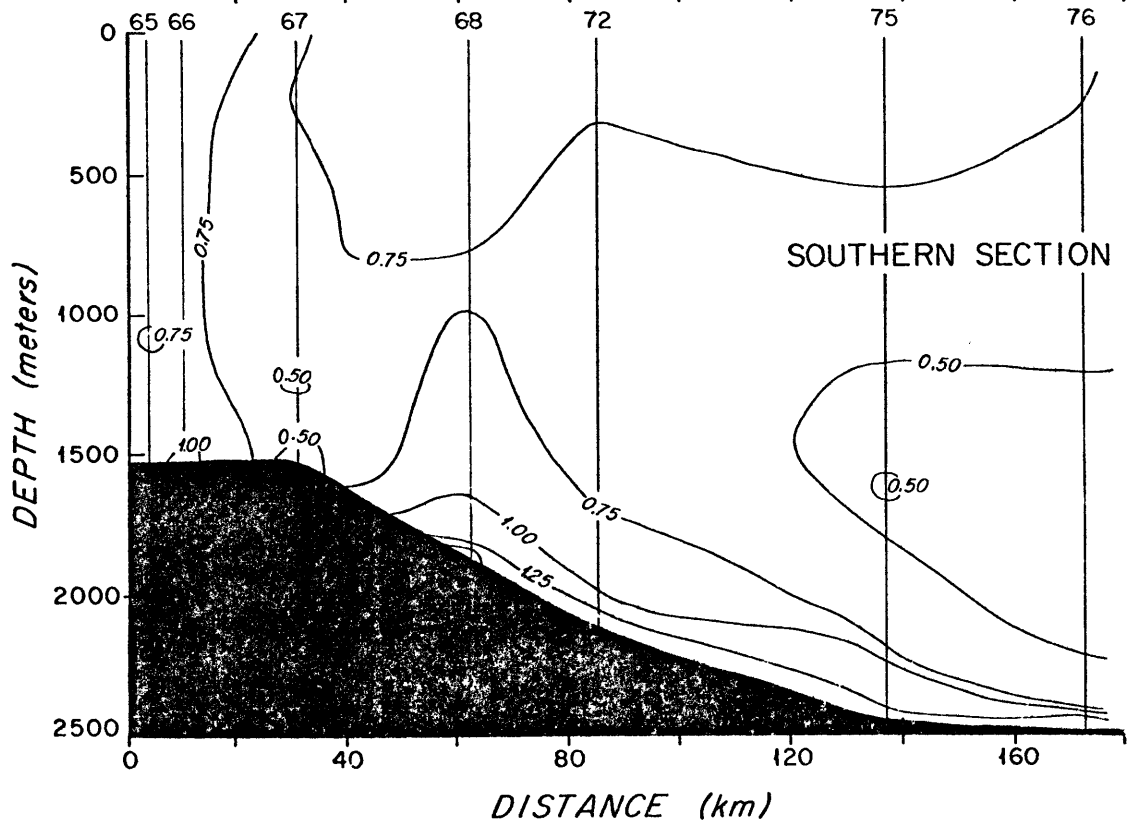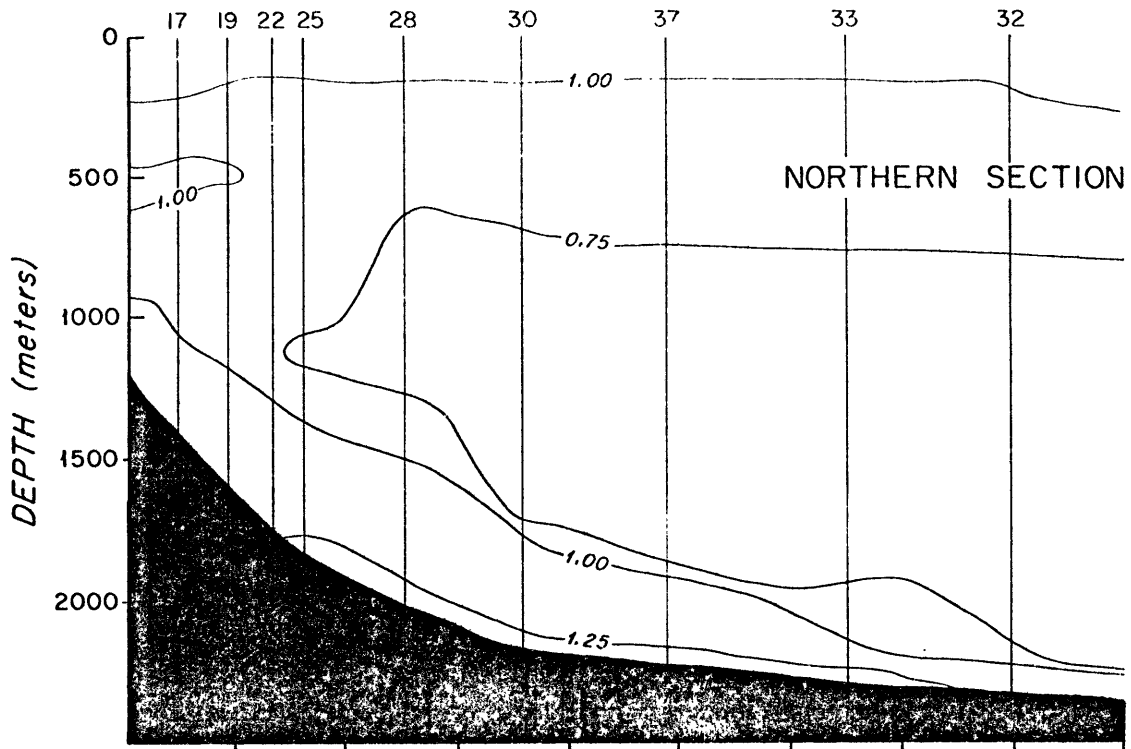
SIZE DISTRIBUTION ANALYSES

SPM size distributions have been examined throughout the oceans, but primarily in the surface waters (Sheldon et al., 1972). The presence and patchiness of biological components in the surface waters dramatically affects the size distributions of SPM. For this reason, both latitudinal and seasonal variations have been noted (Sheldon et al., 1972). Below the surface waters (upper few hundred meters) the particle size distributions change. Distributions in surface waters are often characterized by a predominant modal size, whereas in deep water the particle size spectrum is one of approximately equal amounts of material in logarithmically increasing size grades (Sheldon et al., 1972), at least up to the 100 μm size studied.

Particle size distributions are most often displayed in terms of number, volume, or weight of particles per logarithmic size grade. Since this work deals with volume or weight concentrations rather than numbers of particles, all of the data will be displayed in terms of volumetric measurements.

Iceland Rise

Water samples were obtained from above and within the near-bottom nepheloid layer in order to compare characteristics of the SPM. Two stations (25 and 39) are used here as examples to demonstrate the differences in the percent volume size distributions between clear water and the nepheloid layer. Station 25 is located

along the northern section in the Iceland Rise region at 1804 m, in

the axis of the bottom current. A nephelometer profile obtained at

the same site (Figure 3.7) was compared with SPM concentrations from

the water bottles to verify which bottles were within the nepheloid

layer. The size distribution from bottle 1 at 1780 m, within the

nepheloid layer, shows a distribution with low variance (Figure

3.10). The modal size is an equivalent spherical diameter of

5.6 μm. The shape of this distribution stands in marked contrast to

the more typical deep-water profile of equal volumes of material in

the size grades from 1-20 μm (Sheldon et al., 1972). This more

typical distribution, with high variance, is seen in bottle 4

(790 m), in clear water at the same station (Figure 3.10).

Similar features are seen at Station 39 at 2163 m, farther down

the ridge flank (Figure 3.11). The nephelometer profile for this

station (Figure 3.7) shows a sharply defined nepheloid layer. From

this profile, two bottles, B1 and B5, were selected for comparison

of particle size distributions. Bottle B5 at 2145 m shows a low

variance distribution as does the nepheloid-layer sample at Station

25, but the modal size of this distribution is larger (∿9 μm).

Bottle B1, at 1205 m, has an irregular, high variance distribution,

as does the clear-water sample from Station 25.

Western North Atlantic

Size distributions were also compared for clear- and nepheloid-

layer waters in the western North Atlantic. In this region,

Figure 3.10   Coulter counter volumetric size histograms from
               station 25 in the Iceland rise region. See Figure 3.7
               for the location of the clear-water and nepheloid-
               layer samples with respect to the light-scattering
               profile. Note the lower variance of the nepheloid-
               layer sample.

STATION 25
1804m

790 m

CLEAR WATER

1780 m

NEPHELOID LAYER

% TOTAL VOLUME

DIAMETER (μm)
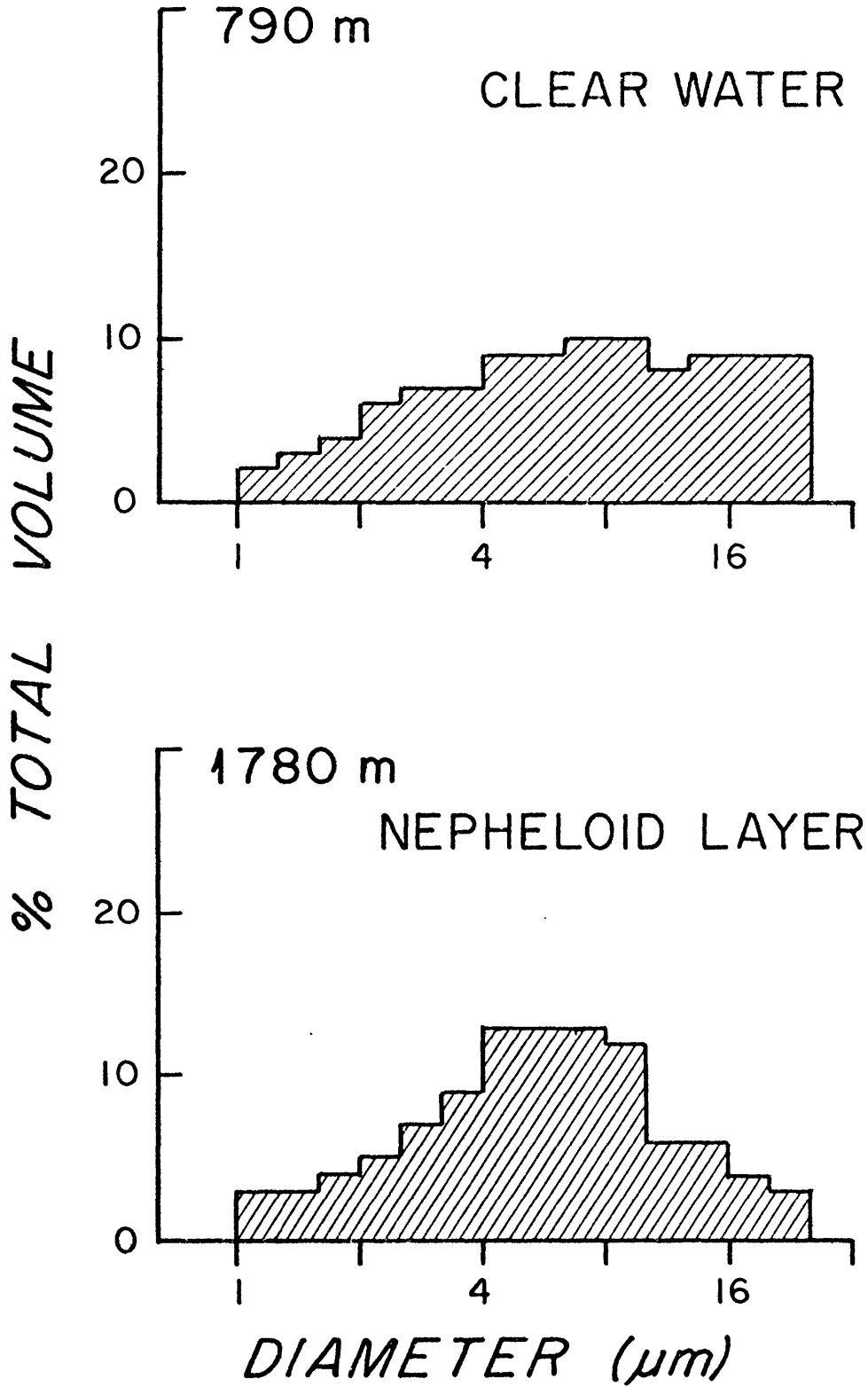
Figure 3.11   Coulter counter volumetric size histograms from station
39 in the Iceland Rise region. See Figure 3.7 for the
location of the clear-water and nepheloid-layer
samples with respect to the light-scattering profile.
Note the lower variance of the nepheloid-layer sample.

STATION 39
2163m

DIAMETER (μm)
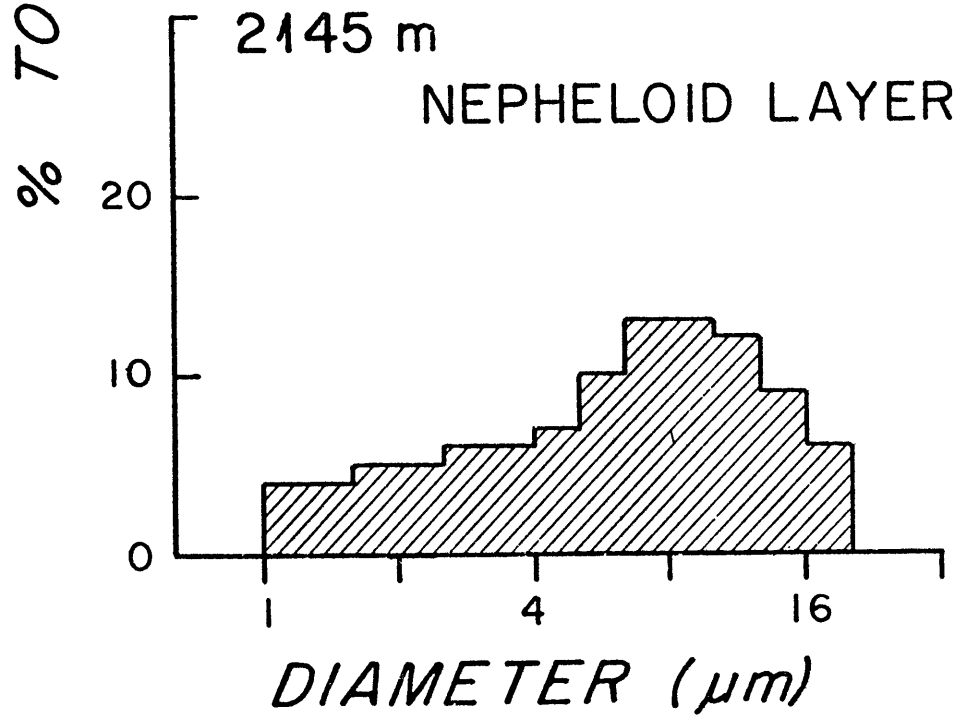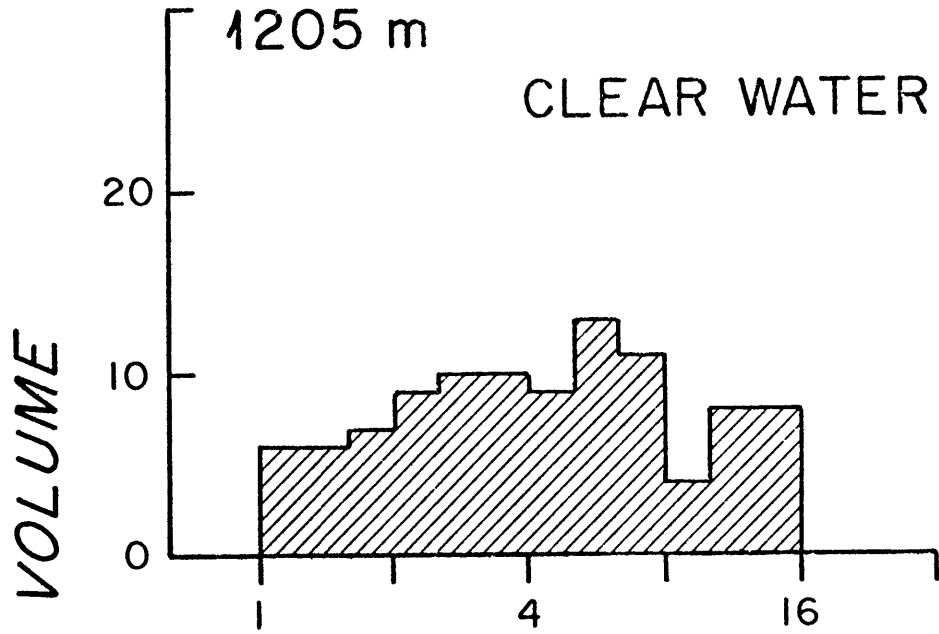
nephelometer profiles were not available at the hydrographic stations, so the nepheloid layer was judged to begin at the sharp increase in concentration in the near-bottom waters. The general results of the comparison made between clear-water and nepheloid-layer samples are similar to those from the Iceland Rise. The nepheloid-layer samples (e.g., OC6, 718, bottle 1, 4462 m) have low variance distributions with the modal size at 3 μm, whereas clear-water sample distributions have higher variance (Figure 3.12).

Both standardly drawn samples and "dregs" samples were counted with the Coulter counter for nepheloid-layer samples. The nepheloid-layer "dregs" samples exhibit the low variance type distribution even more strongly than do the standard nepheloid-layer samples (Figure 3.12).

COMPOSITION OF SPM

Particles on SEM photomicrographs were counted in this study to determine the difference in composition between the clear-water material and the nepheloid-layer material.

Iceland Rise

Five stations were selected for compositional analysis in the Iceland Rise region (25, 31, 39, 67, and 76; see Figure 2.2) as being representative of the various hydrographic conditions. Station 25 is in the axis of the bottom current; Station 39 is off-axis along the same transect. Stations 31 and 76 are in the

Figure 3.12   Coulter counter volumetric size histograms from
station 718 in the western North Atlantic. Samples
are from clear water, the nepheloid layer and the
"dregs" water from a nepheloid layer sample. Note the
lower variance of the nepheloid-layer standard and
"dregs" samples.

STATION 718
4485 m

1453 m
CLEAR WATER

4462 m
NEPHELOID LAYER

4462 m
NEPHELOID LAYER
"DREGS"

% TOTAL VOLUME

DIAMETER (μm)
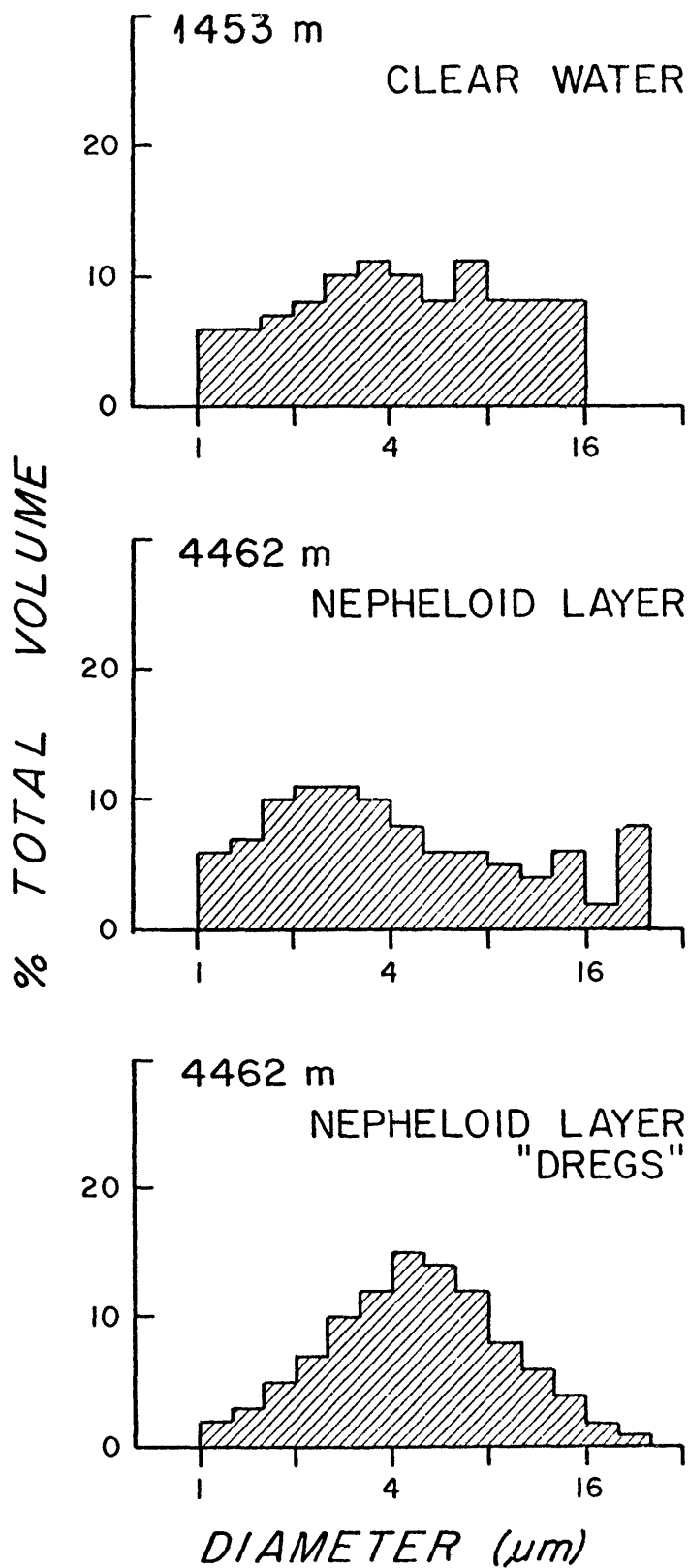
interior of the basin, at the ends of the northern and southern
lines, respectively. Station 67 is located on the nose of the West
Katla Ridge and exhibits no nepheloid layer. Instead, concentra-
tions vary erratically with an overall general decrease with depth.
Two samples were taken from each station, one in clear water at
mid-depths and one in the nepheloid layer or within fifty meters of
the seafloor.

The results of the particle counts for these stations are given
in Figure 3.13 and Table 3.1. These compositional studies (Plate
3.2) show that by number, small coccoliths are the largest component
of the samples (up to 62%). Pennate diatoms, mineral matter, and
clays follow in order as the next largest fractions of the sample.
These are also the components which show major differences between
clear-water and nepheloid-layer samples. Nepheloid-layer samples
have fewer small coccoliths and more pennate diatoms, clays, and
mineral matter than do clear-water samples (Figure 3.13). These
same differences are observed whether or not particles from the
"dregs" water are included. In comparison to the standard,
above-spigot samples, "dregs" samples have fewer small coccoliths,
less organic matter and mineral matter, and more large coccoliths,
centric diatoms, and pennate diatoms. The smaller percentage of
mineral matter in the "dregs" samples is difficult to understand.
One would expect that the larger and denser particles would settle
to the bottom of the bottle. A differentiation is seen for the
biogenic particles, but does not hold for the mineral matter.

—87—

Figure 3.13   Compositional variability of suspended particulate
matter from the Iceland Rise. Counts were made of the
different components from scanning electron microscope
photomicrographs and normalized to total number of
particles counted. Identifiable fragments were
included in the counts. Greatest differences between
clear-water and nepheloid-layer samples are in small
coccoliths, pennate diatoms, and mineral matter.

COMPOSITIONAL VARIABILITY OF SUSPENDED PARTICULATE MATTER
ICELAND RISE

TABLE 3.1

PERCENTAGE OF SPM BY PARTICLE TYPE FROM THE ICELAND RISE
AND WESTERN NORTH ATLANTIC

Station -Bottle	Small Coccoliths	Large Coccoliths	Centric Diatoms	Pennate Diatoms	Dino-Flagellates	Organic Matter	Plankton Fragments	Fecal Pellets	Aggregates	Clays	Mineral Matter	Unidentified Particles	Total Counted
25-4	51	1	5	11	1	2	1	0	3	4	11	12	928
25-4 dregs	39	3	8	21	0	2	2	0	4	4	5	11	163
25-4 total	49	1	5	13	1	2	1	0	3	4	10	11	1091
*25-1	46	5	5	11	1	3	1	1	4	5	12	9	1342
*25-1 dregs	31	11	6	22	1	1	1	1	4	7	6	11	303
*25-1 total	44	6	5	13	1	2	1	1	4	6	11	9	1645
39-B1	55	3	1	7	0	4	2	0	3	6	4	15	473
39-B1 dregs	21	21	8	16	0	1	0	2	2	5	3	21	96
39-B1 total	49	6	2	8	0	3	1	1	3	6	4	16	569
*39-B5	47	2	4	11	1	2	2	0	4	8	10	9	891
*39-B5 dregs	29	9	6	24	0	0	1	0	5	8	7	13	272
*39-B5 total	43	4	4	14	1	2	2	0	5	8	9	10	1163
32-4	62	3	4	2	1	2	1	0	2	3	7	14	377
*32-1	41	5	2	24	2	2	1	0	1	7	7	8	1101
67-B6	51	2	2	9	1	4	1	0	4	6	7	15	509
67-B1	51	3	3	4	0	3	1	0	4	7	11	13	503
76-B6	51	8	3	4	0	2	1	0	2	4	9	16	451
*76-B1	52	7	4	4	0	2	2	0	2	6	10	10	978
718-10	49	3	11	5	0	2	0	0	5	4	3	17	253
718-4	6	4	12	3	0	1	0	0	9	17	26	23	197
734-11	50	2	7	1	0	4	1	0	5	5	9	16	152
734-5	34	5	4	2	0	1	0	0	6	11	25	14	304

*Nepheloid layer samples

-89-

Plate 3.2   SEM photomicrographs of suspended particulate matter
            from clear water and the nepheloid layer from the
            Iceland Rise. 1a and 2a are clear-water samples; 1b
            and 2b are from the nepheloid layer. Sample 1 is from
            Station 25, and sample 2, from Station 76. Sample 3
            is from Station 67, which has no nepheloid layer. 3a
            is from mid-water; 3b, from the near-bottom water.
            See text for interpretation of these samples.
            X 1200.
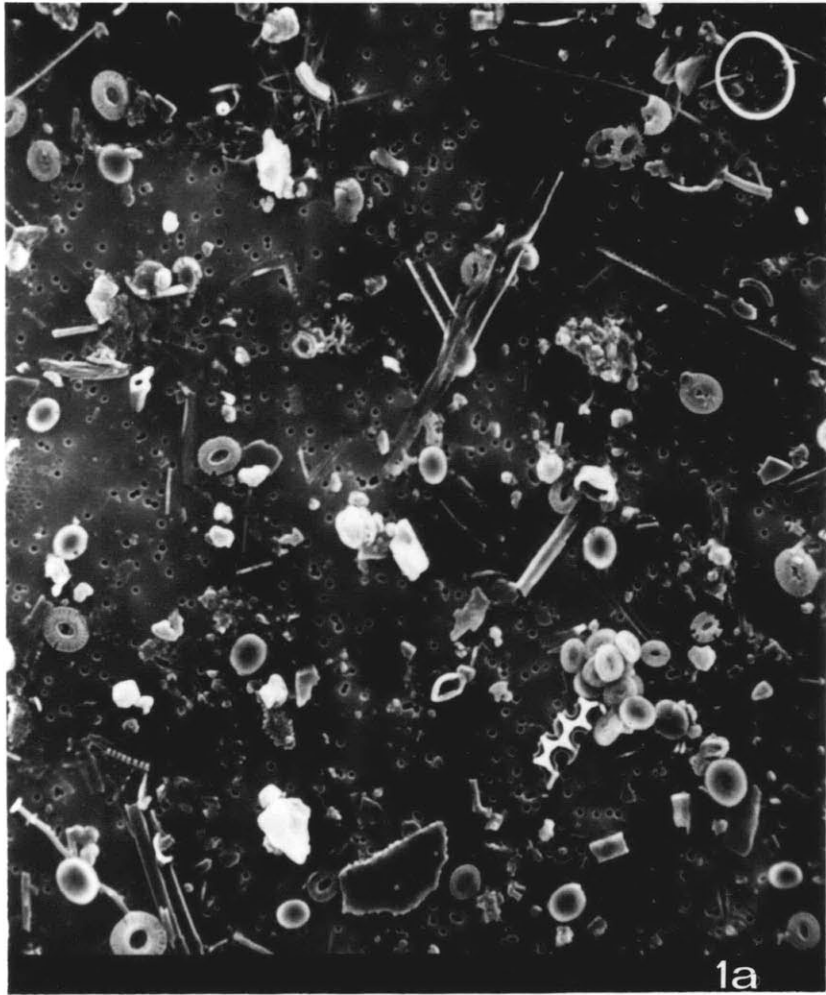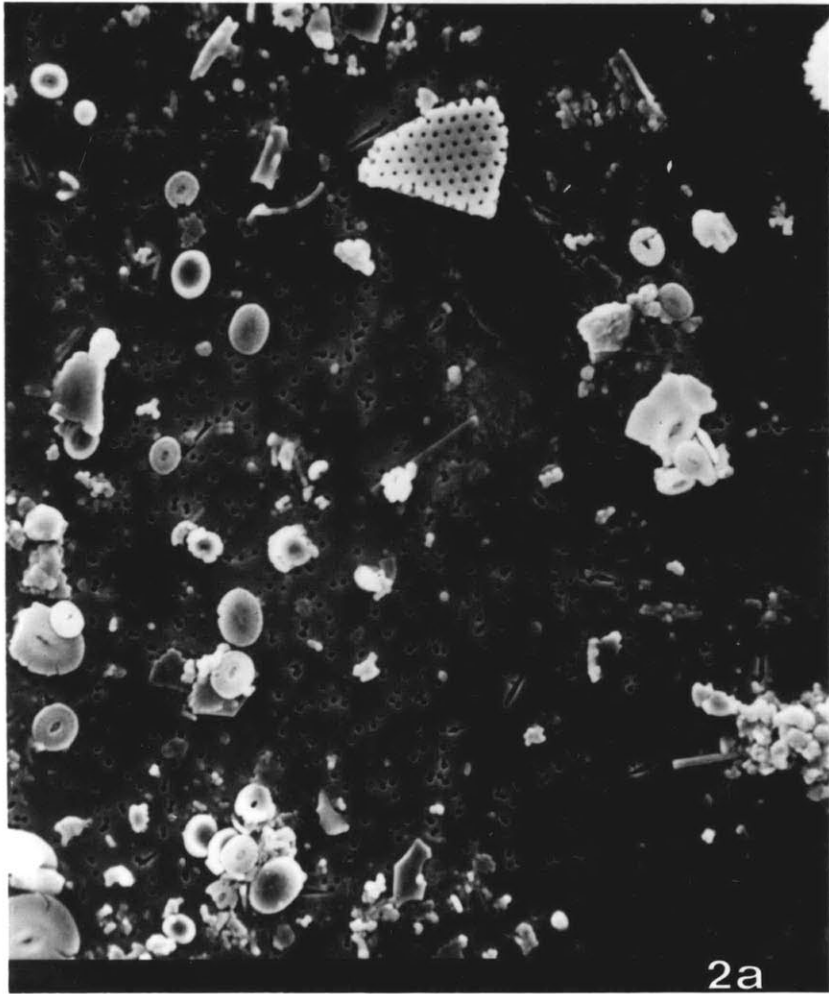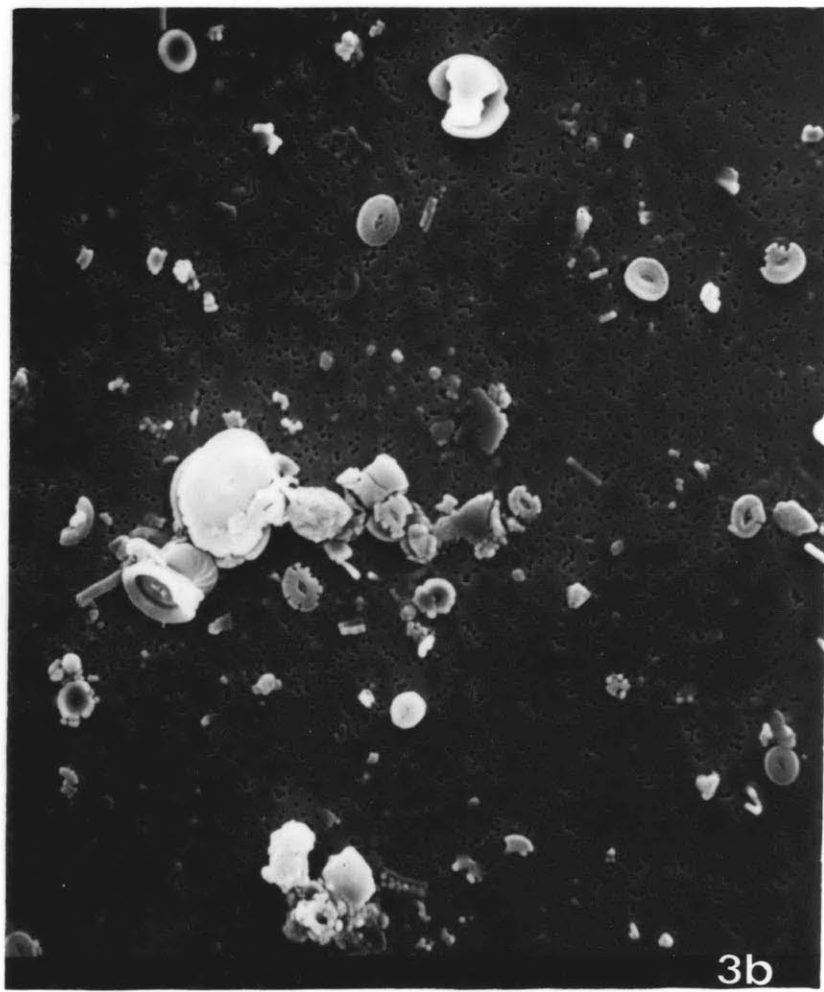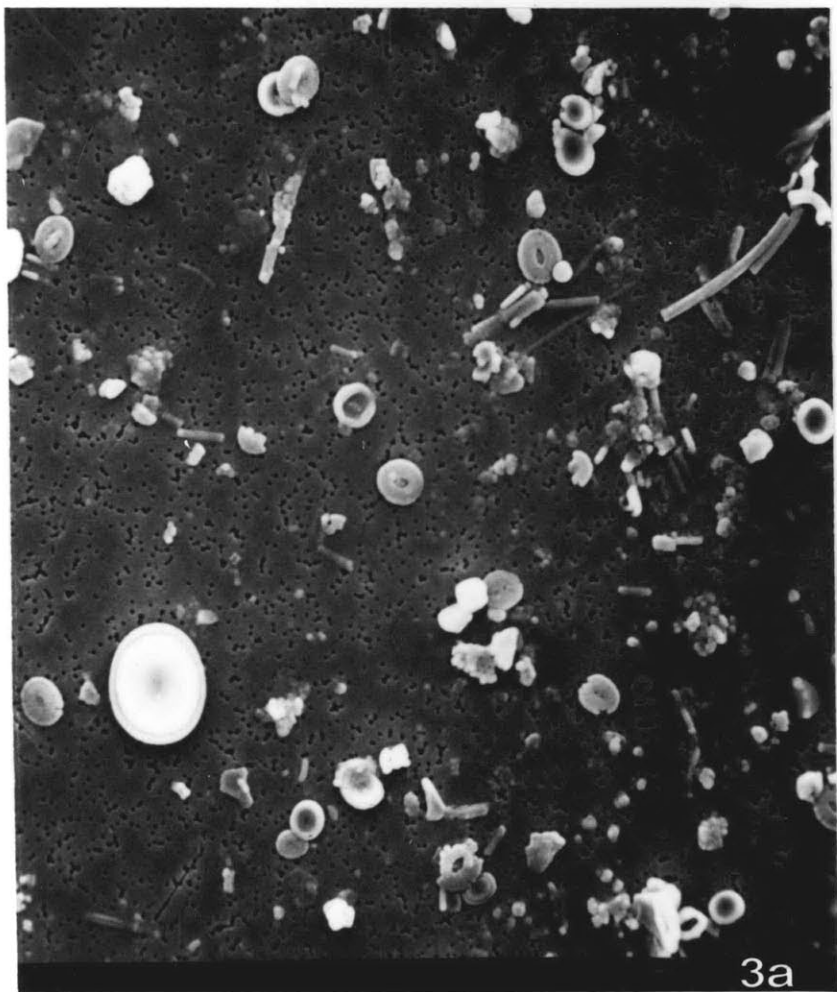
Perhaps the mineral matter is contained in organic aggregates of low density. The results of the chi-square analysis (statistics after Crow et al., 1960) on the compositional data summarized in Table 3.2 indicate that at the 95% confidence level, the random photomicrographs of the filters are representative subsamples of a homogeneous population of material. This result allows summing the counts from many photomicrographs to make additional comparisons. The second chi-square test performed was to determine whether clear-water and nepheloid-layer samples from individual stations are statistically different. This was found to be true at the 95% confidence level. The differences observed were outlined above. Another chi-square test was performed to determine whether the clear-water samples from all stations were statistically different from each other, and whether the nepheloid-layer samples from all stations were statistically different from each other. This hypothesis was also found to be true at the 95% confidence level. The variability between stations is perhaps related to proximity to Iceland. The two stations in the basin generally have less mineral matter and fewer clays and aggregates than the stations along the flanks. For mineral matter, this is true only for the nepheloid-layer samples, indicating that the variability may also be caused by resuspension of mineral matter by the bottom current into the nepheloid layer for the stations along the flanks.

TABLE 3.2

CHI-Square Analysis of Compositional Data from the Iceland Rise
and Western North Atlantic

Station -Bottle	Clear – C Nepheloid – N	Degrees of Freedom	Calculated CHI-Square	95% Confidence Interval
TESTS FOR HOMOGENEITY OF FILTER SAMPLES				
25-4	C	27	35.16	40.11
25-1	N	27	39.83	40.11
39-B1	C	27	25.83	40.11
39-B5	N	27	23.98	40.11
32-4	C	27	31.95	40.11
32-1	N	30	28.93	43.77
67-B6	C	27	19.29	40.11
67-B1	C	27	41.30*	40.11
76-B6	C	24	25.50	36.42
76-B1	N	30	14.15	43.77
TESTS FOR STANDARD VERSUS DREGS SAMPLES				
25-4	C	10	32.70*	18.31
25-1	N	11	70.03*	19.68
39-1	C	10	103.12*	18.31
39-5	N	10	73.96*	18.31
TESTS FOR CLEAR WATER VERSUS NEPHELOID LAYER SAMPLES				
25	C/N	11	38.62*	19.68
39	C/N	10	50.16*	18.31
32	C/N	10	131.90*	18.31
67	C/C	9	16.52	16.92
76	C/N	10	24.07*	18.31
SAME INCLUDING DREGS				
25	C/N	11	48.34*	19.68
39	C/N	10	64.36*	19.68
718	C/N	8	37.46*	15.51
734	C/N	8	145.50*	15.51
TESTS FOR ALL CLEAR WATER SAMPLES				
all clear	C	45	197.28*	61.63
TEST FOR ALL NEPHELOID LAYER SAMPLES				
all nepheloid	N	33	326.15*	45.69

* Significant at 95% confidence interval

Western North Atlantic

Compositional identification and quantification of particles for two stations in the western North Atlantic were performed in a similar fashion to that for the Iceland Rise samples. The dominant components of these samples are small coccoliths, clays, and mineral matter (Figure 3.14, Table 3.1). The variations seen between clear-water and nepheloid-layer samples are also most pronounced for these components. The percentage of small coccoliths drops sharply from clear-water to nepheloid-layer samples, whereas the percentages of clay and mineral matter rise dramatically (Figure 3.14).

A chi-square test to examine the similarity of the clear-water and nepheloid-layer samples verifies that these samples are statistically different at the 95% confidence level (Table 3.2).

DISCUSSION

CORRELATION OF LIGHT-SCATTERING MEASUREMENTS WITH SPM CONCENTRATIONS

A correlation of light-scattering measurements with concentrations of SPM has been used for several years to calibrate L-DGO nephelometer profiles in quantitative terms (Biscaye and Eittreim, 1974; 1977). As part of this study, a relationship was sought between light-scattering observations and SPM concentrations (uncorrected for "dregs" particles) for clear-water samples, nepheloid-layer samples, and the entire water column. Uncorrected

Figure 3.14   Compositional variability of suspended particulate
matter from the western North Atlantic. Note the
pronounced differences in percentages of small
coccoliths, clays and mineral matter between clear
water and the nepheloid layer.

COMPOSITIONAL VARIABILITY OF SUSPENDED PARTICULATE MATTER
WESTERN NORTH ATLANTIC
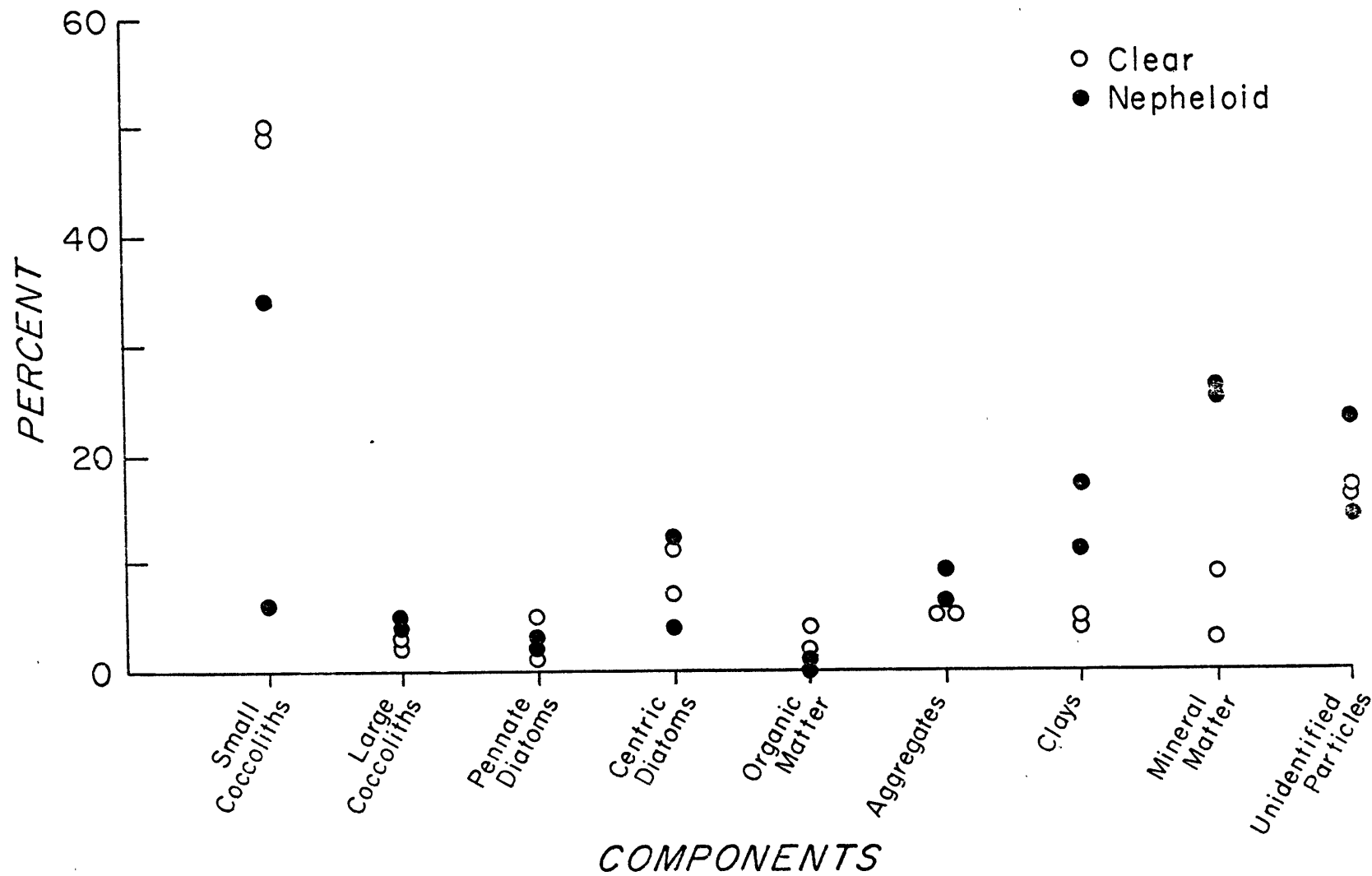
concentrations were used so that a comparison of the relationships given by Biscaye and Eittreim (1974; 1977) to those obtained south of Iceland could be made (Table 3.3).

There are two important comparisons to be made with these regression correlations: first, the comparison between clear-water and nepheloid-layer samples in the Iceland Rise area, and second, the regional comparison between the Biscaye and Eittreim curves and the combined Iceland Rise data.

Analysis of the regression lines for clear-water and nepheloid-layer data shows a statistically significant difference in these two curves at the 95% confidence level (Figure 3.15). This can be interpreted in two ways: either the nephelometer responds differently to the particles in the nepheloid layer versus those in clear water, or the relationship between light scattering and SPM concentration is nonlinear for the full range measured. Theory suggests nephelometers are responsive to particle characteristics other than concentration, such as size and composition from differences in index of refraction (Jerlov, 1968). It has been shown here that the size and composition of suspended material differs between clear-water and nepheloid-layer samples in the Iceland Rise region. Both of these factors are likely to influence the response of the nephelometer; however, it is not yet possible to determine the magnitude of their influence.

The considerable scatter about the regression lines for the Iceland Rise data may originate from numerous sources of error.

Table 3.3

LEAST SQUARE REGRESSION EQUATIONS FOR LIGHT SCATTERING
VERSUS CONCENTRATION CORRELATIONS

BBOR-HAP
from Biscaye and Eittreim (1974)

$\log Y = 1.19 \log X + 0.13$ $(r = 0.91)$

LCR
from Biscaye and Eittreim (1977)

$\log Y = 1.0 \log X + 0.50$ $(r = 0.84)$

Clear water
this study

$\log Y = 0.63 \log X + 0.94$ $(r = 0.62)$
$S_b = 0.106$

Nepheloid layer
this study

$\log Y = 0.36 \log X + 1.35$ $(r = 0.52)$
$S_b = 0.055$

All data
this study

$\log Y = 0.65 \log X + 0.98$ $(r = 0.76)$

Y = concentration ($\mu g/l$)
X = light-scattering (E/E_D)
r = correlation coefficient
S_b = standard error of the regression coefficient, b

test for similarity between clear water and nepheloid layer lines

$$t = \frac{b_1 - b_2}{S_{b_1-b_2}} = \frac{0.63 - 0.36}{0.0124} = 21.77$$

Reject the hypothesis at the 5% significance level that the two
regression lines are the same

statistics after (Crow et al., 1960)

Figure 3.15   Correlation of light scattering and standard concen-
               tration for the Iceland Rise area. The dashed line is
               the regression line for the clear-water samples. The
               inner pair of dashed curves are the 95% confidence
               limits for clear-water concentration values. The
               outer pair represent the 95% prediction interval for
               this regression. The solid line is the regression
               line for the nepheloid-layer samples. The solid
               curves are the same as for the clear-water samples.
               The regression lines for clear water and the nepheloid
               layer, are statistically different at the 95%
               confidence level. The dotted lines are the
               regressions for the BBOR-HAP and LCR of Biscaye and
               Eittreim (1974; 1977).
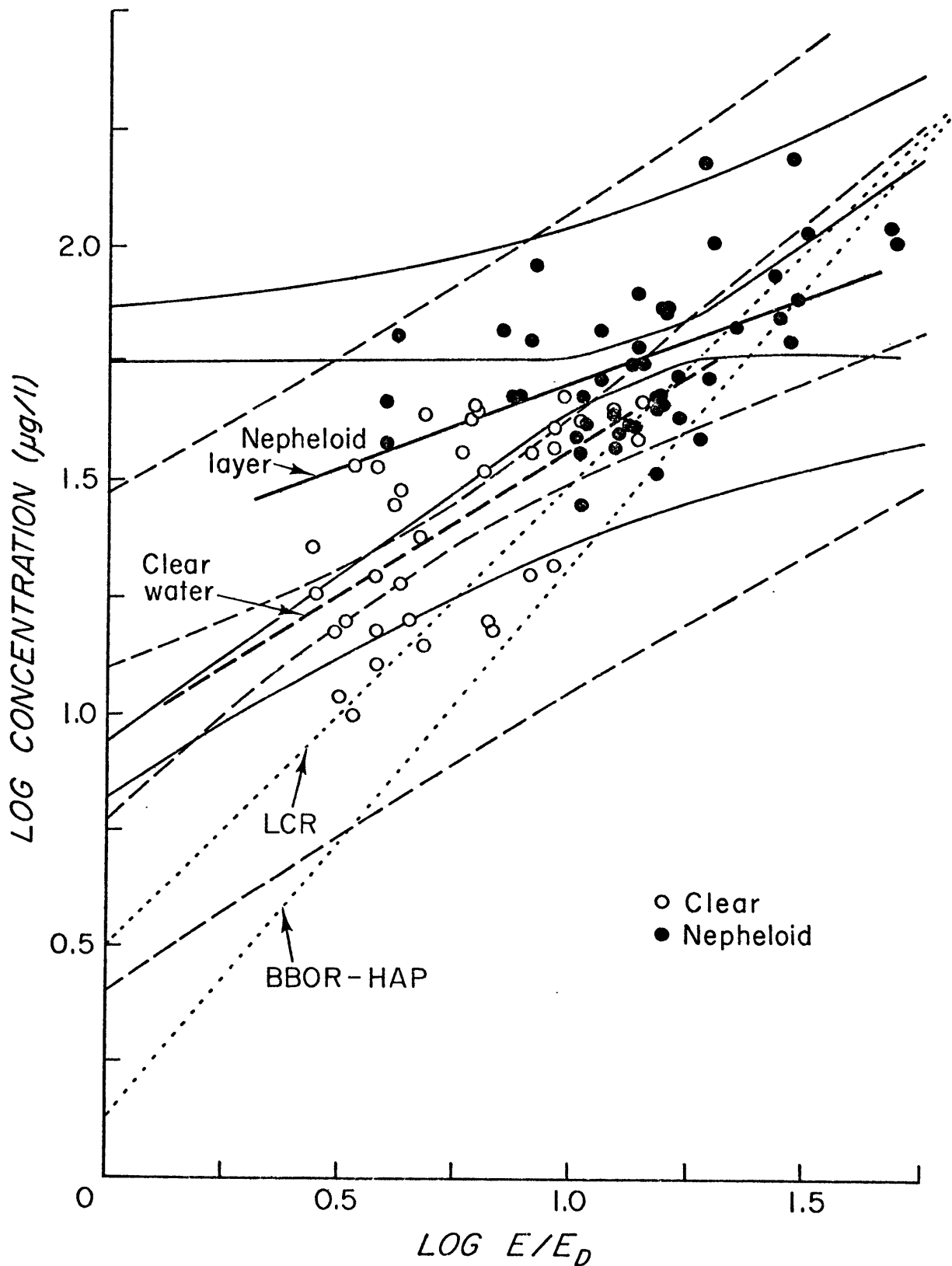
There is analytical error in the concentration measurements
(outlined earlier), error in the light-scattering determinations,
and error in relating the depth of the nephelometer measurements to
the depth of the bottle samples. Perhaps larger than any of these
is the basic difference in the volume of water being examined by
each method. The SPM concentration data are obtained with 5 or 30
liter Niskin bottles, which sample over a vertical scale of one-half
to one meter. The nephelometer, on the other hand, measures light
scattering that is integrated over a vertical distance of 25
meters. In a region of active currents like the Iceland Rise,
temporal variability over a half hour and patchiness in the
concentration of particles in near-bottom water are likely and could
cause differences between the point values of the Niskin bottles and
the integrated values measured by the nephelometer.

Although the Biscaye and Eittreim curves (Figure 3.16) yield
good first-order approximations of SPM concentration, their
calibration curves differ from those of this data set. Calibrations
apparently differ regionally. The data south of Iceland produce a
curve with a gentler slope and a larger intercept than those
obtained by Biscaye and Eittreim (1974; 1977). This reflects
smaller changes in concentration for the same increase in light
scattering when compared with their study. The difference in the
intercepts of these curves indicates that in the BBOR-HAP and LCR
regions, less material is needed for detection of measurable
scattering than south of Iceland. This may be due to a nonlinear

Figure 3.16   Correlation of light scattering and standard
               concentration for the BBOR-HAP, from Biscaye and
               Eittreim (1974). The BBOR-HAP line is the
               least-squares regression line through the data shown.
               Also shown are the regression lines for the LCR from
               Biscaye and Eittreim (1977), and that for the entire
               Iceland Rise data set.
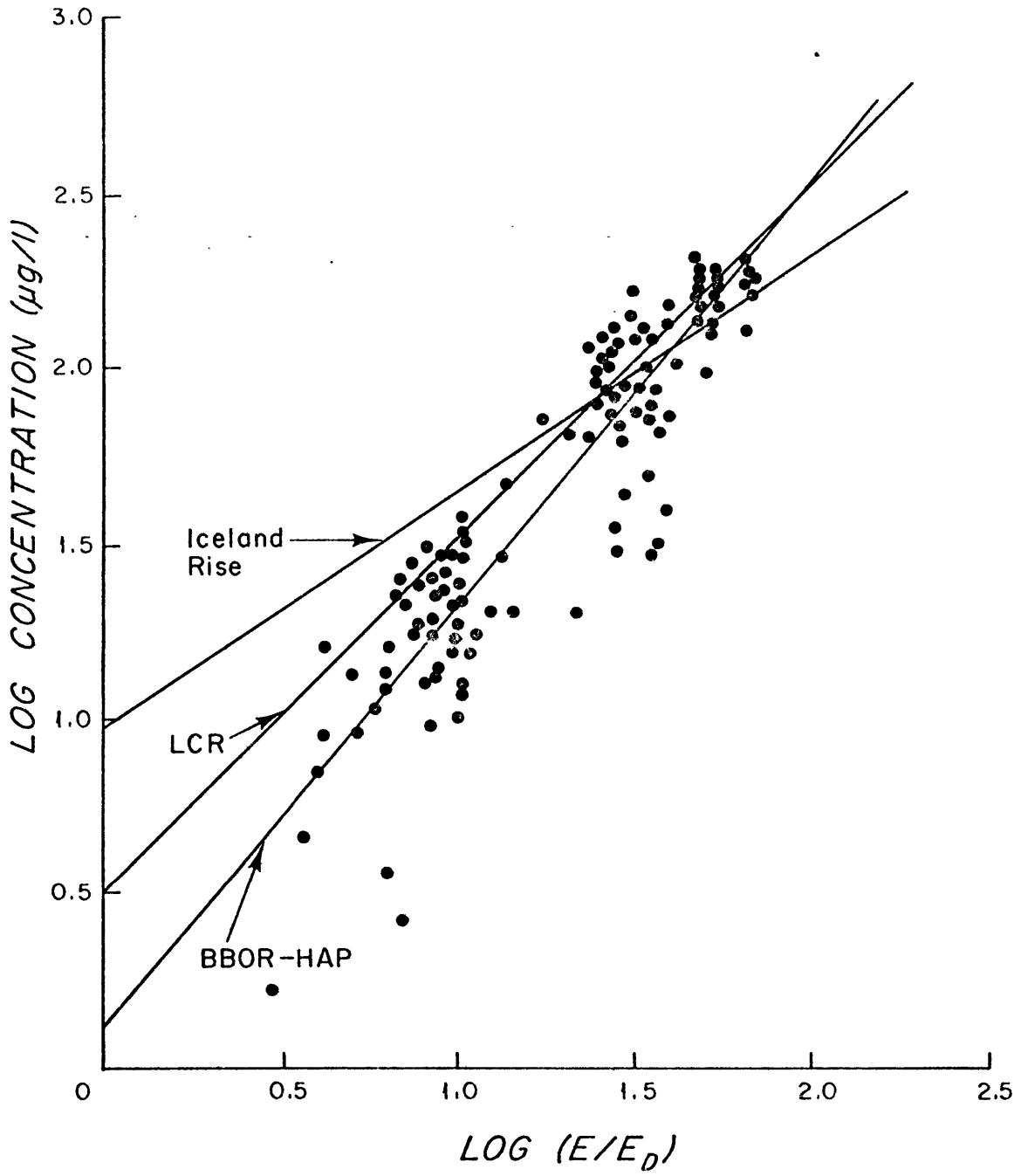
response of the nephelometer, or to a difference in the nature of SPM in the two regions. A comparison of the SPM off Iceland to that along the continental rise off New York indicates that more clays and mineral matter occur at the latter location.

Most light-scattering values observed in these studies fall in the range 0.5 to 1.5 log E/E_D. Over this range of light-scattering values, the differences in prediction of the SPM concentration from the different regression lines vary by a factor of 3.4 for low values of light scattering and by a factor of 1.3 for high values. This appears to indicate significant differences in prediction from the curves. However, the 95% prediction limits for the Iceland Rise data span at least this much variability (Figure 3.15). Information for these limits for the Biscaye and Eittreim curves is not available. Therefore, although there are regionally significant differences in the response of the nephelometer to SPM, used as a predictive tool, the particular correlation employed is unimportant, since the prediction limits are so large.

SIZE DISTRIBUTION VARIATIONS

Particle size distributions were analyzed from clear water and the nepheloid layer from south of Iceland and compared to those from the western North Atlantic to determine whether variation in the size spectra were site specific.

Volumetric Histograms

Histograms of normalized particle volume versus equivalent spherical diameter depict the variations in the distributions between clear water and the nepheloid layer (Figures 3.10, 3.11, 3.12). The clear-water distributions in both regions have relatively constant volumes of material in logarithmically increasing size grades, from 1-20 μm, i.e., distributions with high variance. In contrast, the particles in the nepheloid layer generally have low variance distributions. These variations in particle size distributions between clear water and the nepheloid layer are noted in both areas, and may be due to either differences in the state of aggregation or the composition of the suspended material. Filters of SPM were examined to determine which alternative was more likely.

The percentage of aggregates does not change substantially between clear water and the nepheloid layer for either region. Composition of the SPM does change. Both regions show an increase in relative proportion and total concentration of the clays and mineral matter in the nepheloid layer in comparison to clear water.

The variations in particle size distributions between clear water and the nepheloid layer occur wherever a nepheloid layer is present. In the few stations where nepheloid layers are absent, the size distributions retain a clear-water characteristic, high variance, even near the seafloor (Figure 3.17). This suggests that nepheloid layers are areas of introduction into the water column of material with a given, (site-specific) predominant modal size. With

-108-

Figure 3.17   Coulter-counter volumetric size histograms from station
67 in the Iceland Rise region. See Figure 3.7 for the
location of the mid-water and deep-water samples with
respect to the light-scattering profile. Station 67
does not show a well-defined nepheloid layer.

STATION 67
1522 m

700 m

CLEAR WATER

1479 m

NEPHELOID LAYER

% TOTAL VOLUME

DIAMETER (µm)
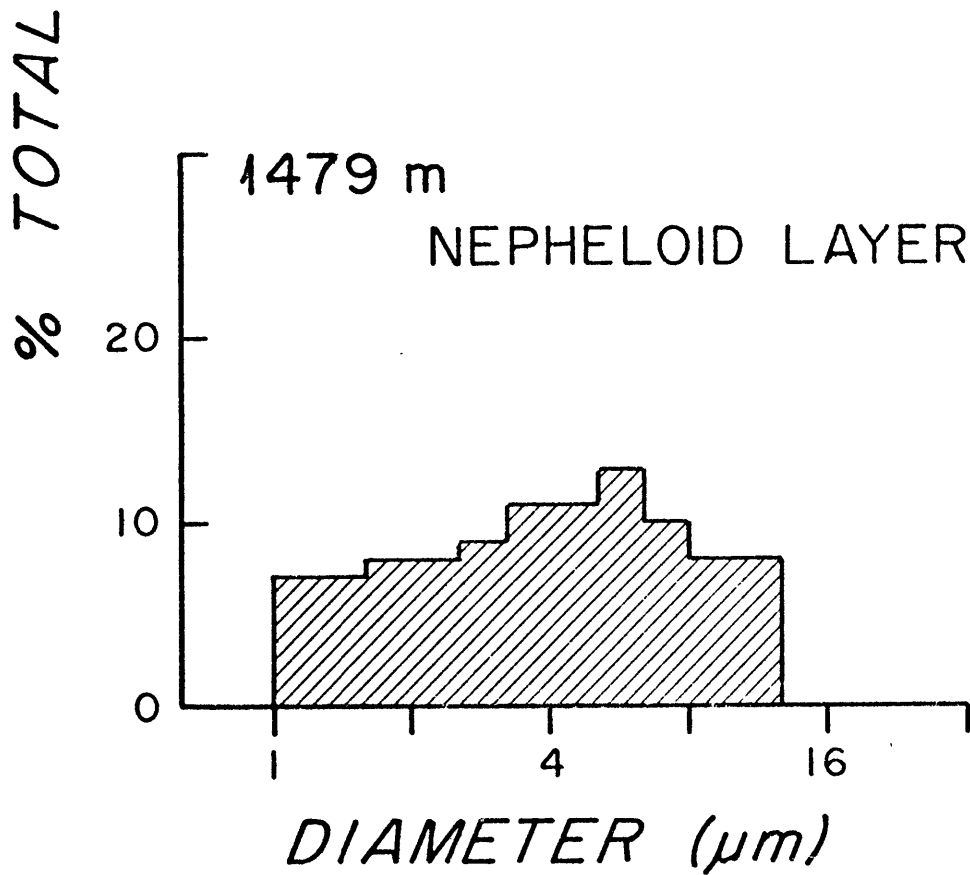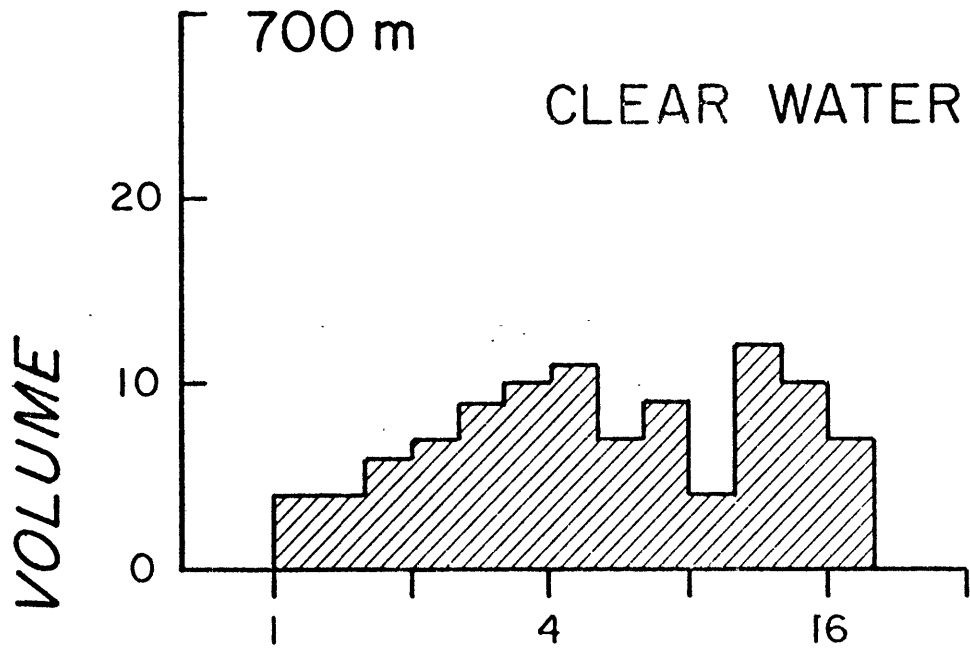
an increasing quantity of resuspended material, a distribution of lower variance with a more well-defined mode develops.

Differential Volume Distributions

Data on marine particle-size distributions are usually expressed as the slope of the cumulative number distribution (Bader, 1970; Carder et al.; 1971, Brun-Cottan, 1971; Sheldon et al., 1972; McCave, 1975; Brun-Cottan, 1976). A slope of minus three is indicative of a distribution with equal volumes of material in logarithmically increasing size grades, the type described here for clear-water samples. In this study of concentration, size, composition, and density, most of which are related to weight or volume of material, the parameters mass and volume are more useful than number. For this reason, the normalized differential volume of particles is used in interpretation rather than the cumulative number distribution. For comparison with other studies, a slope of minus one for a normalized differential volume distribution is equivalent to a slope of minus three for a cumulative number distribution (Figure 3.18).

Slopes from the normalized differential volume distributions were plotted versus depth for all stations from the Iceland Rise region (Figure 3.19). Nepheloid-layer and clear-water points were distinguished to determine trends within these subgroups. It is seen from the plot that the data have too much scatter to reveal any depth-dependent or clear-water versus nepheloid-layer distinctions.

Figure 3.18   Particle size distributions and associated
               parameters. Graph 1a represents a particle size
               distribution with equal volumes of material in
               logarithmically increasing size grades. Graph 1b
               shows the associated differential and cumulative
               number distributions. Graph 1c shows the associated
               volume distribution normalized by the size grade
               interval. Graph 2a illustrates an idealized
               nepheloid-layer, volumetric distribution of lower
               variance. Graph 2b, similar to 1b, demonstrates the
               variability of slope through the distribution, but
               overall having slopes very similar to those in 1b.
               Graph 2c, similar type to 1c, shows both positive and
               negative slopes through the distribution, with the
               overall slope similar to 1c.

1a

% TOTAL VOLUME

20

10

0

1   4   16

1b

NUMBER

512

128

32

Cumulative slope ~ -3.0

Differential slope = -3.0

1   4   16

1c

VOLUME / SIZE INTERVAL

235

59

15

Slope = -1.0

1   4   16

DIAMETER (µm)

2a

% TOTAL VOLUME

20

10

0

1   4   16

DIAMETER (µm)

2b

NUMBER

1000

100

10

Slope ~ -2.5

Slope ~ -2.0

Differential overall slope = -3.0

Cumulative overall slope = -3.6

Slope ~ -4.0

Slope ~ -4.25

1   4   16

DIAMETER (µm)

2c

VOLUME / SIZE INTERVAL

10,000

1000

100

Overall slope = -1.0

1   4   16

DIAMETER (µm)

-112-

Figure 3.19   Scatter plot of the slopes of the curves of the
               normalized differential particle volume versus
               particle diameter, with depth for the Iceland Rise
               region. Slopes of two idealized distributions are
               shown in Figure 3.18.
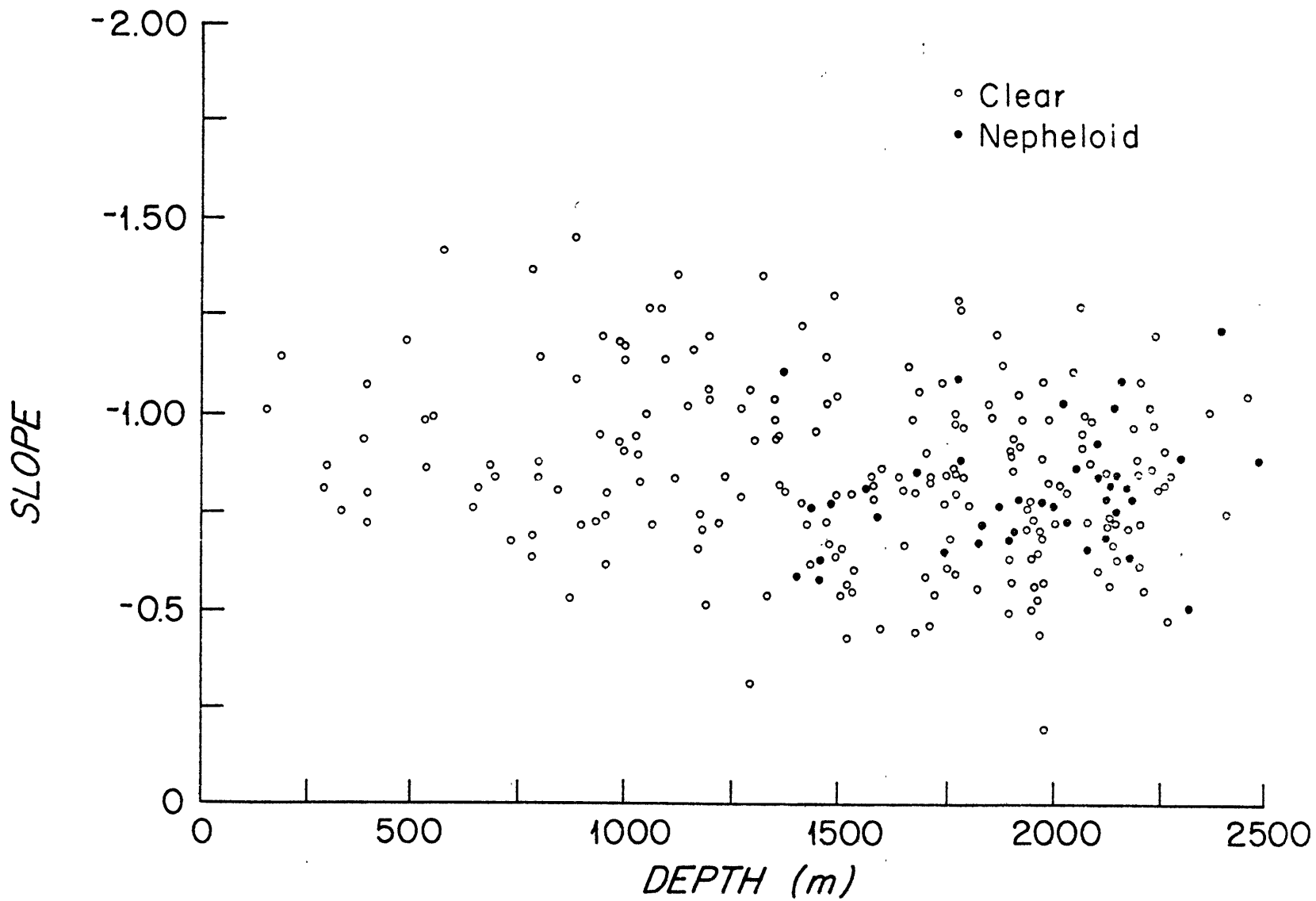
Insight into this phenomenon is gained in examining the slopes of individual profiles (Figure 3.20). Clear-water distributions are well represented by single lines having slopes of approximately -0.9. Nepheloid-layer distributions as single-line representations have slopes similar to those of clear water, but much more scatter. An explanation for the similarity in slopes between clear-water and the nepheloid-layer samples is seen in examining idealized distributions (Figure 3.20). Both idealized clear water (high variance, flat distributions) and idealized nepheloid layer (low variance distributions) have the same slopes of minus 1. However, the nepheloid-layer distributions are much better expressed as two-slope distributions with a slope break at the modal point of the particle volume histograms.

This break in slope has previously been reported for shallow-water data (<200 m)(Bader, 1970; Brun-Cottan, 1971; McCave, 1975) and is here shown to be a feature also of the deep-water nepheloid layer. In shallow water, the meaning of the slope break is unexplained. In this case, for deep water, the two-slope distribution is interpreted to be due to an introduction of resuspended clays and mineral matter into the nepheloid layer.

APPARENT DENSITY

One of the characteristics of suspended particles most difficult to determine is their in-situ bulk density. However, measurements related to the density of SPM may be useful in providing insight

Figure 3.20   Individual profiles of normalized differential particle
                volume versus particle diameter for the clear-water
                and nepheloid-layer samples plotted in Figures 3.10
                and 3.11. Clear-water samples are seen to be well
                represented by a single line through the data.
                Nepheloid-layer samples are better represented as a
                two-slope distribution.
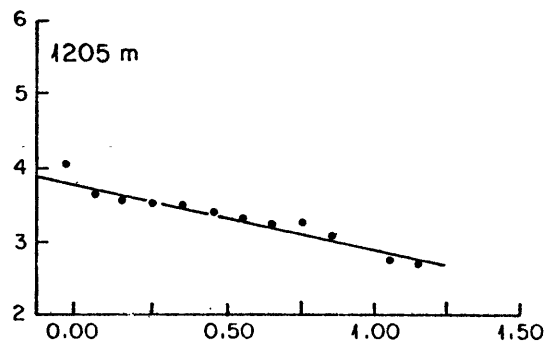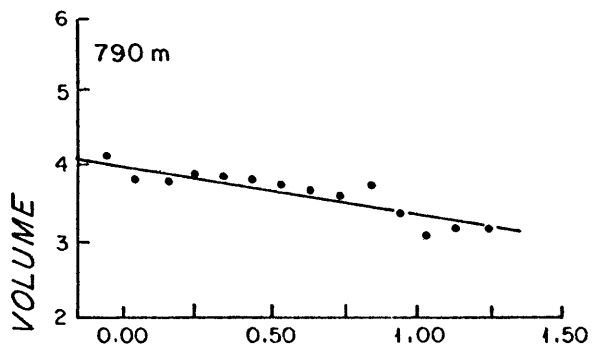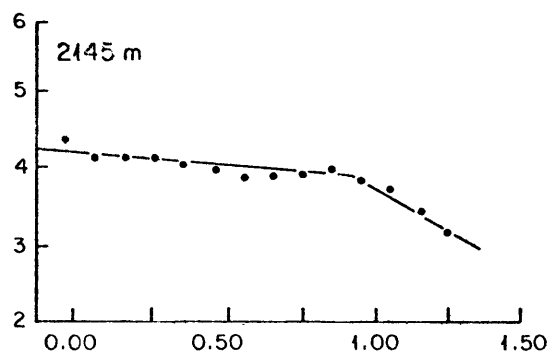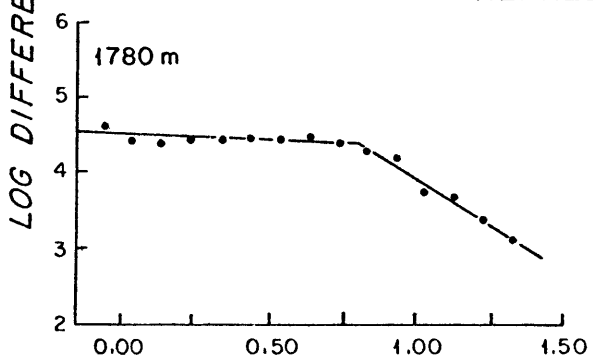
into the differences between clear-water and nepheloid-layer

samples. Biogenic organic-rich matter has a density close to that

of seawater, whereas mineral grains have a density approaching

2.5 g/cm^3. However, few marine particles are composed solely of

either organic matter or mineral grains. Organic-rich matter, fecal

pellets, and aggregates are often composed of varying percentages of

skeletons of plankton, organic matter, and clays.

Contents of organic-matter in SPM drop substantially from 25-50%

in the water column to <2% in surface sediments (Baker et al., 1979;

Rowe and Gardner, 1979). This difference may be useful in

identifying resuspended material, which would tend to have a lower

organic-matter content and therefore a higher density.

Although in-situ particle density cannot now be measured, an

apparent density can be calculated. This parameter is the ratio

between mass and volume concentrations of a sample of SPM. The mass

concentration is determined by filtration and the volume

concentration, by the Coulter-counter analysis. Filtration of SPM

gives a measurement of dry weight of particles per volume of

seawater. The Coulter counter gives a measurement of wet volume of

particles per volume of seawater. The ratio of the two gives a dry

weight of material per wet volume of material.

It is evident that numerous sources of error are included in

estimates of this type. The specific errors in filtration and

Coulter-counter analysis have been detailed previously. The three

major additional sources of variability in this parameter lie in the

difference in the quantity, range, and nature of the measurements. First, filtration integrates over at least 5 (and up to 30) liters of water, whereas the volume of seawater analyzed with the Coulter counter was only a 2 ml aliquot. Second, the Coulter counter was used to measure particles only between 1 and 20 μm, whereas filtration includes all particles greater than 0.4 μm, and some smaller particles are probably collected as well. Third, filtration is a measurement of a dry weight of particles; Coulter-counter analysis measures a wet volume. These sources of error indicate that apparent density cannot be interpreted in terms of actual bulk densities, but it may be a useful parameter for comparative purposes.

Iceland Rise

A plot of mass concentration versus wet particle volume (Figure 3.21) reveals no distinction in the data between the apparent density (the ratio of the two plotted parameters) of the nepheloid-layer and clear-water samples, except that nepheloid-layer samples plot in the upper portion of the graph due to their higher concentrations. The fifty-two clear-water samples give a mean apparent density of 2.00 ± 1.39 g/cm^3, whereas the nepheloid-layer samples yield a statistically indistinguishable 2.38 ± 1.23 g/cm^3.

Western North Atlantic

A similar study was made of the apparent density of particles from the western North Atlantic continental rise. A plot of

Figure 3.21   Apparent density of samples from the Iceland Rise. No
               differentiation by apparent density is evident between
               clear-water and nepheloid-layer samples.

APPARENT DENSITY - ICELAND RISE
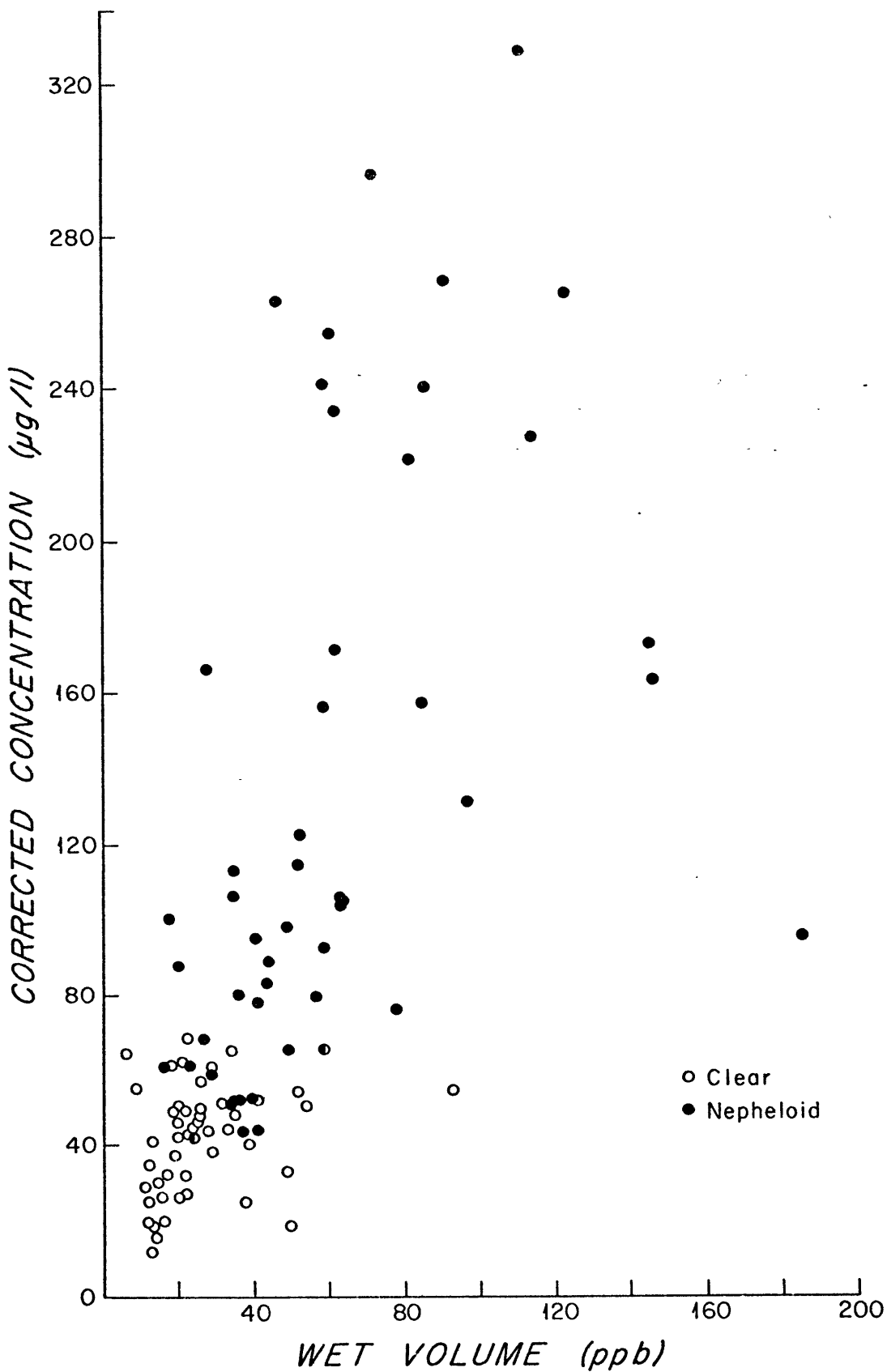
apparent density (Figure 3.22) suggests that the nepheloid-layer

particles have an apparent density greater than that of clear-water

particles. Clear-water samples have a mean apparent density of

0.83 ± 0.40 g/cm^3, whereas nepheloid-layer samples have

significantly larger values (1.34 ± 0.46 g/cm^3). A line of

apparent density at 1.10 g/cm^3 effectively separates most of the

nepheloid-layer samples from clear-water samples.

An explanation for why differences in apparent density between

particles in clear water versus nepheloid water are seen in the

western North Atlantic and not south of Iceland lies in the

composition of the particulate matter. Both regions have

statistically significant differences in the composition of SPM

between clear-water and nepheloid-layer samples. However, the

differences for the western North Atlantic samples are much more

pronounced (Table 3.1). They have a dramatic 16-43% decrease in

coccoliths, a 16-23% increase in mineral matter, and a 6-13%

increase in clays between clear water and the nepheloid layer. The

increase in the clays and mineral matter in the nepheloid layer

serves to increase the apparent density of these particles with

respect to clear-water particles. Compositional variations for the

Iceland Rise samples are not as large. Coccoliths have a 5-6%

decrease; pennate diatoms, a 0-6% increase; clays, a 2% increase;

and mineral matter, a 1-5% increase, between clear water and the

nepheloid layer. These compositional differences are not sufficient

to reflect differences in the apparent densities.

Figure 3.22   Apparent density of samples from the western North
               Atlantic. Clear water samples have apparent densities
               smaller than those for nepheloid-layer samples. A
               line with slope 1.1 g/cm^3 effectively separates the
               two groups.

APPARENT DENSITY   WESTERN NORTH ATLANTIC
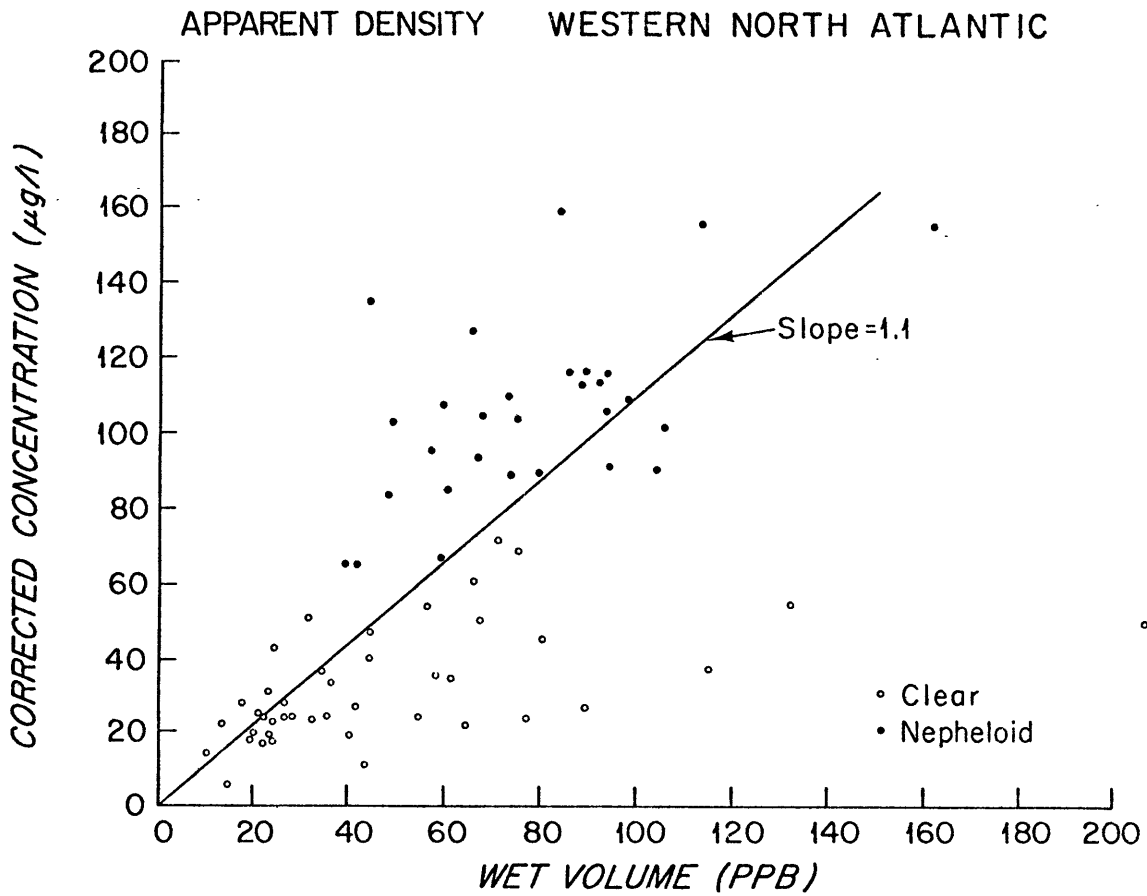
COMPOSITIONAL DIFFERENCES

Filters of SPM from both regions were examined to look for compositional differences between clear-water and nepheloid-layer particles, and to determine whether composition or state of aggregation is a likely cause of the differences in particle size distributions. In the previous section, compositional differences were suggested as an explanation for apparent density changes in the western North Atlantic samples.

Iceland Rise

Chi-square analyses of the compositional results indicate that particles from clear water and the nepheloid layer at individual hydrographic stations differ at the 95% confidence level. In order to determine whether these differences are due to processes causing nepheloid layers, or are simply evidence of dissolution, decomposition, and consumption of particles with increasing water depth, a station with no nepheloid layer was sampled. A chi-square test was made on samples from Station 67 (no nepheloid layer; Figure 3.7) taken from 700 m and 1479 m where the total water depth is 1522 m. The result indicates that at the 95% confidence level these samples are from the same population. These data support the hypothesis that the variability between clear-water and nepheloid-layer samples is due to the existence of the nepheloid layer, and is not simply a function of depth or depth-related processes.

For comparative purposes, the percentages, rather than numbers, of particles in the different compositional classes were used to eliminate the effects of concentration differences between clear water and the nepheloid layer (Figure 3.13). The major variations seen in composition were a decrease in the percentage of small coccoliths and an increase in the percentage of diatoms (particularly Rhizosolenia), clays, and mineral matter in the nepheloid layer relative to clear water. The increase in the percentages of diatoms, clays, and mineral matter is probably caused by resuspension of these components, which are abundant in the local surface sediments into the nepheloid layer. The decrease in the percentage of small coccoliths reflects dilution. The number of small coccoliths does not decrease in the nepheloid layer, but the percentage does (Table 3.1, Figure 3.13). Therefore, the other components of the SPM in the nepheloid layer are preferentially added, resulting in the decrease in percentage of small coccoliths.

State of aggregation of particles was also studied. Aggregates were found in both the clear-water and nepheloid-layer samples, with the percentage of aggregates in both samples being very similar (Table 3.1). Aggregates are sometimes difficult to detect on filters, because drying of the samples removes water and collapses organic matter which may act a binding agent. In clear-water samples, collapsed aggregates were readily detected because there was little material on the filters (Plate 3.2). However, for nepheloid-layer samples, filters were usually covered with material,

in some cases more than a single layer, which made estimation of aggregates more difficult. Therefore, aggregates may have been underestimated in the nepheloid-layer samples.

From the studies on composition and state of aggregation, it appears that compositional differences between clear water and the nepheloid layer, particularly the increases in diatoms and mineral matter, may account for the differences in particle size distributions. Aggregations of particles in the nepheloid layer may be of secondary importance.

The possibility of inorganic flocculation being a contributor to aggregate formation in the nepheloid was assessed on theoretical grounds. Inorganic flocculation occurs by Brownian motion, local shear and differential settling. Einstein and Krone (1962) report equations to calculate the probability of successful collisions by particles in salt water resulting in flocculation. From their equations, and using Iceland Rise data, collisions by Brownian motion would occur once every six months to two years; collisions by local shear would occur once every twenty to eighty days; and differential settling may be important for particles larger than 5.4 μm which comprise <1% by number of the suspended particles. These calculations indicate that inorganic flocculation is not likely to be responsible for aggregate formation in the nepheloid layer on the Iceland Rise. However, organic flocculation may be important.

Western North Atlantic

The compositional differences between particles in clear water and the nepheloid layer are more pronounced in the western North Atlantic region than for the Iceland Rise. This is probably due to the different inputs and processes in the two regions. At present, the Iceland Rise region has a high surface input of both terrigenous and biogenic components, whereas the western North Atlantic has a smaller terrigenous input. For the western North Atlantic, the clear-water samples are mostly composed of biogenic material; the nepheloid-layer samples contain a larger fraction of clays and mineral matter (Figure 3.14). Changes between clear water and the nepheloid layer include a decrease in percentage of small coccoliths and organic matter and an increase in mineral matter, clays, and aggregates.

Water depths are much greater in the western North Atlantic than in the Iceland Rise area. In these increased depths carbonate dissolves at the seafloor (Takahashi, 1975; Broecker and Takahashi, 1978). The coccoliths observed in the nepheloid-layer samples are frequently partially dissolved. Dissolution at the seafloor, and subsequent resuspension, certainly could account for the dramatic decrease in coccoliths from clear water to the nepheloid layer. The increase in clays and mineral matter in the nepheloid layer is partially due to the decomposition and dissolution of other components at the seafloor. However, advection of nonbiogenic material into the region in the bottom boundary layer is another probable cause.

Since current velocities were not measured during this study, assessing the probability of local sediment input is difficult.

Composition and state of aggregation change from clear-water to nepheloid-layer samples. Both of these may cause the differences observed in the particle size distributions. Mineral grains and clays increase substantially in the nepheloid layer. These components usually range in size from 3 to 8 μm and therefore may account for the peak of material in the nepheloid-layer particle size distributions (Figure 3.12). Aggregates observed tended to be larger (> 10 μm), and therefore are not as likely candidates for explaining the size changes observed.

CONCLUSIONS

(1) Analysis of light scattering versus SPM concentration from the Iceland Rise gives three principal results: a) clear-water and nepheloid-layer samples show different relationships of concentration to light scattering, indicating that although the first-order response of the L-DGO nephelometer is a function of particle concentration, second-order responses due to other SPM characteristics such as particle size and composition are not negligible, and/or the response is nonlinear with increasing concentration; b) comparison of the correlation obtained south of Iceland to the BBOR-HAP and LCR regression lines (Biscaye and Eittreim, 1974; 1977) demonstrates that the correlation is somewhat site-specific, with predicted concentrations differing by up to a

factor of 3.4 for light-scattering log E/E_D values between 0.5 and 1.5; and c) but as a means of predicting SPM concentration from light scattering the correlation curves for the two regions are indistinguishable. Limits for prediction of a further observation for the Iceland Rise data include the Biscaye and Eittreim curves for log E/E_D values greater than 0.5.

(2) Particle size analyses show that clear-water and nepheloid-layer samples have different distributions. Clear-water samples are characterized by high variance distributions of roughly equal volumes of material in logarithmically increasing size grades. Nepheloid-layer samples have lower variance distributions with a mean modal size between 3 and 9 μm in the two areas studied. Expressed in terms of normalized differential volume curves, nepheloid layers are shown to have a two-slope distribution, previously reported only in shallow waters. The variations in particle size observed between clear-water and nepheloid-layer samples are interpreted as being due primarily to resuspension of sediment into the nepheloid layer and advection of material into the region in the bottom boundary layer.

(3) Determinations of apparent density from the Iceland Rise area show no differentiation between clear-water and nepheloid-layer samples. However, plots of apparent density from the western North Atlantic do show a marked increase for nepheloid-layer samples. The interpretation of this phenomenon is that the compositional differences for the western North Atlantic samples are much greater

than for the Iceland Rise samples. The dramatic decrease in coccoliths and increase in mineral matter and clays between clear water and the nepheloid layer serves to increase the apparent density of these particles with respect to clear-water particles.

(4) Microscopic examination of filtered particles and application of a chi-square test to the data obtained show that samples from the nepheloid layer are statistically different from clear-water samples. For the Iceland Rise, compositional differences include a decrease in the percentage of small coccoliths and an increase in the percentage of diatoms, clays, and mineral matter in the nepheloid layer relative to clear water. These differences are interpreted as being due to dilution of the coccoliths by other components (diatoms, clays, and mineral matter) which are readily resuspended into the nepheloid layer from the local surface sediments. For the western North Atlantic, the major compositional changes between clear water and the nepheloid layer include a decrease in small coccoliths and organic matter and an increase in mineral matter, clays, and aggregates. These differences are due to dissolution of the carbonate and decomposition and consumption of the organic matter on the seafloor with subsequent resuspension and advection of the refractory material into the near-bottom boundary layer.

CHAPTER IV

COMPARISON OF SEDIMENT TRAP SAMPLES AND THE SURFACE SEDIMENT:

EVIDENCE FOR LOCAL RESUSPENSION

INTRODUCTION

There is ample geologic evidence that resuspension and
redistribution of sediments by deep-sea currents has occurred over
geologic time. The high frequency of hiatuses in DSDP and piston
cores (Watkins and Kennett, 1971; Rona, 1973; Davies et al., 1975;
Berggren and Hollister, 1977; Moore and Heath, 1977) is overwhelming
evidence for periods of erosion and/or nondeposition. Terminating
or outcropping reflectors in continuous seismic profiles corroborate
erosion and nondeposition (Ewing et al., 1970; Tucholke, 1979).
Coarse sediment lag deposits, interpreted as the material left
behind in winnowing by currents, are also indications of erosion, at
least of the fines (Huang and Watkins, 1977; Stow and Lovell, 1979).

Evidence for extensive redistribution and horizontal transport
of deep-sea material is found in the size and structure of the
sediment features in the ocean basins. If pelagic settling were the
only factor in the distribution of sediments, the ocean floor would
be uniformly blanketed with sediments. Instead, large (10's-100's
km) bodies of sediment -- ridges, rises and drifts -- have been
identified in many regions of the ocean basins (Jones et al., 1970;
Tucholke et al., 1973; Hollister et al., 1978). Some of these
features are associated with smaller scale (cm to 100's m)

bedforms -- ripples, furrows and mud waves (Hollister et al., 1974; Bouma and Treadwell, 1975; Jacobi et al., 1975; Lonsdale and Spiess, 1977; Flood, 1978). Formation of these sediment features may indicate sediment redistribution during the present day and up to millions of years ago.

Another probable indication of resuspension and transport of material by deep-sea currents comes from examining the components of the sediment. Distinctive tracers from a single source, e.g., Antarctic diatoms (Burckle and Biscaye, 1971; Johnson et al., 1977) and hemipelagic red clay (Ericson et al., 1961; Heezen et al., 1966; Hollister, 1967; Zimmerman, 1972) have been useful in inferring the paths of bottom currents. These tracers are transported and deposited by the currents, outlining the flow of Antarctic Bottom Water and the North Atlantic Western Boundary Undercurrent, respectively.

There is abundant geological evidence for resuspension and extensive transport of material having been important processes over time. A purpose of this chapter is to determine whether resuspension is occurring now or was restricted to phases of more vigorous bottom-water flow such as may have occurred during Pleistocene glacial epochs (e.g., Ledbetter and Johnson, 1976).

The approach used to test for present day resuspension in this chapter is to compare the material in the water column to that on the seafloor. Samples were obtained with sediment traps through the lower 500 m of the water column and from box core samples of the sediment surface layer.

OBJECTIVES

The principal purpose of this work is to determine whether resuspension of deep-sea material is presently occurring on a time scale of days to weeks and to determine the influence of resuspension on suspended particulate matter. In carrying out this study, the focus is on the following objectives:

(1) To examine samples of particulate matter from the water column and the seafloor below to assess and interpret the changes that occur to particles in transit through the water column and while residing on the seafloor.

(2) To look for components of material in the water column which may be clearly identified as having previously resided on the seafloor, as evidence of resuspension.

(3) To assess the vertical settling velocity versus horizontal current velocity scales involved to constrain the possible sources and distances of transport of the resuspended material.

METHODS

SUSPENDED PARTICULATE MATTER

Three moorings of sediment traps were deployed in the Iceland Rise region for periods from 4 to 13.5 days (Table 4.1). Two moorings were located along the northern transect at 1596 and 1971 m (Figure 4.1), with traps at 13, 103, 493 and 503 m above bottom (mab)(Figure 4.2). The third mooring was located in a turbidity-

Table 4.1

SEDIMENT TRAP MOORINGS

Mooring No.	Station	Time Deployed	Time Recovered	Depth (m)	Location	Height of Traps Above Bottom (m)
1	12	0200 June 27	1500 July 10	1971	62° 18.6'N 17° 26.2'W	13, 103, 503
2	14	0630 June 27	1500 July 3	1596	62° 28.5'N 17° 53.8'W	13, 103, 493
3	51	1153 July 5	1200 July 9	2146	61° 45.4'N 18° 39.2'W	13, 14, 54, 104, 494

Figure 4.1   Bathymetry of the study area with mooring locations and
              box cores identified.   Three moorings and fourteen box
              cores were obtained from the study area.   Samples were
              collected in the channel between the two ridges
              (Mooring 3, box cores 6, 7, 9, 10, 11 and 12) and
              along transects under the influence of the bottom
              current (Moorings 1 and 2, box cores 2, 3, 4, 5, 8,
              13, 14, 15).
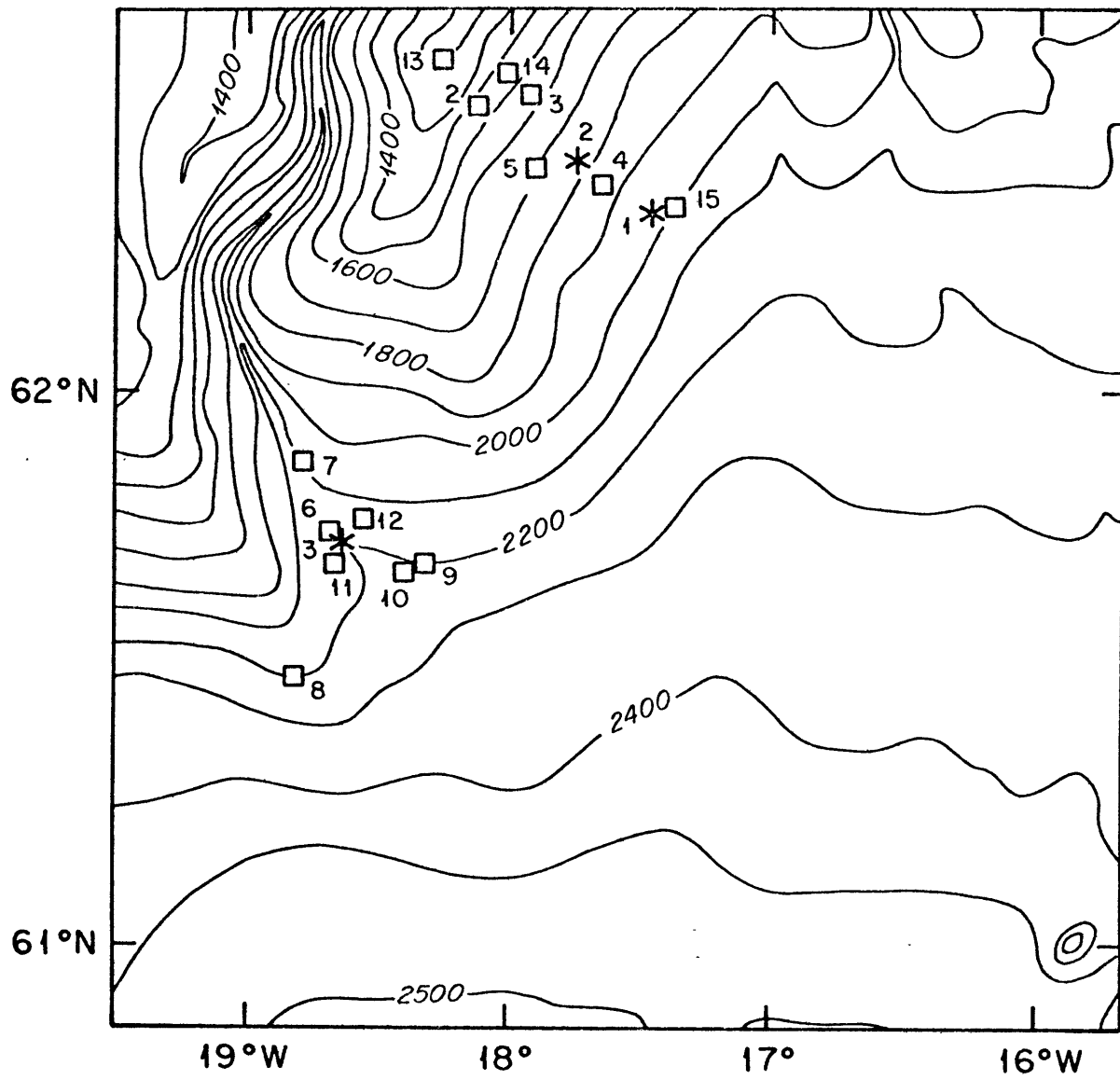
□ BOX CORES   ＊ MOORINGS

Figure 4.2   Diagram of sediment trap moorings from the northern
              transect. Traps were located at 503, 103 and 13 mab
              for Mooring 1 and 493, 103 and 13 mab for Mooring 2.

FLAG, RADIO, FLASHER

FLOTATION SPHERES

~500 mab
SEDIMENT TRAP

TIMED RELEASE

MESSENGER

~100 mab
SEDIMENT TRAP

MESSENGER

~10 mab
SEDIMENT TRAP

TIMED RELEASE

RELEASE ARM

ANCHOR
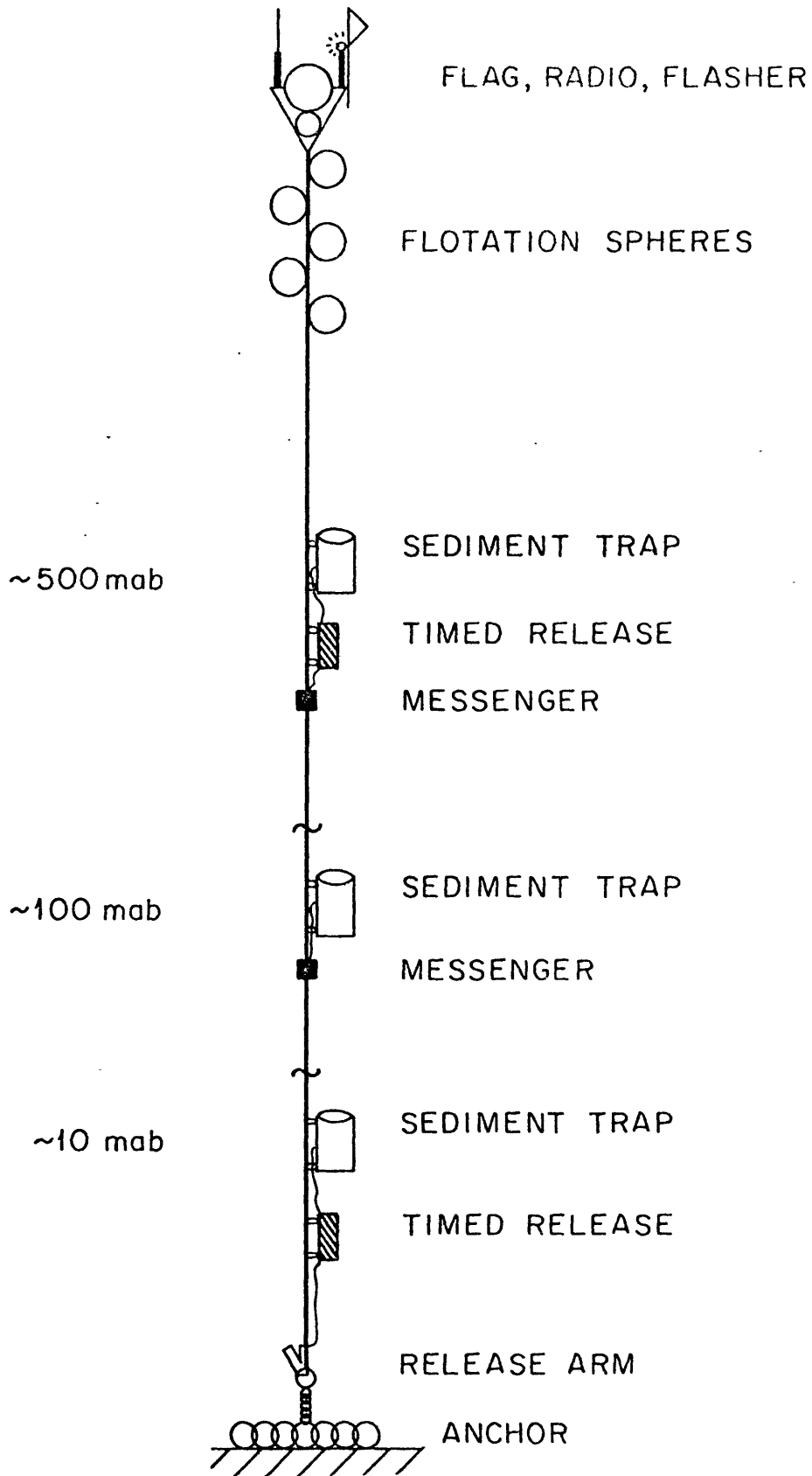
current canyon at 2146 m with additional traps at 53 and 13 mab (Figure 4.3). In the rest of this chapter the traps are referred to as being at 10, 50, 100 and 500 mab; these are their approximate heights above bottom and this description is used for convenience in comparison from one mooring to another. Water depths for the moorings are rounded to 2000, 1600, and 2150 m for moorings 1, 2, and 3, respectively.

The sediment traps used in this study were a modification of the type used by Gardner (1977a). The traps are PVC cylinders 25 cm in diameter and 62 cm in height (Figure 4.4). The lid of the trap is a butterfly valve recessed 30 cm from the top edge. The lid is held open by a spring-loaded PVC clamp. The valve is closed either by burning a nichrome wire attached to the spring mechanism or alternatively by dropping a messenger which releases a taut line to the spring mechanism. The burning of the wire or dropping of a messenger is actuated by a timed release.

SURFACE SEDIMENT SAMPLES

Sediment samples were obtained throughout the study area by piston coring and box coring. Box-core samples were used in this work since box corers more reliably recover the surface sediments. Fourteen box cores were obtained in the Iceland Rise region (Table 4.2, Figure 4.1). The box corer used is that described by Bouma (1969, p. 339-342). Surface scrapings from the top 1 cm were taken from the cores for comparison with the sediment-trap samples.

Figure 4.3   Diagram of sediment trap mooring from the channel
              station, Mooring 3.   Traps were located at 494, 104,
              54, 14 and 13 mab.   The trap at 14 mab was a different
              design from the other traps and did not function
              properly.

FLAG, RADIO, FLASHER

FLOTATION SPHERES

SEDIMENT TRAP

TIMED RELEASE

MESSENGER

~500 mab

SEDIMENT TRAP

MESSENGER

~100 mab

SEDIMENT TRAP

~50 mab

SEDIMENT TRAP

~12 mab

SEDIMENT TRAP

~10 mab

TIMED RELEASE

RELEASE ARM

ANCHOR
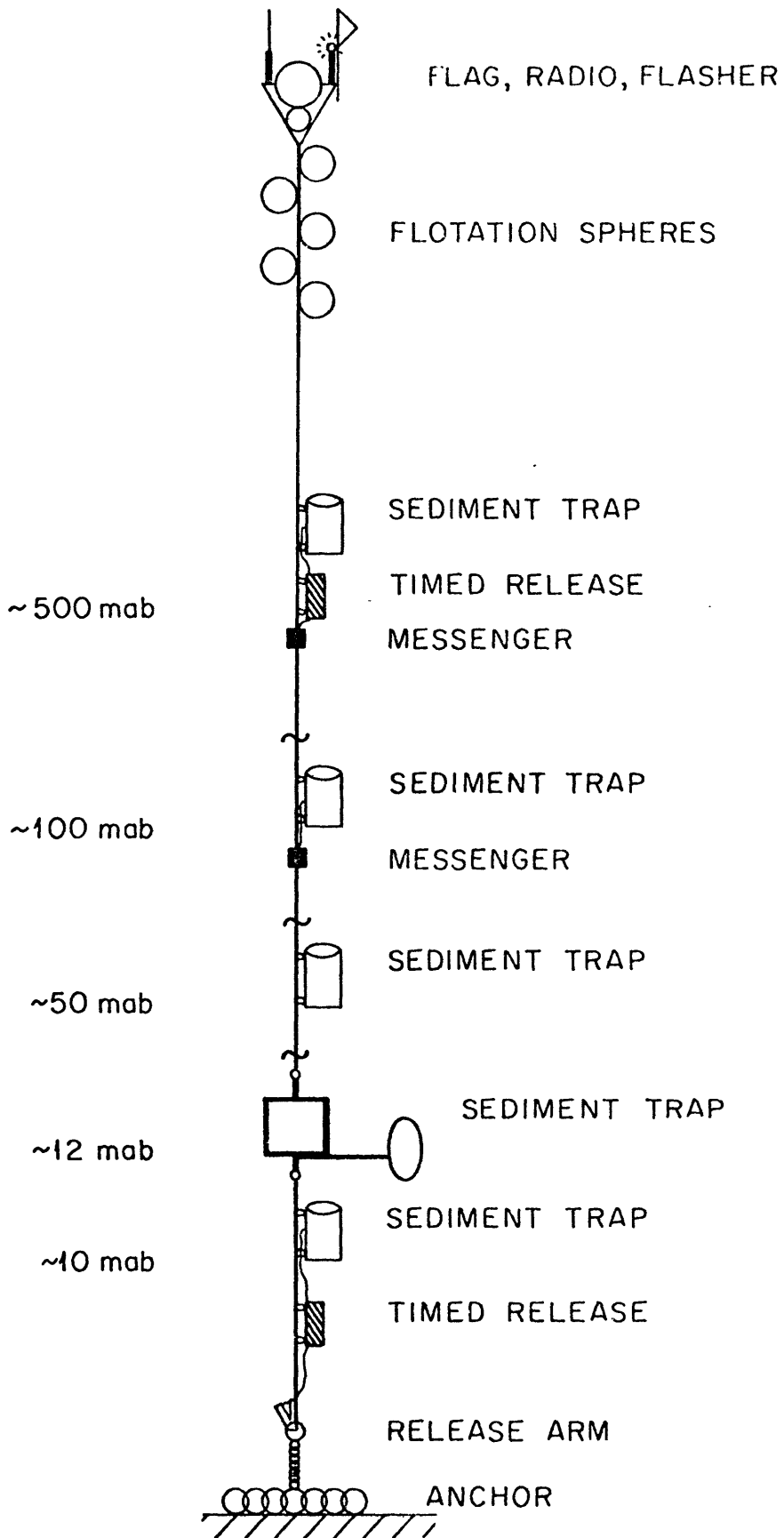
Figure 4.4   The sediment trap used in this study. The trap is a
              PVC cylinder with a height to width ratio of 2.5. The
              closing mechanism is a butterfly valve actuated by a
              timed release.

25 cm

NANSEN
BOTTLE
RELEASE

BUTTERFLY
VALVE

62 cm

SPRING
(SURGICAL
TUBING)
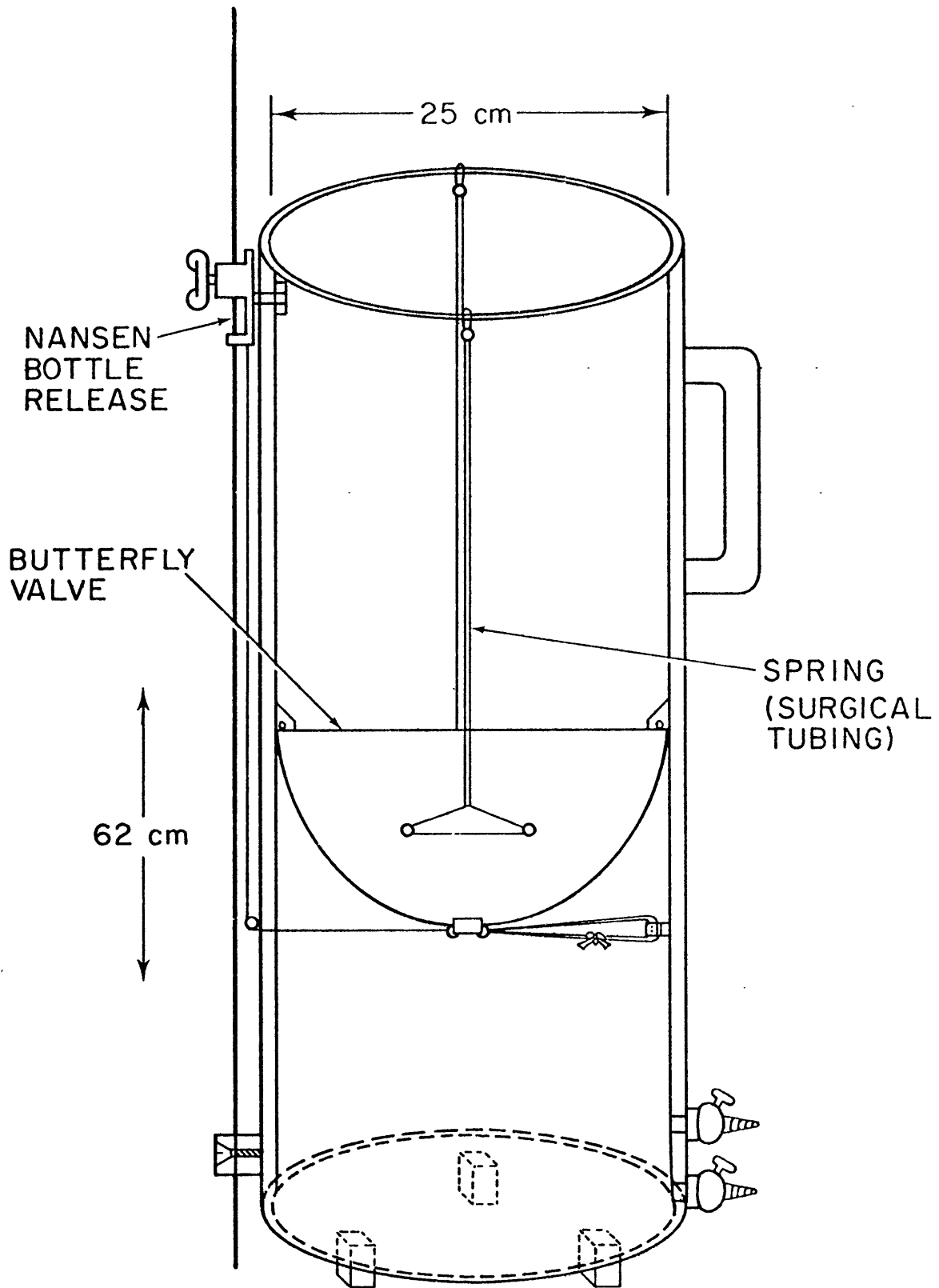
Table 4.2

BOX CORES

Station	Core No.	Depth (m)	Latitude	Longitude	Remarks
1	1-BC	4539	40°35.1'N	63°04.4'W	72 cm sample
21	2-BC	1391	62°30.4'N	18°06.4'W	1 kg sample
24	3-BC	1509	62°29.6'N	17°59.3'W	26 cm sample
43	4-BC	1839	62°22.5'N	17°35.8'W	
48	5-BC	1687	62°26.3'N	17°50.3'W	10 cm sample
56	6-BC	2175	61°44.0'N	18°39.0'W	
60	7-BC	2128	61°50.3'N	18°47.9'W	
73	8-BC	2203	61°31.0'N	18°46.5'W	
77	9-BC	2205	61°41.0'N	18°25.1'W	
78	10-BC	2248	61°40.5'N	18°27.2'W	
79	11-BC	2154	61°41.2'N	18°39.0'W	
80	12-BC	2133	61°45.6'N	18°37.0'W	
82	13-BC	1198	62°33.2'N	18°14.3'W	1/2 kg sample
83	14-BC	1409	62°31.8'N	18°02.0'W	1 kg sample
86	15-BC	1998	62°17.6'N	17°25.1'N	

SIZE DISTRIBUTION ANALYSES

Particle size analyses were performed on sediment trap material and surface sediments. Samples were wet sieved with gentle agitation at 250, 125, 63, and 20 μm, yielding five size fractions per sample. Samples were sieved with seawater as distilled water might disperse the aggregates and loosely bound fecal pellets. Some particles smaller than the grid size remained on the sieves due to agglomeration with larger particles. Each size fraction was separately filtered onto 0.4 μm Nuclepore filters or pre-combusted glass fiber filters (nominal pore size of 1 μm), for weight determination. Samples were rinsed ten times with 10 ml aliquots of filtered, buffered to pH 7, distilled water to remove residual salt.

OPTICAL IDENTIFICATION

Components of sediment trap samples and surface sediment samples were identified by optical microscopy and scanning electron microscopy. A binocular microscope was used to study the >63 μm fractions of the samples which comprised 37-70% of the total trap samples by weight. Counts were made of the major constituents of the samples. These include: foraminifera, radiolaria, pteropods, diatoms, dinoflagellates, fecal pellets, unidentified biogenic material, volcanic glass, mineral grains, and aggregates. Counts were made directly from filters obtained in the size-fraction analysis for the sediment-trap samples for all but the traps at 10 mab. The sieved fractions of the surface-sediment and

sediment-trap samples from 10 mab were later split into smaller, manageable fractions with a microsplitter before counting. Scanning electron microscopy was used to obtain photomicrographs of the various constitutents in the samples.

MINERALOGY

X-ray diffraction was used to determine the mineralogy of surface-sediments and sediment-trap samples from 10 mab; trap samples above 10 mab had insufficient material for these analyses to be made. Bulk powder mounts were used to determine the overall composition of the samples, and oriented mounts of the $<2\ \mu m$ fraction were used for clay mineralogy (Hathaway, 1972).

CARBONATE DETERMINATIONS

The calcium carbonate content of sediment-trap samples and surface-sediment samples was determined by acidification of a fraction of the samples. Sediment-trap samples were wet split with a plankton splitter into fractions small enough to be concentrated onto 25 mm diameter precombusted, preweighed glass-fiber filters. The samples were digested with 2N HCl and rinsed ten times with distilled water. Calcium carbonate content was calculated from weight loss.

ORGANIC CARBON AND NITROGEN ANALYSES

Organic carbon and nitrogen contents were determined for both the sediment-trap and surface-sediment samples. Samples obtained at

sea were fractionated by wet splitting and filtering these portions onto precombusted glass-fiber filters. These filters were frozen at sea to minimize organic decay. Subsequently, in the laboratory they were thawed, acidified to remove carbonate, and analyzed with a Perkin Elmer #240 elemental analyzer, to obtain organic carbon and nitrogen contents of the samples.

RESULTS

All of the sediment trap moorings were successfully recovered, with almost complete success with the sediment traps. All traps were recovered with good samples except for the traps at 500 and 100 mab from Mooring 3. Material from these traps may have been partially washed out in the surface waters, because they remained open and subject to the pumping action of the swell before recovery.

MASS COLLECTED BY THE SEDIMENT TRAPS

The quantity of material collected by the sediment traps increases substantially from 500 to 10 mab, particularly between 100 and 10 mab (Table 4.3). The greatest increase, more than two orders of magnitude, is for Mooring 2, located in the axis of the bottom current.

Apparent vertical fluxes of material can be calculated from the sediment-trap data (Figure 4.5; Gardner, 1977a). At 500 mab, apparent fluxes varied by a factor of 2, from 1.8 $mg/cm^2/yr$ at Mooring 2 at 1600 m to 3.6 $mg/cm^2/yr$ at Mooring 1 at 2000 m.

Table 4.3

MASS OF SEDIMENT TRAP SAMPLES

	MAB (m)	Mass Collected (mg)
Mooring 1	500	68.0
	100	147.6
	10	3867.
Mooring 2	500	15.9
	100	36.4
	10	4072.
Mooring 3	500	18.7*
	100	54.3*
	50	55.3
	10	1895.

* traps returned open

Figure 4.5   Apparent vertical fluxes of material through the water
column. Weight of material collected by the traps is
divided by the area of the opening and duration of
trapping. A dramatic increase in apparent flux is
observed from 100 to 10 mab. The trap data from 500
mab and 100 mab from Mooring 3 are questionable since
these traps were recovered open.
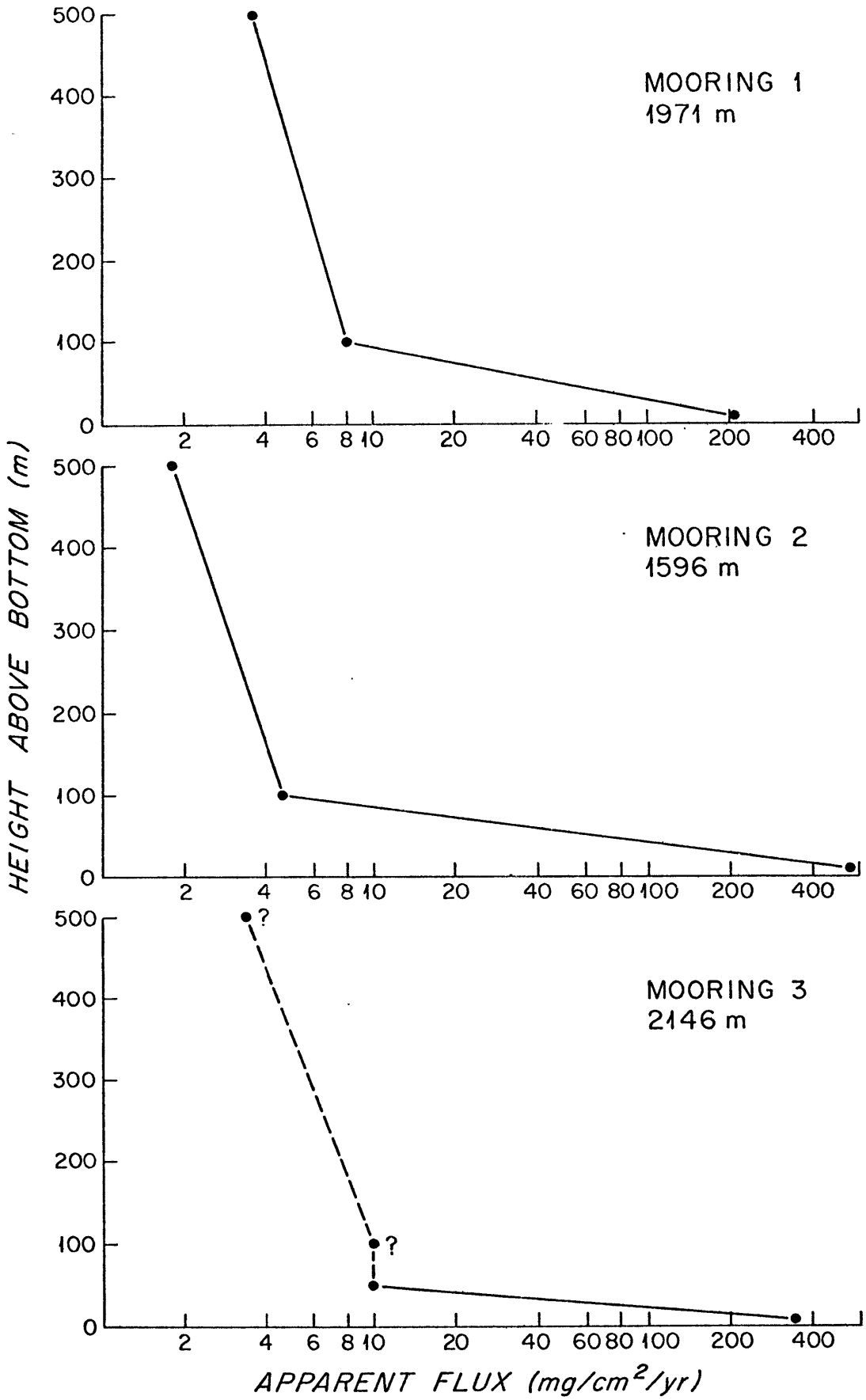
Traps were spaced up to 500 mab because it was thought that 500 m would be high enough to be above the nepheloid layer, and would catch only primary, surface-source material. However, from the light-scattering profiles discussed in Chapter III (Figure 3.8), the traps at 500 mab on Moorings 1 and 3 were still within the nepheloid layer; the 500 mab trap from Mooring 2 was above it. Apparent fluxes at 100 mab varied by a factor of 1.9, with the higher value at the deeper station, Mooring 1. At 10 mab, the fluxes vary by a factor of 2.3 with the highest flux, 474 mg/cm^2/yr at Mooring 2, in the axis of the bottom current.

PARTICLE SIZE DISTRIBUTIONS

Particle size distributions were examined for sediment-trap samples and nearby surface sediments to determine if grain size varies with water depth or between material in the water column and that on the underlying seafloor.

Sediment Traps

Particle size distributions vary considerably through the water column, but show the same general trends from mooring to mooring (Figure 4.6). Traps at 500 mab have roughly similar amounts in all size fractions >20 μm. The <20 μm fraction is a large percentage of the samples, 33 to 42%. This high proportion of small particles indicates that although large particles may theoretically compose a substantial portion of the vertical flux of material through the

–153–

Figure 4.6   Particle size distributions for sediment trap samples
              by weight. Distributions were determined for two
              splits of the samples which are represented by the
              solid bars. The average size distribution of the
              combined splits is given as the open bars.
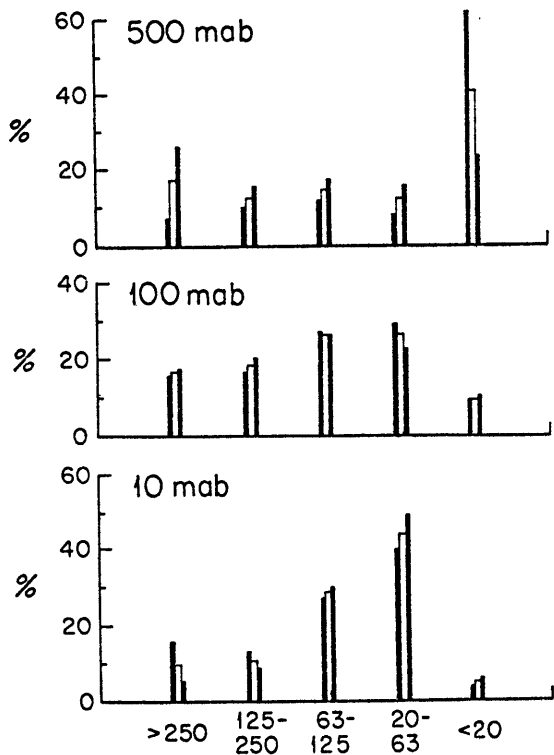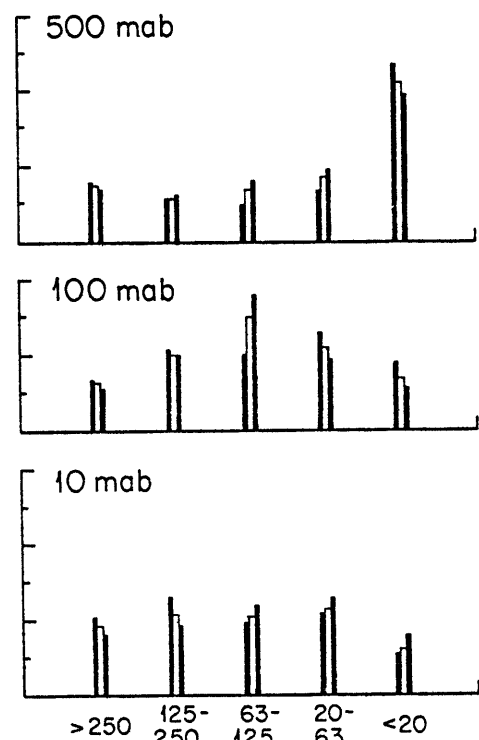
MOORING 1   MOORING 2   MOORING 3
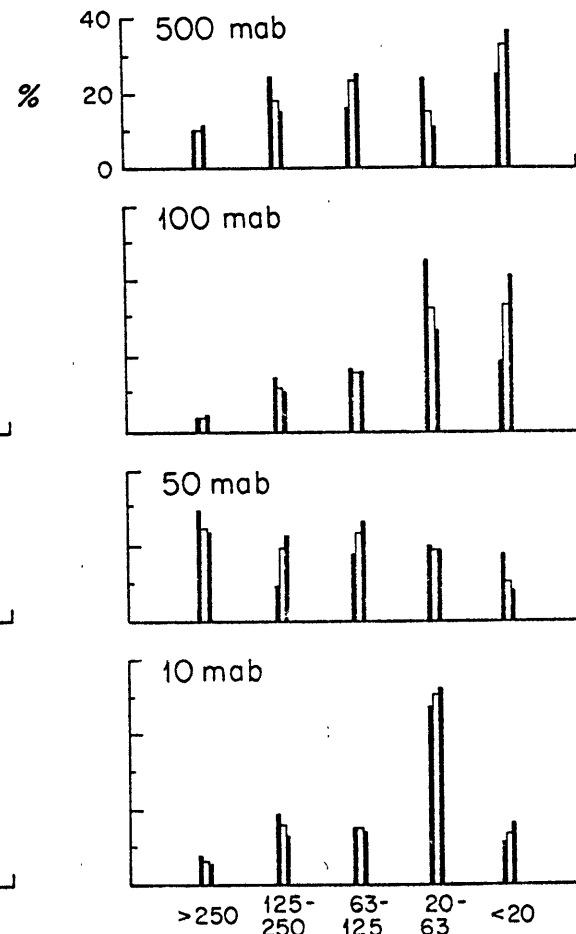
SIZE   FRACTION   (μm)

water column (McCave, 1975), small particles are equally important in this particular area.

The traps at 100 mab along the northern transect have a peak in the 63-125 μm size fraction. The 50 mab trap from the channel mooring (the only trap at this height) has roughly equal amounts of material in the size fractions >20 μm, as do the traps at 500 mab, but has a decrease in material <20 μm.

The material from traps at 10 mab are more variable in their size distributions. A general trend among these three samples is low percentages of material <20 μm. This may be artificial. For these traps, up to one gram of material was sieved. The 20 μm sieve would frequently clog, and sieving at this size fraction took several attempts to complete. Some material smaller than 20 μm undoubtedly remained on the sieve due to the large amount of material processed. This could account for the strong decreases in the <20 μm size fraction for these samples.

A general trend observed among the trap samples is a decrease with depth in the percentage of material <20 μm.

Surface Sediments

Box cores were taken along the northern transect and in the channel. The samples recovered are somewhat biased, since some attempts made to recover box cores in the current axis along the northern line, were unsuccessful due to wash-out of the coarse sediments during recovery. Cores taken in the channel have fine

grained sediments, up to 96% <63 μm (Figure 4.7). Cores along the
northern transect tend to be composed of coarser material. Cores 3,
5, and 15 (Figure 4.7) and gravity cores 1, 5, and 11 (Shor, 1979)
have surface sand layers from which the fines seem to have been
winnowed.

OPTICAL IDENTIFICATION

The coarse material (>63 μm) in flux at various depths in the
water column was identified and counted to compare this material to
that on the seafloor.

Sediment Traps

Foraminifera

Planktonic foraminifera comprise by number from 2 to 54% of the
size fractions >63 μm of the sediment-trap samples (Table 4.4).
The >250 μm size fraction had the largest percentage of planktonic
forams; smaller size fractions had smaller percentages. The
planktonic foraminifera >150 μm in the sediment trap samples from
10 mab were identified to compare the trap species in the traps with
those in the surface sediments. Forams < 150 μm were generally too
small for reliable identification of species. Species identified
and counted include Neogloboquadrina pachyderma (dextral and
sinistral), Globigerinita glutinata, Globigerina bulloides,
Globigerina quinqueloba and Globorotalia inflata (Plate 4.1, 3-8;
Table 4.5). Some of the planktonic forams in the samples were
coated with iron oxide (Plate 4.1,8; Table 4.5).

Figure 4.7   Particle size distributions for surface sediment
              samples. Samples were wet sieved and filtered on
              glass fiber filters for weight determination.
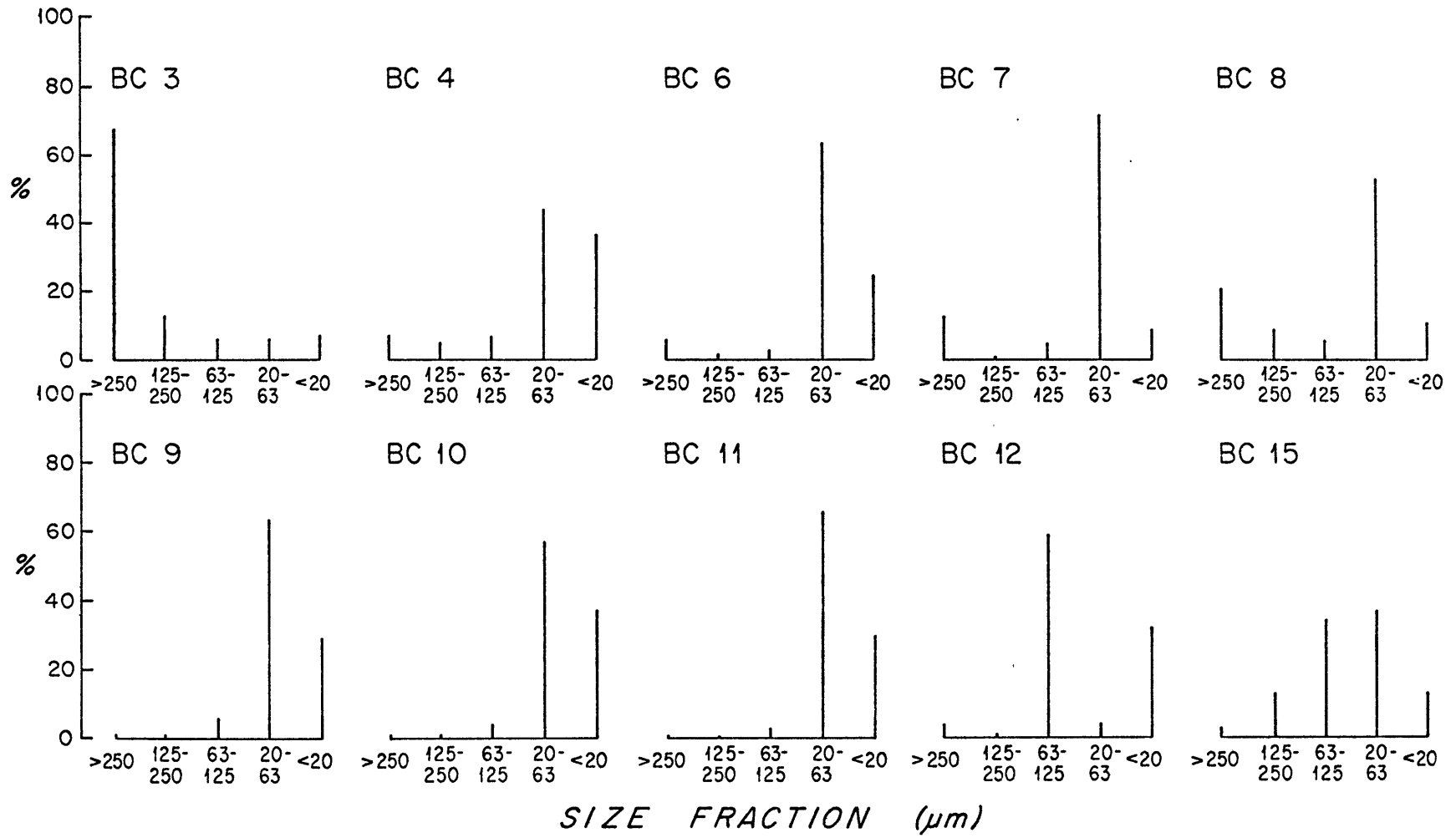
SIZE FRACTION (μm)

Table 4.4

Percentage of Sediment Trap Samples By Particle Type

	Size Fraction	Sample Split	Forams	Radiolaria	Pteropods	Diatoms	Dino-Flagellates	Fecal Pellets	Unidentified Biogenics	Volcanic Glass	Mineral Matter Aggregates	Total Counted
Mooring 1 500 mab	250	1/4	31	2	3	0	31	7	19	2	5	58
	125-250	1/4	30	1	12	2	9	11	7	22	5	325
	63-125	1/4	23	5	4	1	5	2	9	46	6	698
100 mab	250	1/4	54	8	3	1	0	13	13	0	10	80
	125-250	1/4	43	5	4	1	0	10	4	30	3	653
	63-125	1/4	34	3	1	2	1	0	5	53	1	2946
10 mab	250	1/4	15	9	1	1	0	1	2	2	71	1785
	125-250	1/512	6	3	1	4	0	0	4	8	74	574
	63-125	1/512	12	2	1	2	0	0	3	24	56	775
Mooring 2 500 mab	250	1/4	7	0	2	0	0	29	7	0	54	41
	125-250	1/4	6	5	1	11	0	36	7	0	34	149
	63-125	1/4	7	9	4	12	16	24	8	6	14	403
100 mab	250	1/4	8	0	8	15	0	15	15	8	31	13
	125-250	1/4	12	2	1	9	3	16	6	42	10	232
	63-125	1/4	11	2	1	5	2	2	5	57	17	1533
10 mab	250	1/32	54	0	0	1	1	0	3	18	25	1467
	125-250	1/512	35	1	0	0	0	0	6	23	34	235
	63-125	1/2048	5	6	0	6	0	0	10	36	37	395
Mooring 3 500 mab	250	1/4	0	0	0	23	0	27	38	4	8	26
	125-250	1/4	9	1	2	13	4	8	6	48	10	126
	63-125	1/4	1	2	1	18	3	4	7	42	22	551
100 mab	250	1/4	9	2	11	4	0	47	7	0	20	45
	125-250	1/4	2	3	2	5	0	85	1	1	1	932
	63-123	1/4	6	6	2	3	1	61	1	17	2	2088
50 mab	250	1/4	17	2	42	4	0	28	4	0	4	53
	125-250	1/4	10	5	4	6	1	65	1	8	5	327
	63-125	1/4	16	8	2	5	1	20	2	42	5	1024
10 mab	250	1/4	4	5	38	6	0	0	4	15	28	178
	125-250	1/128	2	5	0	9	0	0	3	8	73	672
	63-125	1/32	3	3	0	6	0	0	13	33	42	326

Plate 4.1   SEM photomicrographs of particles from the sediment traps.

1) Pteropod from Mooring 1, 10 mab, scale bar 200 μm, X 65.
2) Pteropod from Mooring 1, 500 mab, scale bar 50 μm, X 400.
3-8) Planktonic foraminifera from Mooring 2, 10 mab:
   3. Neogloboquadrina pachyderma (dextral), scale bar 50 μm, X 250;
   4. Globigerina glutinata, scale bar 50 μm, X 240;
   5. Globigerina bulloides, scale bar 50 μm, X 200;
   6. Globigerinata quinqueloba, scale bar 50 μm, X 380;
   7. Neogloboquadrina pachyderma (sinistral), scale bar 50 μm, X 270;
   8. Globorotalia inflata, note the surface texture; this foram has an iron-oxide coating representative of residence at the seafloor, scale bar 50 μm, X 260;
9-12) Benthic foraminifera from traps at 10, 100 and 500 mab:
   9. Parafissurina sp., from Mooring 2, 10 mab, scale bar 50 μm, X 240;
   10. Uvigerina peregrina, from Mooring 2, 100 mab, scale bar 20 μm, X 500;
   11. Cassidulina sp., from Mooring 2, 100 mab, scale bar 20 μm, X 700;
   12. Astrononion sp., from Mooring 1, 500 mab, scale bar 50 μm, X 380.
13-16) Radiolaria from the sediment traps:
   13. Phaeodarian, Protocystis xiphodon, from Mooring 2, 500 mab, scale bar 20 μm, X 950;
   14. Nassellarian, Botryostrobus aquilonarias, from Mooring 1, 500 mab, scale bar 20 μm, X 610;
   15. Smullerian, family Phacodiscidae, from Mooring 1, 10 mab, scale bar 50 μm, X 270;
   16. Smullerian, family Lithelidae, from Mooring 1, 10 mab, scale bar 50 μm, X 340.
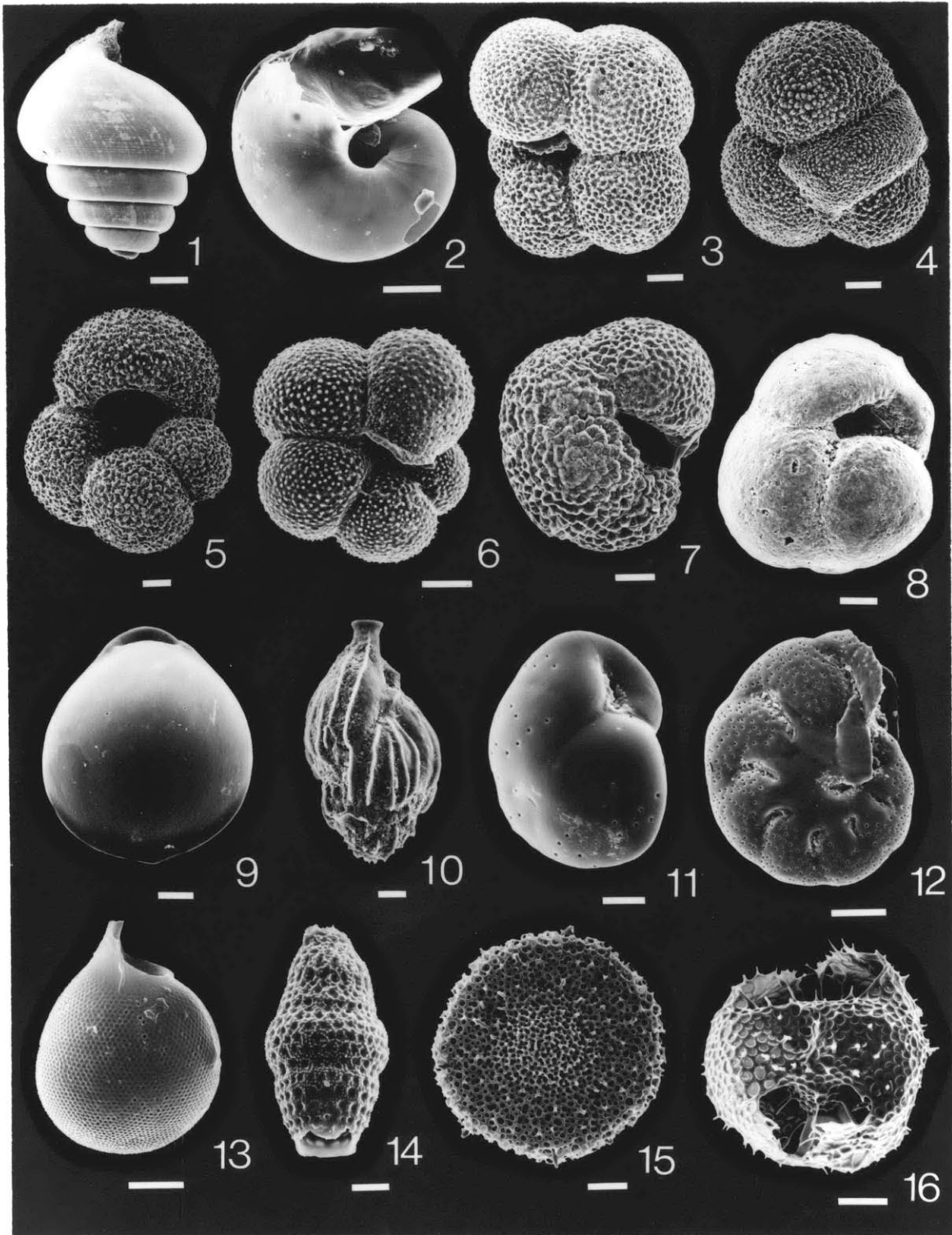
Table 4.5

FORAMINIFERA IN THE SEDIMENT TRAP AND SURFACE SEDIMENT SAMPLES

%

	size fraction (m)	N. pachyderma (sinistral)	N. pachyderma (dextral)	G. inflata	G. quniqueloba	G. glutinata	bulloides	benthics	fragments	others and unknowns	iron-oxide coated	total planktonics	total forams
Mooring 1													
100 mab	250	0	10	5	13	20	45	0	7	8	3	40	43
	250	2	20	2	23	16	32	3	8	5	6	243	274
Mooring 2													
10 mab	250	4	47	3	1	10	31	2	12	3	33	688	799
10 mab	125-250	4	63	1	4	20	5	2	6	3	26	197	216
Box Core 3	150	15	43	7	4	11	14	6	5	6	45	319	359
Box Core 4	150	19	35	11	1	8	21	3	18	6	35	359	456
Box Core 5	150	11	43	11	0	11	16	3	14	9	34	313	375
Box Core 6	150	0	46	2	4	19	22	13	8	7	1	140	176
Box Core 8	150	30	44	4	0	8	11	1	11	4	22	329	376
Box Core 10	150	2	49	6	5	16	15	2	12	8	1	107	124
Box Core 15	150	9	46	2	2	18	16	2	13	6	23	335	394

Benthic foraminifera were also found in the sediment-trap samples (Plate 4.1, 9-12). All traps at 10 mab and 100 mab contained at least a few benthic specimens. The trap at 500 mab from mooring 1, at 2000 m, contained 3 small (<100 μm) benthic forams (Plate 4.1, 12). Some identified were Uvigerina sp., Parafissurina sp., and Cassidulina sp.

Due to the small size of the samples from the traps located at 500 and 100 mab, differentiating of the planktonics by species was not done, only the total number of individuals was counted. The presence or absence of benthic forams, the glacial assemblage foram, Neogloboquadrina pachyderma (sinistral), and iron-oxide staining in these samples was recorded since occurrences of these indicate resuspension of seafloor material.

Radiolaria

Radiolaria of the three major groups (spumellarians, nassellarians, and phaeodarians) were observed in the sediment trap samples (Plate 4.1, 13-16). They comprise < 10% by number of all the samples and are absent entirely from some of the > 250 μ m size fractions (Table 4.4). The percentage of nassellarians and phaeodarians generally decreases between 500 and 10 mab. This agrees with the observations by Takahashi and Honjo (1980) that spumellarians are less subject to dissolution than the nassellarians and phaeodarians.

Pteropods

Pteropods were found in most of the sediment-trap samples (Table
4.4). Specimens were large, a millimeter or more in diameter, and
have fragile transparent to translucent tests (Plate 4.1, 1-2).
Pteropods comprise <7% by number of the total samples considering
all size fractions. However, for the >250 µm size fraction at the
channel station, Mooring 3, they are the dominant component, forming
42% of the trap sample at 50 mab. In general, the percentage of
pteropods in trap samples decreases toward the seafloor. At Mooring
2, at 1600 m, no pteropods were observed in the trap at 10 mab.

Pteropods are composed of aragonite, with which the bottom water
may be undersaturated (Berner, 1977). The specimens observed in the
traps probably fell rapidly through the water column from their
surface source and have so far escaped dissolution. Some of the
pteropods collected were so fragile that touching them with a wet
fine-tipped brush caused them to break into several fragments.

Diatoms

Both centric and pennate diatoms were found in the sediment-trap
samples. Rhizosolenia was most prevalent (Plate 4.2, 8), but
Coscinodiscus, 60-80 µm in diameter, (Plate 4.2, 9) was also
common. Diatoms comprise by number 11% or less of the bulk
sediment-trap samples; individual size fractions have <1 to 15%
diatoms. The two moorings along the northern transect show opposite
trends with depth. For Mooring 1, 2000 m, diatoms increase in
percentage from 500 to 10 mab, whereas for Mooring 2, 1600 m, a
decrease is observed (Table 4.4).

Plate 4.2   SEM photomicrographs of particles from the sediment
             traps and surface sediments. 1-12 are trapped
             sediments; 13-17 are from the surface sediments.

1) Fecal pellet, Mooring 3, 50 mab, see Figure 4.8a for X-ray
   of elements present. Calcareous, siliceous, and clay
   material is seen at higher magnification. Scale bar
   50 µm, X 230.
2) Fecal pellet, Mooring 3, 50 mab, see Figure 4.8b for X-ray
   of elements present. Silica and calcium are the only
   elements detected. Scale bar 50 µm, X 330.
3-7) Dinoflagellates from Mooring 2, 500 mab:
     3. Ceratium, scale bar 20 µm, X 510;
     4. Dinophysis, scale bar 20 µm, X 940;
     5. Ceratium, scale bar 50 µm, X 220;
     6. Ceratium, scale bar 20 µm, X 420;
     7. Peridinium, scale bar 20 µm, X 610.
8) Diatom, perhaps part of Rhizosolenia, Mooring 2, 500 mab,
   scale bar 20 µm, X 390.
9) Diatom, Coscinodiscus, Mooring 2, 500 mab, scale bar 20 µm,
   X 800.
10-12) Volcanic shards and mineral grains from Mooring 2,
   10 mab:
     10. Vesicular volcanic shard, see Figure 4.8c for X-ray
         of elements present, scale bar 50 µm, X 230;
     11. Quartz grain with iron-oxide coating, see Figure 4.8d
         for X-ray of elements present, scale bar 50 µm,
         X 230;
     12. Altered volcanic shard, see Figure 4.8e for X-ray of
         elements present, scale bar 50 µm, X 330.
13-17) Volcanic shards and mineral grains from box core 5:
     13. Vesicular volcanic shard, see Figure 4.9a for X-ray
         of elements present, scale bar 50 µm, X 270;
     14. Volcanic shard, see Figure 4.9b for X-ray of elements
         present, scale bar 50 µm, X 360;
     15. Mineral grain, see Figure 4.9c for X-ray of elements
         present, scale bar 50 µm, X 310;
     16. Mineral grain with iron-oxide coating, see Figure 4.9d
         for X-ray of elements present, scale bar 100 µm,
         X 130;
     17. Quartz grain, see Figure 4.9e for X-ray of elements
         present, scale bar 50 µm, X 250.
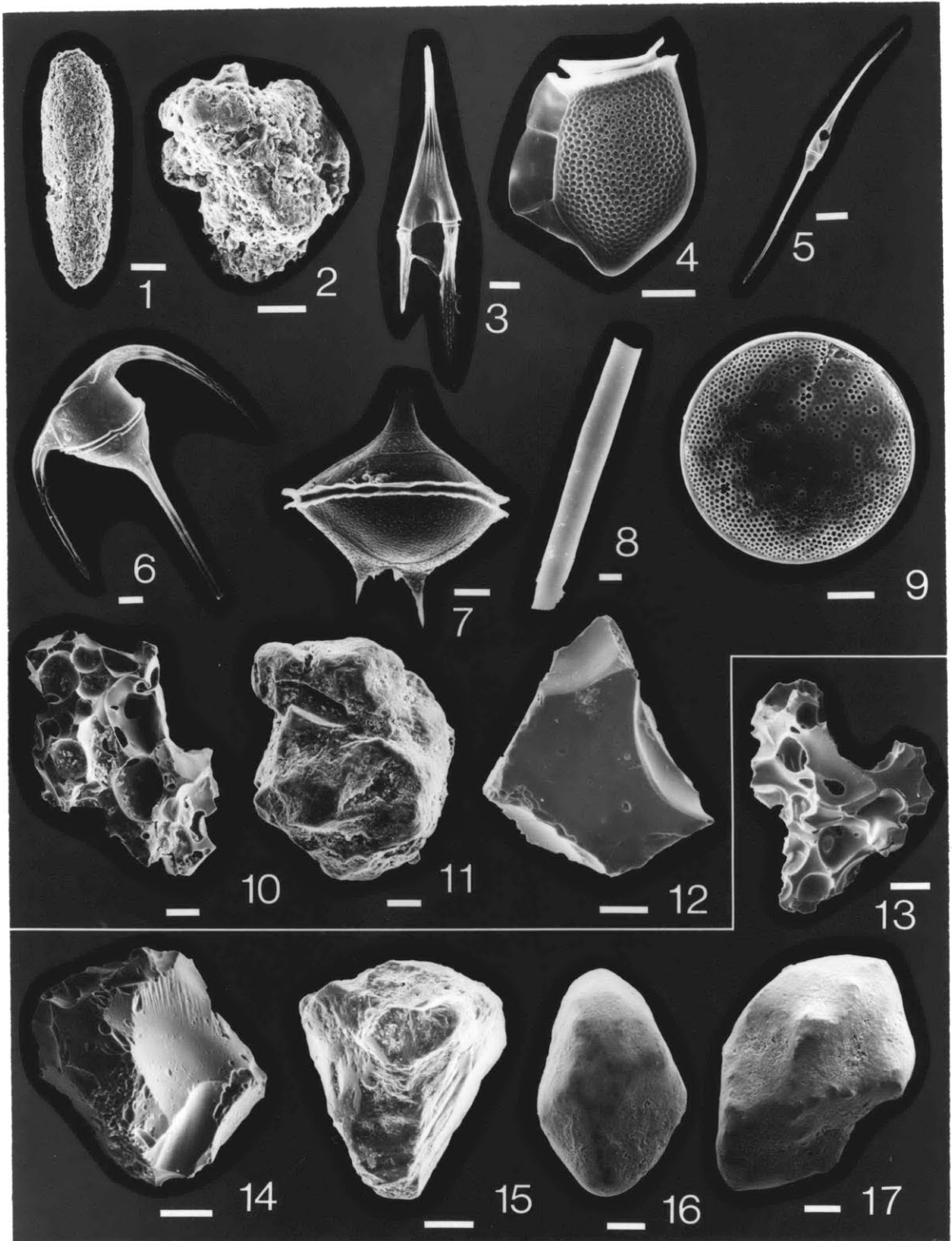
Dinoflagellates

The principal genera of dinoflagellates observed in the sediment traps were Ceratium, Peridinium and Dinophysis (Plate 4.2, 3-7). They are found predominantly in the samples from 500 and 100 mab in the 63-125 μm size fraction, usually comprising only a few percent by number of the samples. Few specimens were observed at 10 mab. These organisms have tests of organic material, which is highly susceptible to degradation in the water column and/or at the seafloor.

Fecal Pellets

Fecal pellets of many shapes, colors, and sizes were found in the sediment traps (Plate 4.2, 1-2; Figure 4.8 a,b). Most were >125 μm. The percentage, by number, of fecal pellets decreased toward the seafloor (Table 4.4). At 50 mab at Mooring 3 in the canyon, the sample is composed of 31% fecal pellets. This sample contains both well-formed tan to brownish fecal pellets and white fecal material as well. Traps at 100 mab at the other mooring sites have less than 5% of the sample composed of fecal pellets. Unfortunately, the traps at 500 and 100 mab from Mooring 3 did not function properly to determine if this high percentage of fecal material at 50 mab is regionally controlled. Counts of the samples from these two traps, which were open show ambiguous results. In the trap at 500 mab, 5% of the sample was fecal pellets, where in the trap at 100 mab, the figure was 68%.

Figure 4.8   Energy dispersive X-ray spectroscopy of sediment trap
              material;   a) fecal pellet from Mooring 3, 50 mab, see
              Plate 4.2, 1 for photomicrograph; b) fecal pellet from
              Mooring 3, 50 mab, see Plate 4.2, 2 for
              photomicrograph; c) vesicular volcanic shard from
              Mooring 2, 10 mab, see Plate 4.2, 10 for
              photomicrograph; d) quartz grain with iron-oxide
              coating from Mooring 2, 10 mab, see Plate 4.2, 11 for
              photomicrograph; e) altered volcanic shard from
              Mooring 2, 10 mab, see Plate 4.2, 12 for
              photomicrograph.
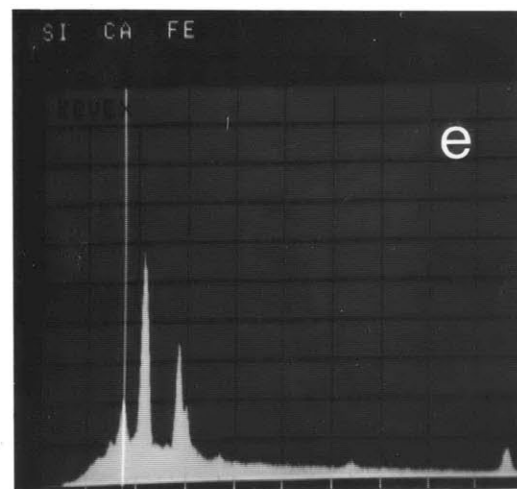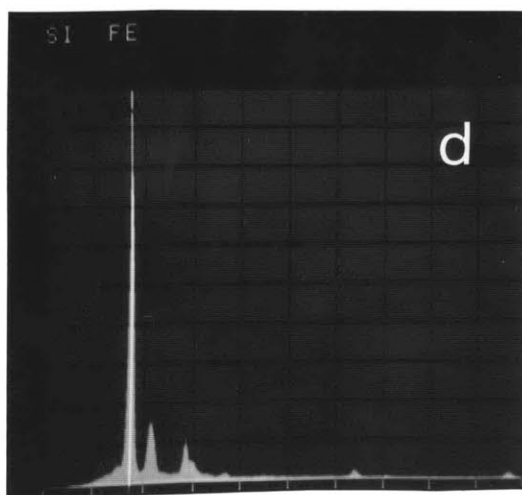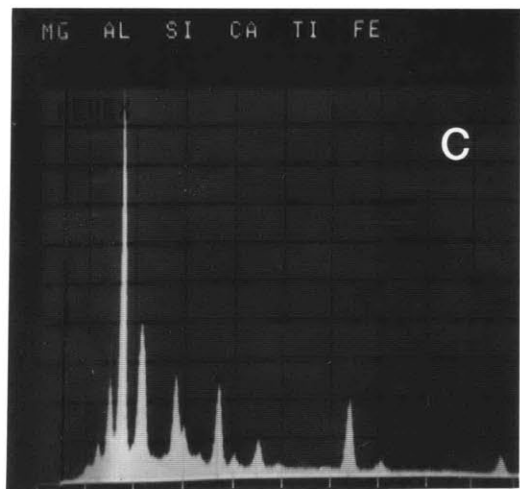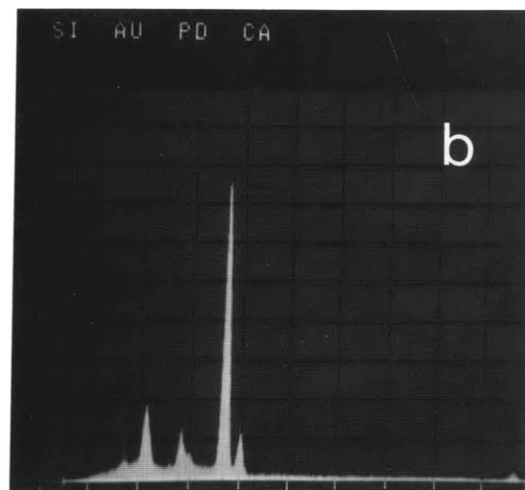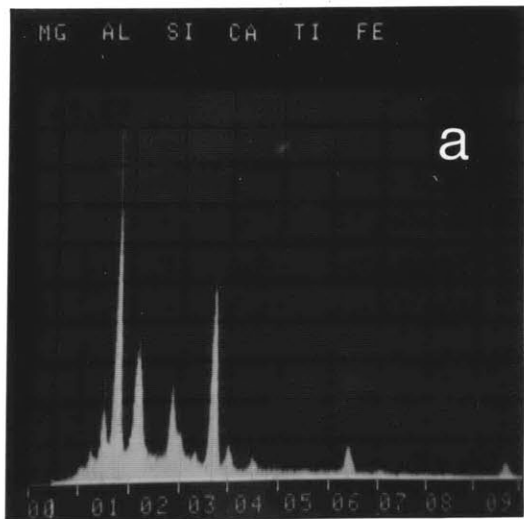
Unidentified Biogenic Material

Unidentified biogenic material comprising < 10% by number of the sample constituents was found in all size fractions of all the sediment traps. A general trend observed in the samples is a decrease in this group of particles toward the seafloor (Table 4.4). This category includes biogenic material too small to be definitively identified, biogenic aggregates, and unidentified test fragments.

Volcanic Glass

Two types of volcanic glass were observed in the trap samples; smooth glass shards and very vesicular fragments (Plate 4.2, 10,12; Figure 4.8, c, e). Both types were observed in all traps and in most size fractions. Volcanic glass was most prevalent in the small size fraction counted (63-125 μm), comprising up to 53% of this fraction. Some glass had smooth, shiny, sharp surfaces, while most volcanic shards showed alternation of its surface. A likely source of this component is Iceland.

Mineral Grains and Aggregates

Mineral grains and aggregates were combined in counting. Rounded particles and clay aggregates were the primary constituents in this category (Plate 4.2, 11; Figure 4.8 d). These components were found in all size fractions in most trap samples (Table 4.4). There is a dramatic increase in these components toward the

seafloor. For the traps at 10 mab, up to 60% of the trap sample >63 µm is composed of mineral grains and aggregates. For the traps above, 13% or less of the sample is composed of these particles.

Surface Sediments

Surface sediments from box cores 3, 4, 5, 6, 8, 10 and 15 were sieved at 63 µm to examine the coarse fraction of material and at 150 µm to separate juvenile forams. Percentages of a particular component were determined as a fraction of the total number of particles counted.

Foraminifera

Planktonic foraminifera are one of the major components of material >150 µm in the surface sediments (Table 4.6). Percentages of forams in this size fraction range from 12 to 65% and do not appear to be regionally controlled. The species of the forams do show some regional differences. N. pachyderma (dextral and sinistral), G. bulloides, G. glutinata, G. quinqueloba, and G. inflata (Plate 4.3, 1-6) were identified. N. pachyderma (sinistral) comprise 9-30% of the samples from box cores 3, 4, 5, 8 and 15, which all are located below the bottom current (Table 4.5). This same species comprises only 0-2% of the species from box cores 6 and 10 from the channel sites (Table 4.5). Other general trends are more N. pachyderma (dextral), G. bulloides, and G. quinqueloba in the box cores from the channel in comparison to the box cores

Table 4.6

PERCENTAGE OF SURFACE SEDIMENTS BY PARTICLE TYPE

Box Core	Size Fraction	Split	Forams	Radiolaria	Pteropods	Diatoms	Dino-flagellates	Fecal Pellets	Unidentified Biogenics	Volcanic Glass	Mineral Matter Aggregates	Total
3	150	1/64	17	0	0	1	0	0	9	33	40	1942
	150	1/2056	4	1	0	2	0	0	7	44	42	427
4	150	1/16	33	0	0	0	0	0	5	36	26	763
	150	1/256	1	1	0	1	0	0	2	71	25	907
5	150	1/16	19	0	0	0	0	0	5	27	49	1820
	150	1/512	1	1	0	1	0	0	2	77	20	650
6	150	1	12	1	0	0	0	0	0	0	87	1493
	150	1/64	6	0	3	0	0	0	3	45	30	943
8	150	1/64	46	0	0	0	0	0	3	7	44	598
	150	1/256	12	6	0	1	0	0	5	58	19	473
10	150	1	37	23	0	13	0	0	14	10	2	305
	150	1/64	6	9	0	1	0	0	0	4	77	524
15	150	1/64	65	0	0	0	0	0	8	19	8	135
	150	1/512	4	7	0	4	0	0	2	72	10	509

Plate 4.3   SEM photomicrographs of particles from the surface
             sediments.

1-6) Planktonic foraminifera:
    1. Neogloboquadrina pachyderma (sinistral), scale bar
       50 µm, X 290;
    2. Neogloboquadrina pachyderma (dextral), scale bar 50 µm,
       X 300;
    3. Globigerina bulloides, scale bar 50 µm, X 190;
    4. Globorotalia inflata, scale bar 50 µm, X 190;
    5. Globigerina glutinata, scale bar 50 µm, X 340;
    6. Neogloboquadrina pachyderma (sinistral), same species
       as (1) but have an iron-oxide coating, scale bar
       50 µm, X 300.
7-12) Benthic foraminifera, 7-11 from box core 5; 12 from box
       core 6:
    7. Parafissurina sp., scale bar 50 µm, X 320;
    8. Trifarina sp., scale bar 50 µm, X 190;
    9. Planulina wuellerstorfi, scale bar 50 µm, X 290;
   10. Melonis barleenum, scale bar 50 µm, X 230;
   11. A milliolid, Quinqueloculina or Trioculina, scale
       bar 50 µm; X 280.
   12. Pleurostomella sp., scale bar 100 µm, X 100.
13-16) Radiolaria from box cores 10 and 15:
   13. Nasselarian, Anthocyrtidium ophirense, scale bar
       50 µm, X 330;
   14. Nasselarian, Botryostrobus aquilonaris, scale bar
       20 µm, X 630;
   15. Smullerian, family Phacodiscidae, scale bar 50 µm,
       X 300;
   16. Smullerian, family Lithelidae, scale bar 20 µm, X 430.
17) Diatom fragment, perhaps Rhizosolenia, from box core 15,
    scale bar 100 µm, X 140.
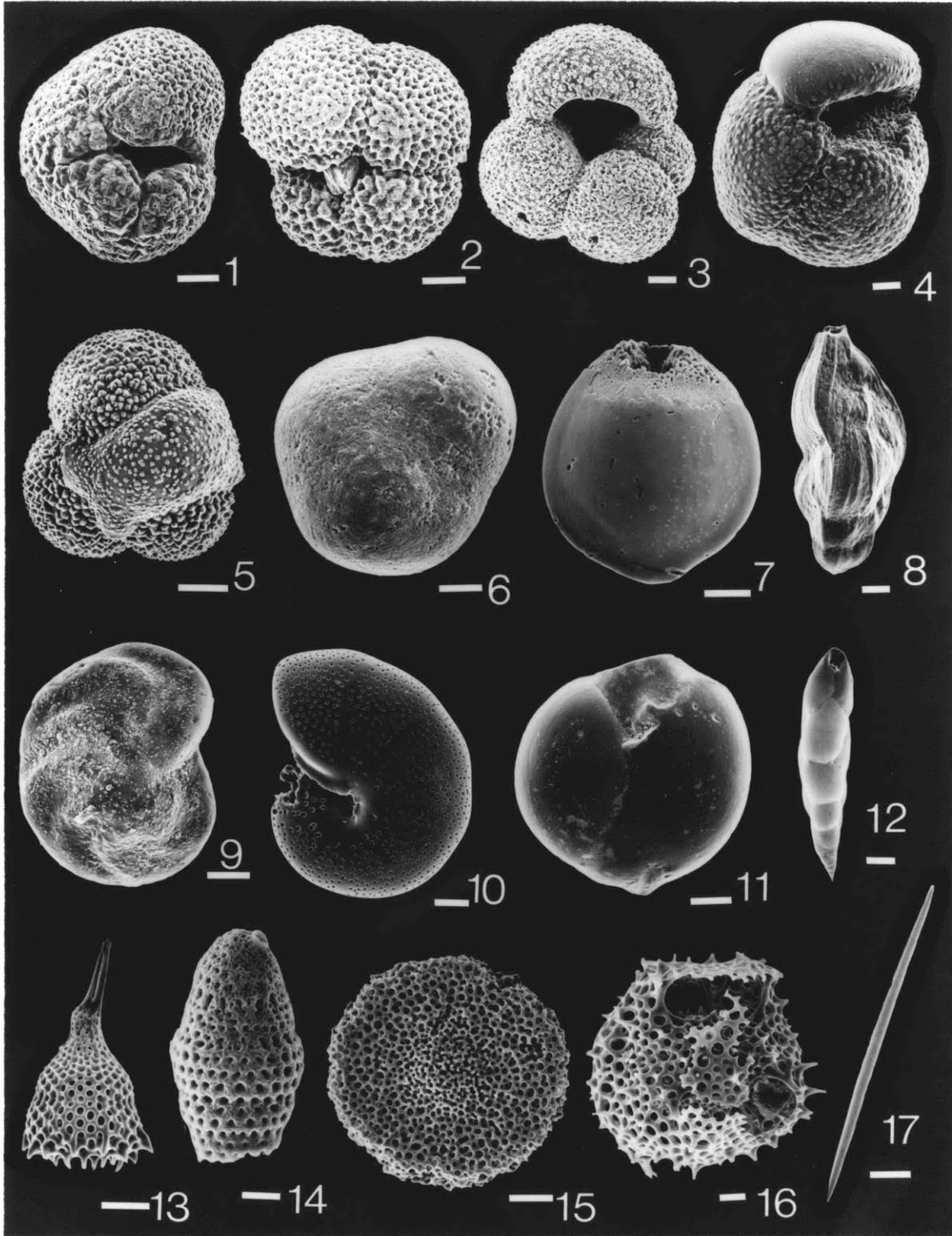
beneath the bottom current. The distribution of iron-oxide coatings on the forams is similar to that of N. pachyderma (sinistral). Only 1% of the forams from the box cores in the channel are iron-oxide coated; 22-45% of the forams from the box cores beneath the bottom current have the coating. In the size fraction <150 µm forams compose a much smaller percentage of the sample (1-6%).

Benthic forams were found in all the sediment samples. Some observed were Parafissurina sp., Trifarina sp., Planulina wuellerstorfi, and Melonis barleeanum (Plate 4.3, 7-12). Benthic forams constituted 1-13% of the total number of forams present. The benthic forams of a channel box core (core 6) were dominated by Pleurostomella sp. This same species was not observed in nearby box core 10.

Radiolaria

Radiolaria comprise only a few percent of the <150 µm and >150 µm size fractions for the box cores taken beneath the bottom current (Table 4.6). Within the canyon, radiolaria are relatively more abundant (Plate 4.3, 3-16). Spumellarians were the dominant group of radiolaria found in the sediments. Some nasselarians, but no phaeodarians, were present.

Pteropods

No pteropods were found in any of the surface sediment samples examined. However, layers of pteropods have been observed to be common down core in one piston core in the canyon (Shor, 1979).

Diatoms

Diatoms are generally absent from the >150 μm size fraction.
However, 13% of the sample from box core 10 in the channel is
composed of diatoms. Diatoms, mostly Rhizosolenia (Plate 4.3, 17),
are a few percent of the <150 μm size fraction.

Dinoflagellates, Fecal Pellets and Unidentified Biogenic Material

Dinoflagellates and fecal pellets were absent from the sediment
samples examined (Table 4.6). Unidentified biogenic material was
found as only a very minor component of box core 15 (Table 4.6).

Volcanic Glass

Volcanic glass is the most abundant component of the sediment
samples (Plate 4.2, 13, 14; Figure 4.9a,b), comprising from 31-71%
by number of the particles counted (Table 4.6). It is more common
in the <150 μm fraction than the >150 μm fraction. Some of the
glass shards show surface alteration.

Mineral Grains and Aggregates

Mineral grains and aggregates are another principal constituent
of the sediment samples (Plate 4.2, 15-17; Figure 4.9c-e). They
comprise 3-41% of the samples >63 μm (Table 4.6). Most particles
counted were single grains. However, in box core 6 from the
channel, the majority (87%) of the material >150 μm was composed of
clay aggregates that were not disaggregated by sonification.

Figure 4.9   Energy dispersive X-ray spectroscopy of surface
              sediments from box core 5; a) vesicular volcanic
              shard, see Plate 4.2, 13 for photomicrograph; b)
              volcanic shard, see Plate 4.2, 14 for photomicrograph;
              c) mineral grain, see Plate 4.2, 15 for
              photomicrograph; d) mineral grain with iron-oxide
              coating, see Plate 4.2, 16 for photomicrograph; e)
              quartz grain, see Plate 4.2, 17 for photomicrograph.
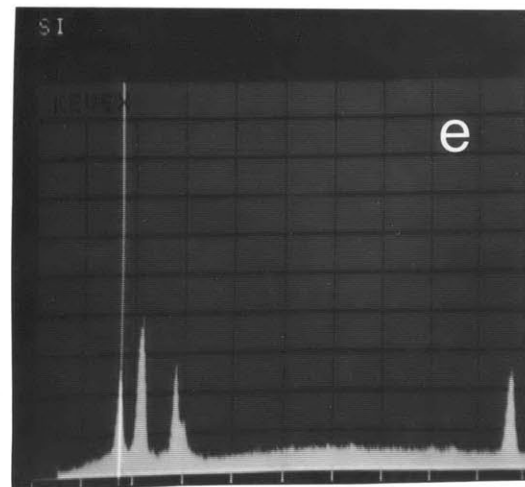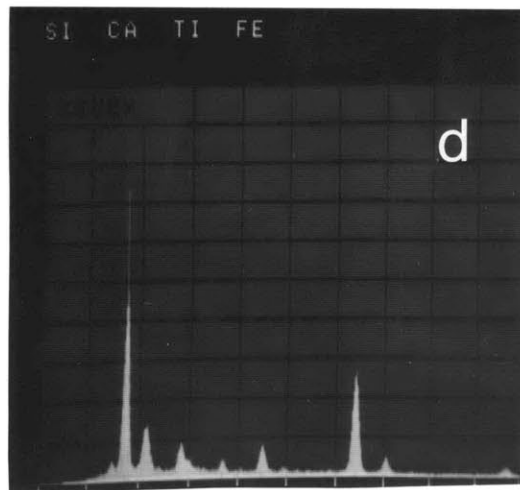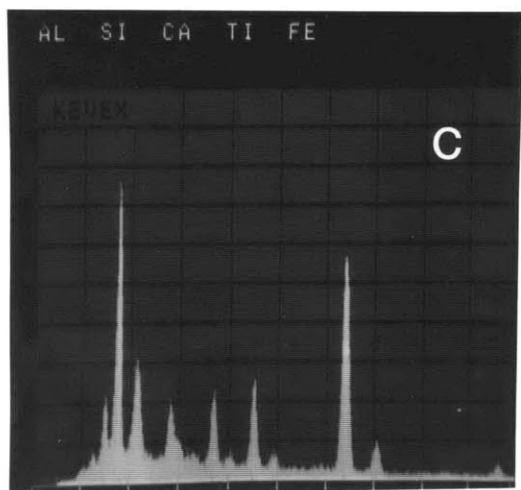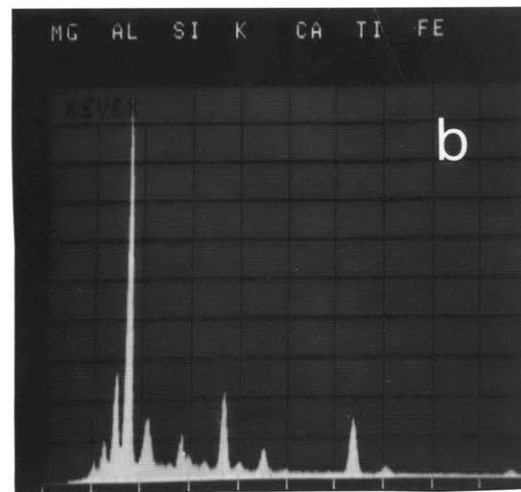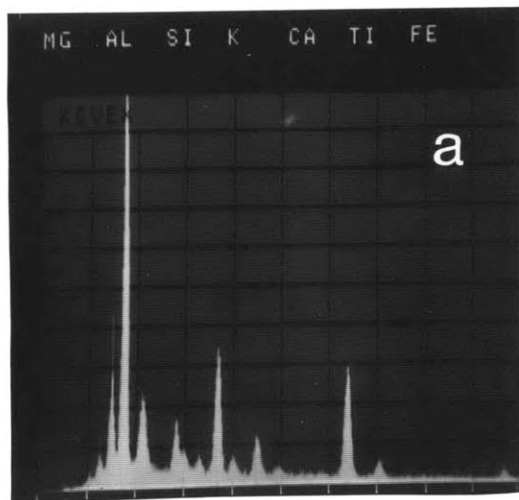
Combining the categories of volcanic glass and mineral grains

and aggregates demonstrates that the majority of the particles

preserved at the seafloor are not biogenic. Together these

categories comprise from 53 to 85% of the sediment samples.

MINERALOGY

Sediment Traps

Due to the limited amount of material collected by the sediment

traps, powder mounts for bulk composition by X-ray diffraction were

made only for the surface sediment samples. However, enough

material from sediment traps at 10 mab was available to make

oriented mounts of the <2 μm fraction which was filtered onto silver

filters. This procedure precludes semiquantitative analysis; only

presence or absence of particular minerals can be determined. The

principal minerals detected were quartz, feldspar, calcite, and some

clays (Figure 4.10). The quartz and feldspar are from volcanic

material and mineral grains; the calcite is biogenic. Clays were

not well detected due to dilution by the other constituents. Those

detected were chlorite, smectites, and illite. Illite was detected

only at Mooring 2, in the axis of the bottom current.

Surface Sediments

Surface sediments from box cores have the same components as the

sediment traps at 10 mab. Semiquantitative analysis was performed

by using peak areas on the diffractograms of the minerals present

Figure 4.10   X-ray diffractogram for a sediment trap sample.
               Minerals detected are calcite, quartz, feldspar,
               montmorillonite, chlorite and illite.

X-RAY DIFFRACTOGRAM
FROM MOORING 2, 1600 m
TRAP AT 10 mab
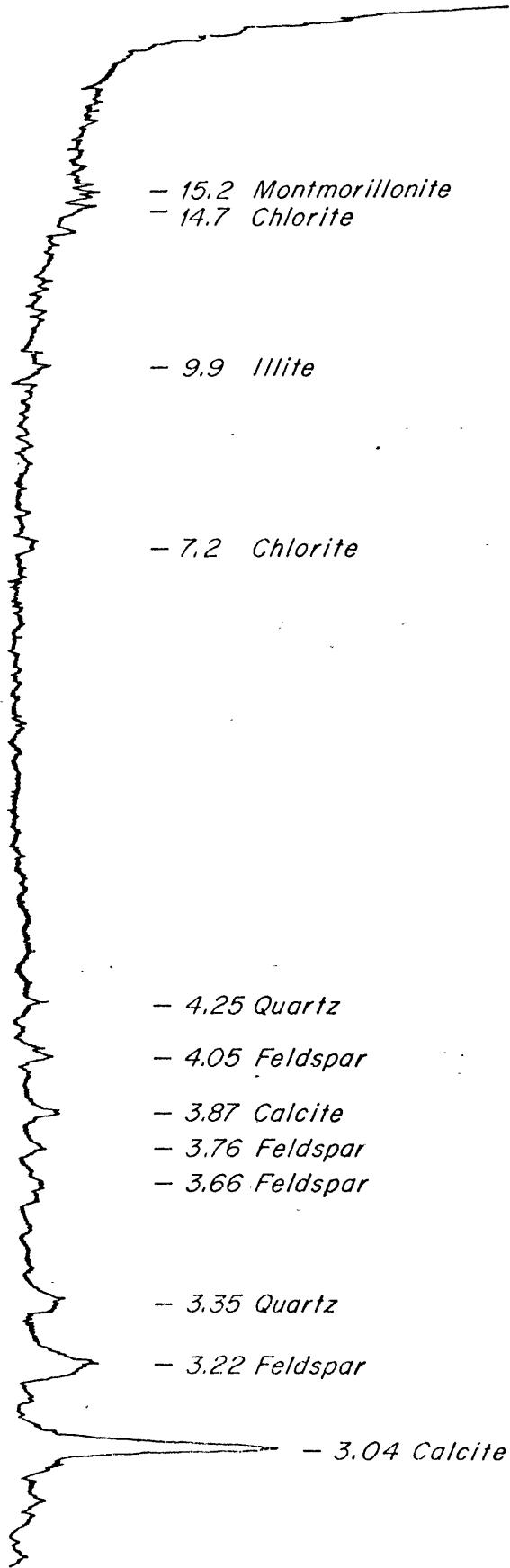
— 15.2 Montmorillonite
— 14.7 Chlorite

— 9.9 Illite

— 7.2 Chlorite

— 4.25 Quartz

— 4.05 Feldspar

— 3.87 Calcite
— 3.76 Feldspar
— 3.66 Feldspar

— 3.35 Quartz

— 3.22 Feldspar

— 3.04 Calcite

(Table 4.7). Quartz, feldspar, and calcite are the dominant
minerals detected (Figure 4.11). Montmorillonite, chlorite, and
illite are the clays present. Illite is absent from, or composes a
smaller percentage than, montmorillonite or chlorite in the channel
box cores (Table 4.7). For the box cores taken beneath the axis of
the current, the percentage of illite is greater than or equal to
the percentages of montmorillonite or chlorite. This suggests a
differentiation of the clay minerals that may be controlled by the
bottom current or channel.

CARBONATE CONTENT

The carbonate content of the sediment-trap samples decreases
from 500 mab to 10 mab and then further to the surface sediments
(Figure 4.12). From optical identification of the particles in the
trap samples, both forams and pteropods comprise the coarse
carbonate fraction. Acidification indicates that carbonate
comprises up to 90% of the trap samples at 500 mab. Surface
sediments at the mooring sites have values as low as 15%.

Carbonate percentages of the surface sediments vary regionally
(Figure 4.13). Low values (9 to 21%) are found for the northern
transect box cores and box core 8 atop the channel level, along the
southern transect. The box cores within the channel have higher
carbonate contents (21-30%). This indicates that the channel may be
preferentially retaining or obtaining carbonate material, or the
bottom current is preferentially removing it.

Table 4.7

SEMIQUANTITATIVE MINERALOGY OF SURFACE SEDIMENTS*

Box Core	Calcite	Quartz	Feldspar	Montmor- illonite	Chlorite and Kaolinite	Illite
3	15	9	11	0.8	0.5	0.7
4	12	11	14	8	4	4
6	30	6	12	6	7	3
7	25	4	10	2	1	–
8	30	13	14	3	2	3
9	41	4	10	13	3	–
10	35	6	13	17	6	2
11	25	6	11	11	8	2
12	30	5	15	14	4	–
15	31	6	10	3	1	2

*Values are recorded as the percentage of the samples composed of each mineral. Peak areas were compared to peak areas of standards to obtain relative percentages.

Figure 4.11   X-ray diffractogram for a box core sample. Minerals
detected are quartz, feldspar, calcite, mont-
morillonite, chlorite and illite.

X-RAY DIFFRACTOGRAM
BOX CORE 3
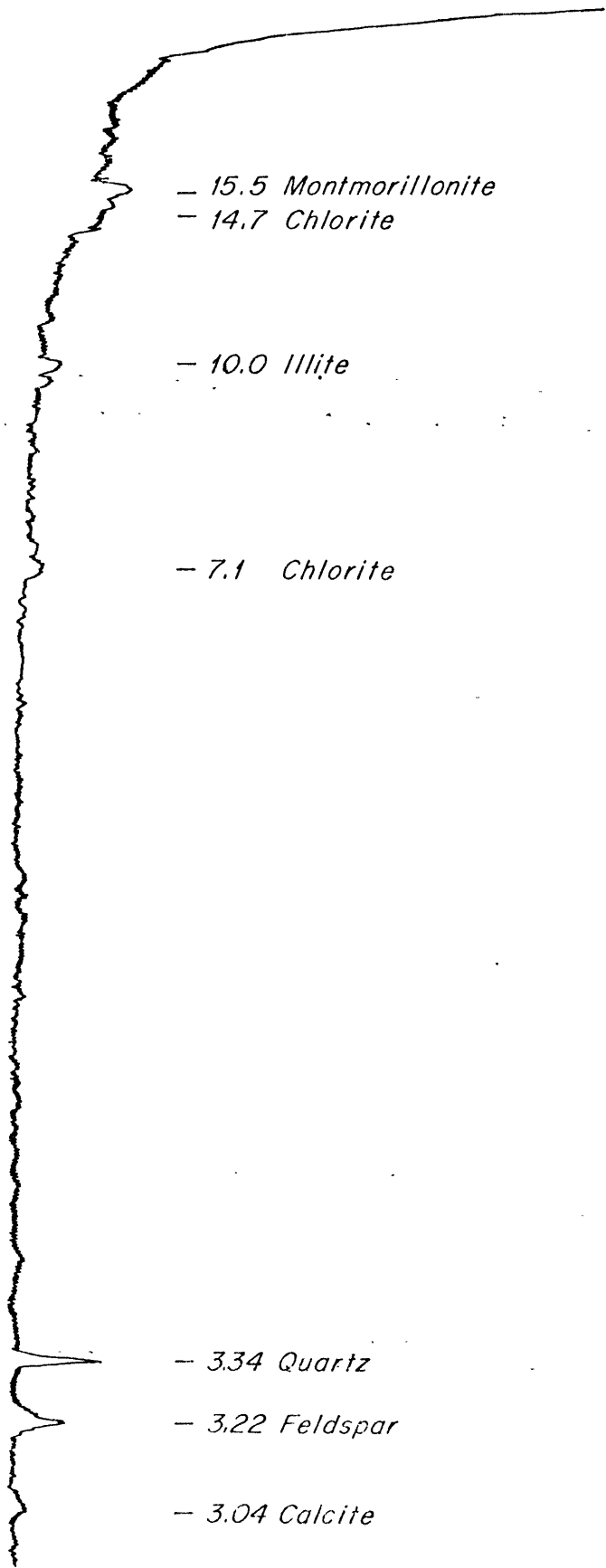
— 15.5 Montmorillonite
— 14.7 Chlorite

— 10.0 Illite

— 7.1 Chlorite

— 3.34 Quartz

— 3.22 Feldspar

— 3.04 Calcite

-186-

Figure 4.12   Carbonate percentage in sediment trap and box core
               samples. Percentage of carbonate decreases with depth
               through the water column to the surface sediments.

CARBONATE PERCENTAGE
IN SEDIMENT TRAP AND
BOX CORE SAMPLES

MOORING 1   MOORING 2   MOORING 3

HEIGHT ABOVE BOTTOM (m)
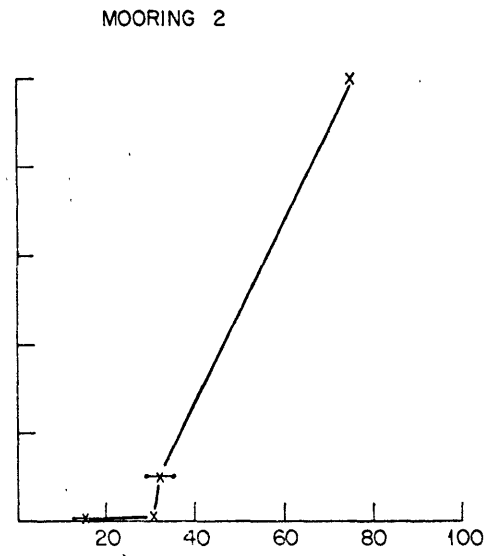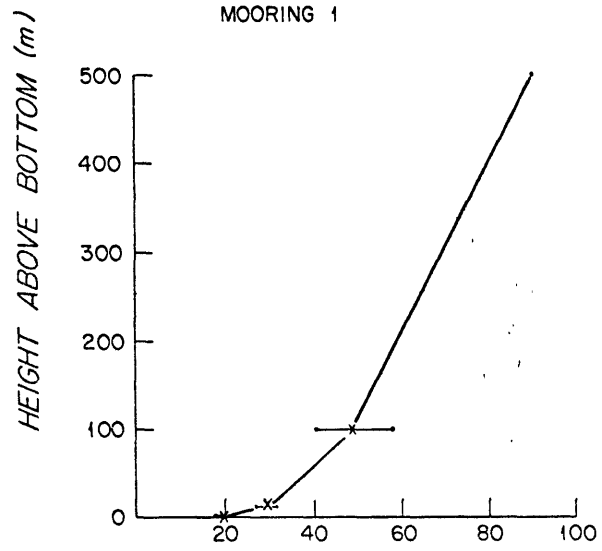
$CaCO_3$ (%)
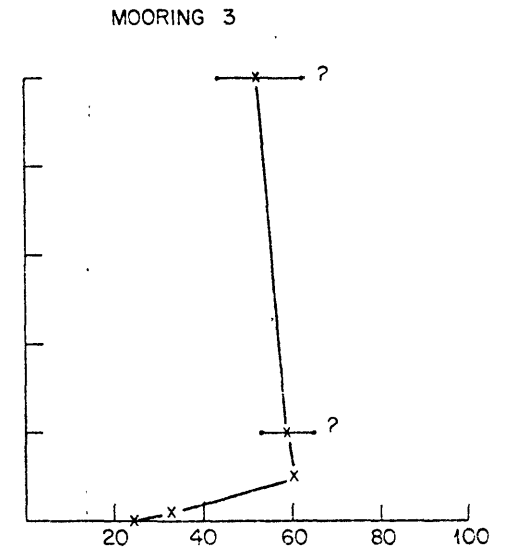
Figure 4.13   Calcium carbonate percentages for box core surface
               samples. The distribution of carbonate varies
               throughout the region with higher values in the
               channel stations.
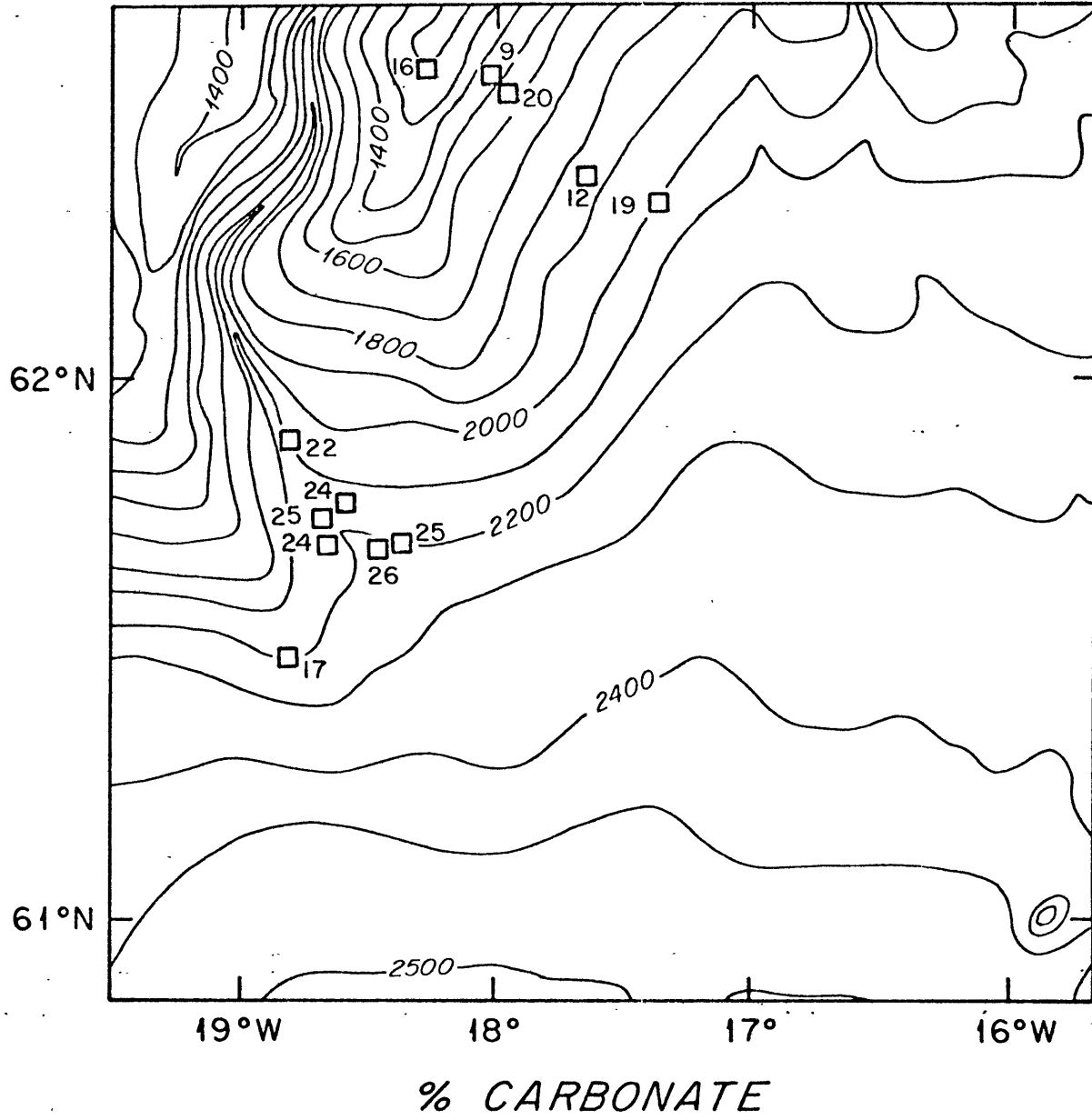
% CARBONATE

ORGANIC CARBON AND NITROGEN CONTENTS

As with carbonate percentages, organic-carbon percentages in the sediment-trap samples show a decrease toward the seafloor (Figure 4.14). However, mooring 1, at 2000 m, shows a low organic carbon content at 500 mab, smaller than those values at 100 mab and 50 mab for the same mooring. This low value is anomalous, particularly since this sample has an overwhelming (90%) percentage of carbonate. In this case, organic carbon is unexpectedly not directly associated with biogenic calcium carbonate (Heath et al., 1977). Organic-carbon contents decrease from >1.25% for the trap samples at 10 mab to < 1.25% in the surface sediments.

The regional picture for the content of organic carbon in the surface sediments shows the same trends as for carbonate (Figure 4.15). Box cores from the channel have higher organic carbon content, >0.80%. Cores taken along the northern and southern transect strongly influenced by the bottom current, have lower organic carbon contents (0.16-0.50%).

Ratios of organic carbon to nitrogen also vary through the water column (Table 4.8). The moorings along the northern transect have high ratios (>7.8), but there are no consistent trends with depth. The sediments beneath these moorings also have high ratios (7.9-9.6). The channel mooring has lower ratios (8.4 and 7.0 at 50 and 10 mab, respectively), and ratios in box core surface sediments range from 6.9 to 7.6 (Table 4.9). These differences are not as distinct as those for the content of organic carbon.

Figure 4.14   Organic carbon percentages in sediment trap and box core samples. Values generally decrease through the water column to the surface sediments.

ORGANIC CARBON PERCENTAGE IN SEDIMENT
TRAP AND BOX CORE SAMPLES

MOORING 1   MOORING 2   MOORING 3
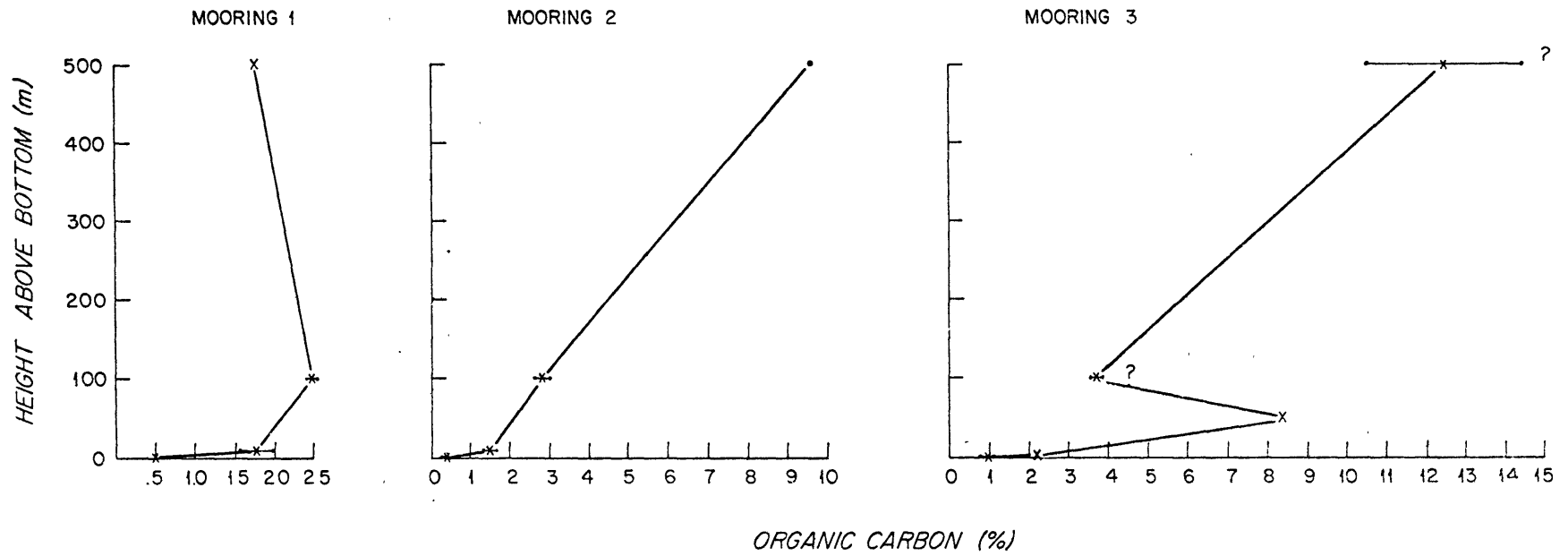
ORGANIC CARBON (%)

Figure 4.15   Organic carbon percentages for box core surface
               samples. The distribution of organic carbon varies
               throughout the region with higher values at the
               channel stations.
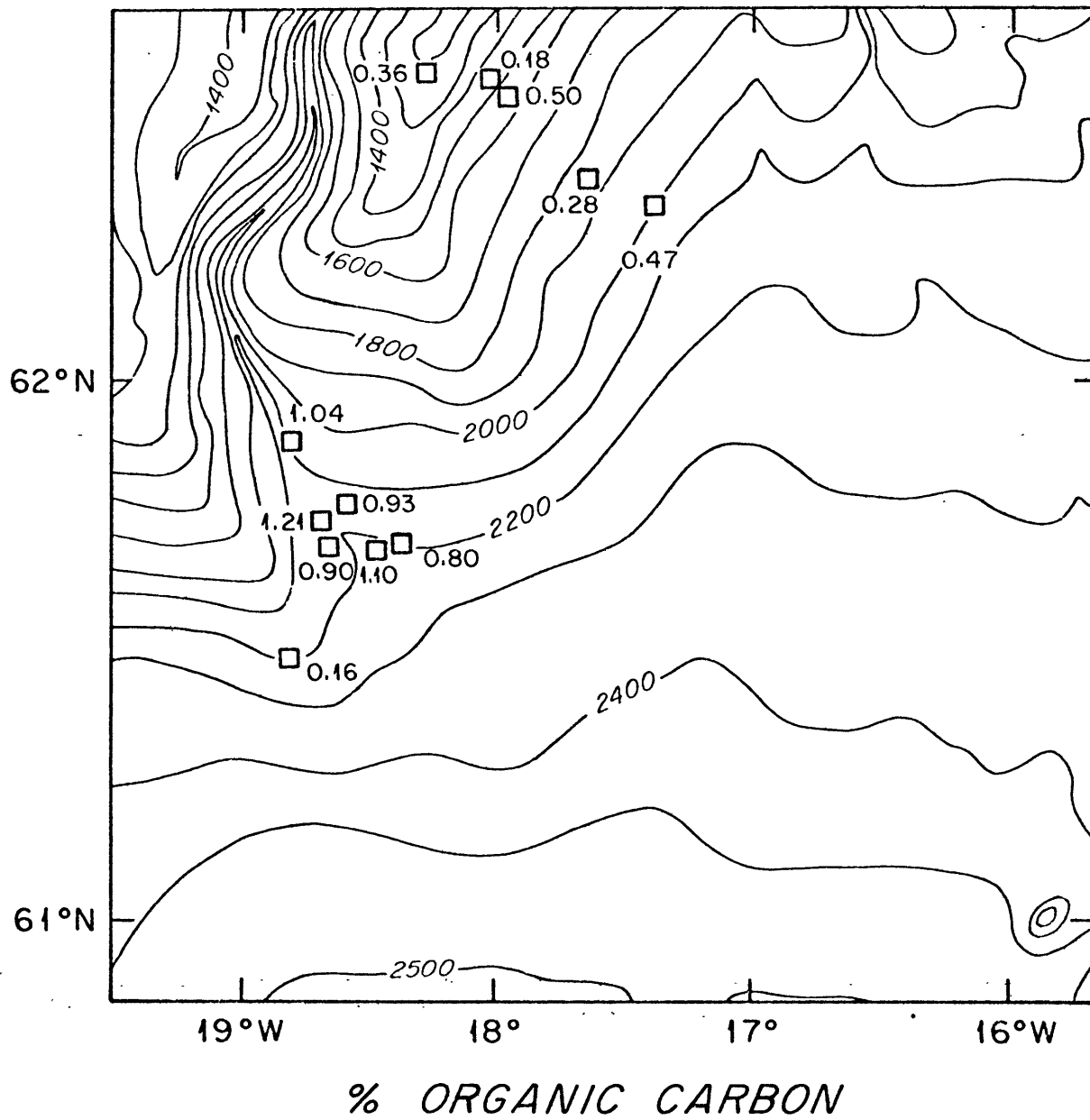
% ORGANIC CARBON

Table 4.8

CARBONATE, ORGANIC CARBON AND NITROGEN FROM SEDIMENT TRAPS

| Mooring	Mab	Split	Filter#	Total Weight (mg)	$CaCO_3$	C(µg)	N(µg)	C/N	%$CaCO_3$	%OC
1	500	1/128	587	2.83	2.55	49.7	5.5	9.0	90	1.76
1	100	1/64	585	3.25	1.89	78.7	10.0	7.9	58	2.42
1	100	1/64	586	3.50	1.41	87.7	9.0	9.7	40	2.51
1	10	1/256	583	26.03	8.07	532.	46.9	11.3	31	2.04
1	10	1/256	584	24.33	6.31	375.	47.9	7.8	26	1.54
2	500	15/128	552	1.76	1.33	168.	19.9	8.4	76	9.35
2	100	1/8	553	4.44	1.29	135.	14.2	9.5	29	3.04
2	100	15/128	554	4.67	1.63	129.	15.4	8.4	35	2.76
2	10	1/64	557	76.75	22.79	1192.	132.	9.0	29	1.55
2	10	1/64	558	78.42	25.25	1136.	146.	7.8	32	1.45
3	500	1/8	568	1.46	0.63	212.	19.6	10.8	43	14.52
3	500	15/128	569	1.04	0.64	109.	11.8	9.2	62	10.58
3	100	1/16	571	2.20	1.44	79.5	9.9	8.0	65	3.61
3	100	1/16	572	1.96	1.03	75.0	9.3	8.1	53	3.83
3	50	1/16	573	1.33	0.80	112.	13.3	8.4	60	8.42
3	10	1/64	582	25.71	8.43	570.	82.0	7.0	33	2.22

Table 4.9

CARBONATE, ORGANIC CARBON AND NITROGEN FROM SURFACE SEDIMENTS

Box Core	Filter#	Total Weight (mg)	CaCO$_3$	C(μg)	N(μg)	C/N	%CaCO$_3$	%OC
3	3213	71.79	14.0	360.	37.4	9.6	20	0.50
4	3214	44.03	5.35	125.	16.7	7.5	12	0.28
6	3216	57.82	14.27	697.	99.1	7.0	25	1.21
7	3217	43.19	9.68	449.	64.3	7.0	22	1.04
8	3218	65.64	11.30	108	25.8	4.2	17	0.16
9	3219	44.60	11.06	358.	47.4	7.6	25	0.80
10	3220	77.33	20.46	854.	123.	6.9	26	1.10
11	3221	44.33	10.57	401.	54.3	7.4	24	0.90
12	3222	43.57	10.5	410.	56.3	7.3	24	0.93
13	3223	60.90	9.52	218.	25.1	8.7	16	0.36
14	3224	97.27	8.52	179.	29.0	6.2	9	0.18
15	3226	46.05	8.77	217.	27.4	7.9	19	0.47

A parameter which shows a clear distinction between samples from the channel and those from beneath the bottom current is the ratio of the percentages of organic carbon to calcium carbonate. Cores from the channel have a ratio of 0.041 ± 0.006; cores from beneath the bottom current, 0.022 ± 0.003. These ratios reflect that less organic carbon is found beneath the bottom current than in the channel cores with respect to calcium carbonate. This may be due to greater input or preservation of organic carbon in the channel, or alternatively, increased degradation beneath the bottom current. Another possibility would be that this ratio reflects differences in the sediment grain size or age. The material beneath the current is coarser and older than that in the channel.

DISCUSSION

The data obtained here are used to verify local resuspension and transport by the bottom current, assess changes that occur to particulate material in transit through the water column, and estimate the distance of transport of the material collected in the traps.

PRESENT-DAY RESUSPENSION OF SEDIMENTS

Four components of the size fraction greater than 125 μm, for the traps at 10 mab, substantiate present-day local resuspension by the bottom current.

Benthic foraminifera (e.g., _Parafissurina_ sp. and _Uvigerina_ sp.) were collected in all the traps at 10 mab in the study area. These forams provide conclusive evidence of active, present-day resuspension. Benthic foraminifera reside on the seafloor, and therefore must have been resuspended from the seafloor into the traps. These forams are larger than 125 μm and therefore have high settling velocities, (some >1 cm/sec), which would indicate that they are locally derived. Distance of transport of the trapped material is discussed in a later section.

Another component of the sediment-trap material indicative of active erosion is _N. pachyderma_ (sinistral). The typical Recent subpolar assemblage in this area is composed of _N. pachyderma_ (dextral), _G. bulloides_, and _G. quinqueloba_ (Ruddiman and McIntyre, 1976). Indeed, these are the predominant foraminiferal species present in the trap samples. However, the single species which defines the polar water and Pleistocene glacial assemblage of this region, _N. pachyderma_ (sinistral) (Ruddiman and McIntyre, 1976), is also present. This suggests that either glacial sediments are presently being eroded or _N. pachyderma_ (sinistral) are being advected from polar regions. Surface sediments in the region contain _N. pachyderma_ (sinistral), so extensive advection does not need to be invoked to explain the data.

A third line of evidence for present-day erosion of material lies in the condition of the planktonic foraminifera in the traps. Planktonic forams secrete their tests in surface waters. Forams

falling directly from the surface are translucent to white, and some
still have spines (Bé, 1977). Some forams which have resided on the
seafloor develop an iron-oxide staining to their tests and become
orange in color. Numerous forams coated with iron oxide were
observed in the surface sediments of the region (Table 4.5). Some
iron-oxide-coated planktonic forams were observed in the sediment
traps at 10 mab (Table 4.5), giving additional evidence of present-
day resuspension.

Further evidence for resuspension is the increase in the
percentage of volcanic glass and mineral matter collected in the
sediment traps with depth (Table 4.4). Percentages of these
components in the $> 250\,\mu m$ size fraction increase from $< 1-7\%$ at
500 mab to 15-67% at 10 mab. Surface sediments near the moorings
have 27-87% volcanic glass and mineral matter in the $> 250\,\mu m$ size
fraction (Table 4.6). Dissolution and degradation of biogenic
material at the seafloor probably accounts for the percentage
differences seen from 500 mab to the surface sediments, while the
increase from 500 mab to 10 mab (Table 4.4) is attributed to
resuspension of the biogenic-poor surface sediments.

The size fraction of material from 63-125 μm that is caught by
the sediment traps is composed primarily of juvenile foraminifera,
diatoms, fecal pellets, volcanic glass, and clay aggregates. A few
tiny ($< 125\,\mu m$) benthonic forams were also found in this size
fraction. These particles can be transported greater distances by
the bottom current than those $> 125\,\mu m$ before they are deposited. In

the traps at 10 mab, the 63-125 μm size fraction is dominated by volcanic glass and clay aggregates, but in the upper traps, forams and diatoms are also important.

Some benthic forams were found in the traps at 100 mab in the 63-125 μm size fraction. In one case, three benthic forams were found in the trap at 500 mab from Mooring 1. These occurrences suggest that some small resuspended seafloor material is found up to 500 mab.

Resuspended material (benthic foraminifera, iron-oxide-coated planktonic foraminifera, and glacial-assemblage planktonic foraminifera, together with an increase in volcanic glass and mineral matter with depth) has been found in sediment traps located at 10 mab with some found up to 500 mab. These components of the sediment-trap material particularly at 500 mab, may conceivably have come from an upslope source and been transported downslope to the traps. However, the large size and fast settling velocities of the foraminifera and volcanic and mineral grains argues for a local source and local resuspension. An assessment of the distance of transport of the resuspended material is contained in a later section.

ADVECTIVE TRANSPORT BY THE BOTTOM CURRENT

The bottom current transports large quantities of material into and out of the study area. A relationship of the potential temperature to suspended particulate matter distributions, the quantity of material transported by the current and its variability

with time, and a comparison of horizontal and vertical fluxes are discussed in this section.

Relationship of the Bottom Water to Suspended Particulate Matter

The distribution of suspended particulate matter reflects the influence of the bottom current. A well developed near-bottom nepheloid layer is present throughout most of the region (Figure 3.8). An association between the bottom water and the nepheloid layer is brought out in a compilation of the data on potential temperature and light scattering from the hydrographic stations.

There is a sharp increase in light scattering in water colder than $3.3^{o}C$ potential temperature (Figure 4.16). A diagram of potential temperature versus salinity shows that water colder than $3.3^{o}C$ has a large component of Norwegian Sea Deep Water (Figure 4.17). Above $3.3^{o}C$, the salinity range increases dramatically due to the introduction of Labrador Sea Water. The $3.3^{o}C$ boundary is below the reference level used by Shor (1979) in calculating volume transport through this region. His reference level was intended to be a level of no motion. The $3.3^{o}C$ boundary separates water of Norwegian Sea origin from that having a strong component of Labrador Sea Water and may indicate the boundary of the strong flow of the bottom current. The association of the bottom water with the high light-scattering values suggests that the current carries large quantities of suspended sediment through the region and may locally resuspend material from the seafloor without significant mixing between the current and the surrounding water of the basin.

Figure 4.16   Potential temperature versus light scattering plot. A
sharp increase in light scattering is seen below
$3.3^{\circ}C$ potential temperature indicating an
association between high concentrations of suspended
matter and the strong bottom current.

ICELAND RISE
NORTHERN SECTION
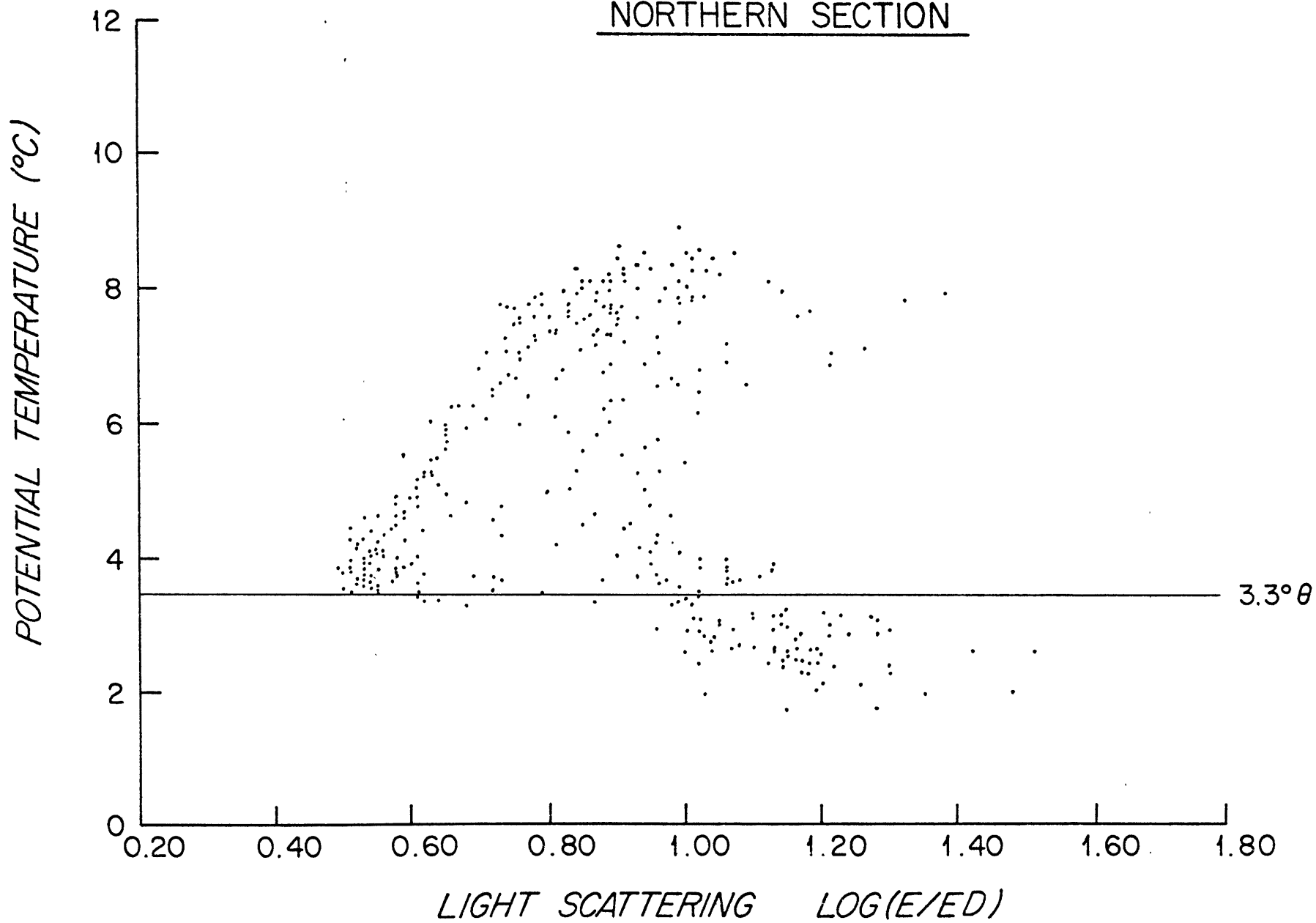
Figure 4.17   Potential temperature versus salinity plot showing the difference between the Shor (1979) reference level and the 3.3°C potential temperature boundary. The latter minimizes the Labrador Sea Water component.
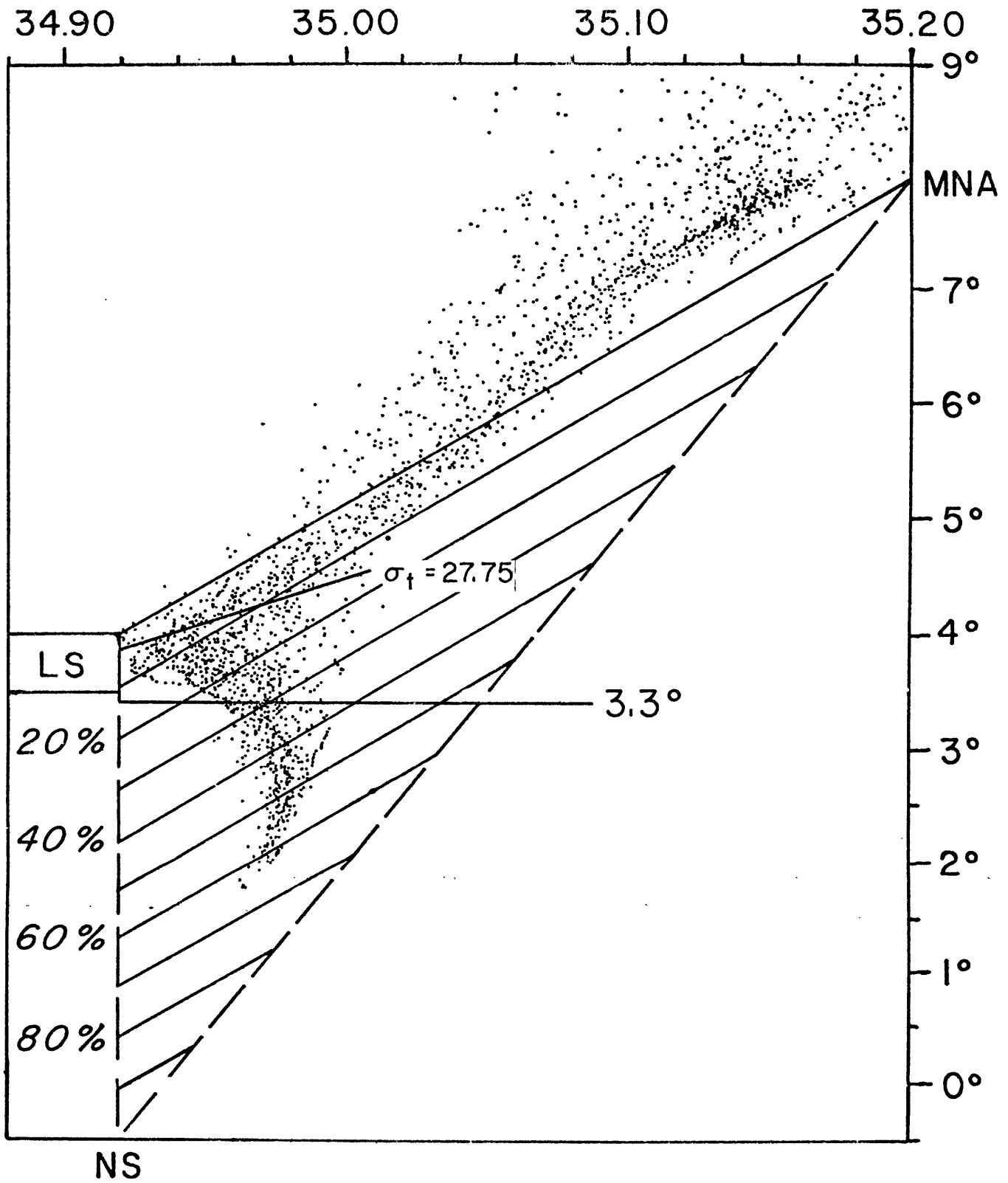
Quantity and Variability of Advective Transport

Routh estimates of horizontal fluxes of suspended particulate matter can be computed by multiplying current velocities by suspended-matter concentrations. Based on geostrophic calculations of water velocities (Shor, 1979) and suspended-particle concentrations from filtration of water samples, the amount of material advected through the northern transect of stations (Figure 2.2) is on the order of 50-200 kg/sec, using standard concentrations and corrected concentrations, respectively. Shor (1979) estimated the horizontal flux using light-scattering measurements converted to suspended-matter concentrations and obtained 100 kg/sec. These estimates of horizontal flux are subject to a large amount of temporal variability and measurement uncertainty.

A reoccupation of Station 28 at approximately 2000 m was made (Station 84), which provides one estimate of the variability in the geostrophic volume transport of water. Transport across the northern transect of stations using Station 28 yields a flow of 5.6×10^6 m^3/sec; substitution of Station 84 into the northern section results in transports of 5.0×10^6 m^3/sec (Shor, 1979). The difference in the transport estimates between the nearest stations upslope and downslope of Stations 28 and 84 is 2.5×10^6 and 1.9×10^6 m^3/sec. Based on the hydrographic stations a temporal variability of at least 30% should be considered reasonable in estimates of water transport.

Current velocities measured by the current meters are uniform
and steady in the axis of the bottom current (Figure 2.5). East of
the axis of the current (at approximately 2000 m) flow speed varies
by an order of magnitude, from current meter stall speeds < 2 cm/sec
to speeds in excess of 20 cm/sec. These measurements were taken on
the boundary of the current and probably reflect spatial meandering
of the current rather than temporal variability of the bottom
current velocity.

Based on the nephelometer lowerings at Stations 28, 40, and 84,
net particulate standing crops (Biscaye and Eittreim, 1977) were
calculated to be 4075, 1834, and 1775 $\mu g/cm^2$ respectively. These
values indicate temporal variation in suspended matter by at least a
factor of two.

Combining the variations in water transport and in suspended-
particle concentrations suggests that during this study, temporal
variability of the horizontal flux of suspended particulate matter
is approximately a factor of 2.5.

HORIZONTAL VERSUS VERTICAL FLUXES

Estimation of the apparent vertical flux of material to the
bottom from the surface waters can be made with the sediment traps
located at 500 mab. Apparent fluxes measured by the traps are
~ 2 mg/cm^2/yr, which together with a density estimate of
1.5 g/cm^3 implies a sedimentation rate of 3 cm/1000 yr. This rate
is low in comparison to the long-term deposition rates for the

Recent measured in cores in the Iceland Basin, >30 cm/1000 yr (Shor, 1979). The rate measured by traps compares most closely with the sedimentation rate observed beneath the current axis (<1-2 cm/1000 yr), which certainly is not a situation of continuous deposition. Cores from beneath the current have coarse surface sediments, apparently winnowed of fines. If the traps collected an accurate vertical flux of material, as suggested by Gardner (1980), then, additional material must be introduced into the region other than directly from the surface waters, or alternatively, the fluxes were measured for an anomalous period of low surface input. This study was conducted over a short time scale of two weeks during the summer, a period of high biological productivity. Due to melting, the terrestrial input from Iceland would also be greatest during the spring and summer. Therefore, it seems likely that there is additional material input into the region from other than surface waters. The most likely sources for this additional material are turbidity currents or the bottom current. The horizontal flux of material into the region by the bottom current, $\sim$100 kg/sec or 2×10^4 mg/cm^2/yr, is three orders of magnitude greater than the sedimentation rate indicated for the Recent in cores, 30 cm/1000 yr or 20 mg/cm^2/yr, indicating that the bottom current is a likely source of material transported into and deposited in the region, as well as further downstream south of the Iceland Rise. The large quantity of material carried by the current is sufficient to make up the deficit indicated by the sediment trap as well being a likely source of material for the Gardar sediment drift downstream.

ESTIMATES OF THE QUANTITY OF RESUSPENDED MATERIAL

Estimates can be made of the resuspended fraction in the trap samples based on the quantities and percentages of mass, calcium carbonate, and organic carbon. Gardner (1977a) estimated the resuspended component by assuming that the samples at 500 mab are composed entirely of primary material with no resuspended fraction. For the traps below 500 mab, the amount of resuspended material is the quantity of material greater than that collected at 500 mab, i.e.,

$$\% \text{ Resuspended} = \frac{M_{10} - M_{500}}{M_{10}}$$

where M = quantity of material collected by the traps and the subscripts represent heights above the seafloor. Using his method and assumptions, an average of 59% ± 6% of the material caught at 100 mab has a seafloor source (Table 4.10). At 10 mab 98-99% of the material is estimated to be resuspended (Table 4.10).

By assuming that the material in the traps at 100, 50, and 10 mab is a simple mixture of primary material of the composition caught at 500 mab and the surface sediments as obtained with box cores, calculations of the percentage of the resuspended component can be made, e.g.,

$$F \times \% \text{trap}_{500} + (1-F) \times \% \text{core} = \% \text{trap}_{10 \text{ or } 100}$$

where F = fraction of primary material and 1-F = fraction of resuspended material. Calculations are made only for Moorings 1 and 2, since the 500 mab sample at Mooring 3 returned open.

Table 4.10

CALCULATED PERCENTAGE OF RESUSPENDED MATERIAL
FROM MASS, CARBONATE AND ORGANIC CARBON

Mooring	mab	Mass (mg)	% Resusp.	% CaCO$_3$	% Resusp.	% OC	% Resusp.
1	500	68.0	0	90	0	1.51+0.36	0
1	100	147.6	54	49+13	59	2.47+0.06	0
1	10	3867.	98	28+4	89	1.79+0.35	0
Core 15				20+1		0.91+0.62	
2	500	15.9	0	56+28	0	9.55	0
2	100	36.4	56	32+4	60	2.93+0.23	72
2	10	4072.	99	30+2	65	1.50+0.07	87
Core 3				16+4		0.35+0.13	

These calculations lead to the estimate of 59% for the resuspended fraction at 100 mab. For 10 mab the value of the resuspended fraction is 77% ± 17%. Comparing these percentages with those from the mass-flux calculations shows that the estimates of the percentage of resuspended material at 10 mab based on % $CaCO_3$ are low with respect to the estimates based on mass flux, that is, there is more carbonate at 10 mab than predicted from mass-flux calculations.

Similar calculations using organic carbon show that the percentage of resuspended material at 100 mab for organic carbon is 74% ± 3%. At 10 mab, the resuspended fraction is estimated to be 88% ± 1%. A comparison with the mass-flux calculations indicates that there is more resuspended material at 100 mab and less at 10 mab.

An explanation for the differences in the estimates of resuspended material using mass, calcium carbonate, and organic carbon may be due to the simplicity of the assumptions. Dissolution, degradation, and preferential resuspension have been ignored in the assumptions of the mixing scheme; however, these processes must be occurring or there would be no differences noted between the primary material and the surface sediments. Also, the material at 500 mab may not be all primary, but may contain some resuspended material as well.

From the calculations made, there is no significant difference in the calculated percentage of resuspended material at 100 mab

based on $CaCO_3$ and mass (Table 4.1). However, there is more

carbonate based on $CaCO_3$ calculations than is predicted by mass

calculations at 10 mab. The primary process that would affect the

calcium carbonate content is dissolution. However, due to the

shallow depths of the study region, the water column is saturated

with respect to calcite (Takahashi, 1975; Broecker and Takahashi,

1978), so dissolution of forams and coccoliths is unlikely.

However, in the sediments where organic carbon decomposes to

liberate CO_2, local dissolution may occur. Pteropods are composed

of aragonite. Individual specimens, but mostly fragments were found

in the traps at 10 mab, and not in the sediments. Perhaps the

greater quantity of carbonate at 10 mab is due to aragonite

dissolution at the seafloor. An alternative and perhaps more

plausible explanation is that carbonate may be preferentially

resuspended into the sediment traps at 10 mab.

Differences in the percentage of resuspended material at 100 mab

based on organic-carbon and mass-flux calculations indicate that

there is less organic carbon in the trap than would be expected from

the mass calculations. This phenomenon may be due to degradation

and consumption of organic matter in the water column or trap, a

factor ignored in the original assumptions. There is more organic

carbon in the trap at 10 mab than is predicted by mass-flux

calculations. This may be due to increased degradation and

consumption between 10 mab and the seafloor, or preferential

resuspension. The general trend of more carbonate and organic

-213-

carbon at 10 mab than predicted by mass-flux calculations suggests that carbonate and organic carbon being less dense components of the sediments, may be preferentially resuspended.

DISSOLUTION AND DEGRADATION AT THE SEAFLOOR

Profiles of the percentage of calcium carbonate and organic carbon from sediment-trap samples and box core surface sediments generally show a decrease in these components with increasing water depth (Figures 4.12, 4.14). From these figures, it is seen that the percentages of carbonate and organic carbon decrease downward through the water column, with the sharpest decrease from 10 mab to the seafloor. This decrease is on the order of 50% for carbonate and 70% for organic carbon. One possible explanation for this decrease in the lowermost 10 m is additional detrital material from the seafloor enters the system diluting the carbonate. A second hypothesis, and perhaps more plausible, is that present-day conditions are reflected in the water column, but the surface sediments are subject to dissolution and degradation for much longer periods of time than the material in transit through the water column, i.e., material in the water column does dissolve and decompose, but most of the loss occurs at the sediment-water interface. This latter concept is supported by the visual investigation of the trap and surface sediment samples and is in agreement with other investigators (Adelseck and Berger, 1975; Berner, 1977; Takahashi and Broecker, 1977; Honjo, 1977). For

example, aragonitic tests are absent from the surface sediments and organic material is not visually identifiable.

REGIONAL PATTERNS OF SURFACE SEDIMENTS

Distinct regional differences in the surface sediments are seen in the clay mineralogy and in the content of carbonate and organic carbon. Semi-quantitative X-ray diffraction shows that there are relatively higher proportions of illite in the clays present beneath the bottom current than in the channel (Table 4.7). Illite is formed from weathering of ancient continental rocks (Biscaye, 1965). The higher percentage of illite in the sediments beneath the bottom current may reflect extensive advection by the bottom current from weathered continental rocks, the nearest source being Rockall Plateau, ∿500 km. Although Rockall Plateau is southeast of the study area, it is upstream along the current path.

Carbonate and organic carbon are both more abundant in the cores in the channel than in the cores beneath the bottom current (Figures 4.13 and 4.15). These components are also more abundant in the trap sample at 10 mab in the channel (Figures 4.12 and 4.14) than in the other traps. This may reflect a turbidity current component in the channel cores or the influence of the bottom current eroding and/or not depositing Recent sediments and exposing older glacial deposits. Glacial sediments have lower carbonate percentages, and probably less organic carbon (due to the longer period of time available for decomposition and consumption of the organic matter

present). In addition, the cores taken beneath the current have
glacial-assemblage forams in the surface samples, suggesting that
glacial sediments are exposed.

DISTANCE OF TRANSPORT

Specific components of the sediment trap samples are useful in
estimating the distance of transport of the resuspended trapped
material. Iron-oxide coated planktonic foraminifera, benthic
foraminifera, the glacial assemblage foram N. pachyderma
(sinistral), and some of the large (>250 μm) volcanic fragments and
mineral grains found in the traps have a seafloor source. Eighteen
particles from the trap at 10 mab at Mooring 2 were selected for a
settling experiment to determine the particle fall velocities.
Eight planktonic forams (four with iron-oxide coatings), three
benthic forams, one pteropod and six volcanic shards and mineral
grains, most specimens having a diameter of 300 μm, were settled in
filtered fresh water at 20°C in a one liter cylinder with a 6.2 cm
diameter. A 20 cm vertical distance was used for determining fall
velocities. Particles were submerged in water in a small flask,
which was subsequently evacuated to remove any air contained in the
specimens. The particles were transferred to the settling cylinder
by means of a large pipette. Particles were settled three times to
determine repeatability of the fall velocities as a means of
determining whether air was successfully removed from the samples.
A correction to take into account the difference in viscosity

between 20°C fresh water and 5°C seawater decreases the velocities to 63% of the measured values. The results of the experiment are given in Table 4.11.

Planktonic forams fell most slowly, averaging 0.65 cm/sec. Iron-oxide coated forams fell at 0.94 cm/sec and volcanic glass and mineral grains fall at 1.21 cm/sec. The orange iron-oxide coated forams fall from 1.06-1.76 times faster than the white forams. The maximum fall velocity was 1.75 cm/sec for a mineral grain with 185 and 300 μm axes; the minimum was 0.52 cm/sec for a 1.5 mm long pteropod. From these results, it is found that resuspended material is likely to have a higher fall velocity than material settling from the surface waters. Another result of this study is that larger particles do not necessarily fall more rapidly than small ones. In particular, the smaller (250 μm) N. pachyderma (dextral) fell 1.14 times more rapidly than a larger (300 μm) foram of the same species and the largest specimen, the pteropod, had the slowest fall velocity. This may be due to both greater drag and lower density of the larger specimens.

A comparison of the experimentally determined fall velocities to Stokes law show deviations for these large particles. Stokes law applies only up to Reynolds numbers of 1. These particles settled have Reynolds numbers ranging from 3-6. Stokes law,

$$W = \frac{2\Delta\rho g r^2}{9\mu}$$

would predict a fall velocity of 7.3 cm/sec for a 300 μm particle with a density difference of 1.5. With a $\Delta\rho$ of 0.5, the fall

Table 4.11

PARTICLE FALL VELOCITIES FROM MOORING 2, TRAP 10 mab

Particle	Diameter (m) Max.	Min.	Settling Velocity* cm/sec
Pteropod	1500	750	0.52±0.03
N. pachyderma (dextral) - white	250	175	0.69±0.04
N. pachyderma (dextral) - white	300	200	0.60±0.01
G. bulloides - white	300	200	0.68±0.08
N. pachyderma (sinistral) - white	300	225	0.69±0.04
N. pachyderma (dextral) - orange**	300	188	0.69±0.06
G. bulloides - orange** (light iron-oxide coating)	300	200	0.72±0.03
G. bulloides - orange**	300	238	1.19±0.07
N. pachyderma (sinistral) - orange**	300	225	1.16±0.06
Benthic Foram	688	175	0.73±0.04
Benthic Foram	562	350	1.52±0.04
Benthic Foram	300	212	0.67±0.08
Mineral grain	300	188	1.75±0.05
Mineral grain	300	288	1.34±0.03
Mineral grain	500	362	1.68±0.03
Volcanic shard	300	188	0.97±0.01
Vesicular volcanic shard	300	162	1.17±0.01
Vesicular volcanic shard	300	88	0.84±0.04

* Fall velocities were measured in 20°C fresh water. A
viscosity correction was made to yield the fall velocity
in 5°C seawater of 35%, given here.

**iron-oxide coated.

velocity would be 2.4 cm/sec. These values are higher than those measured for particles with a 300 μm diameter. Density differences of ∿0.2, 0.3, 0.3 and 0.4 would be necessary for the white planktonic forams, iron-oxide coated forams, and volcanic shards and mineral grains respectively for Stokes law to apply. The deviations from Stokes law may be due to the use of a maximum diameter in the equation and to the non-spheroidal shapes of the particles. Using the smaller diameters, calculated density differences of ∿0.5, 0.7, 0.8 and 1.5 for the same particles as above are found to be more reasonable.

By knowing the fall velocities of some of the material in the trap, the horizontal distance of transport can be estimated. Assuming that the particles are mixed vertically to the top of the isothermal mixed layer, how far could they travel horizontally in the bottom current and be caught in the traps at 10 mab? Mixed layers along the northern transect are 30-50 m thick. Fall velocities range from 0.60-1.75 cm/sec. Assuming particles are mixed no higher than the top of the mixed layer, particles would fall 40 m (from the top of the mixed layer to the traps at 10 mab) in $2.3 \times 10^3 - 6.7 \times 10^3$ sec. Along the 1800 m isobath (the location of the mooring), in an average current of 20 cm/sec, the distance of transport would be 0.5-1.3 km.

This study was conducted along a ridge flank and in close proximity to Iceland and the Iceland-Faroe Ridge. Is it possible that the material caught in the traps is derived from these

topographic highs? Two hundred meters up the ridge flank is 13.2 km

away. Particles would fall a 200 m vertical distance in 1.1×10^4

to 3.3×10^4 sec. The horizontal current required to transport

the particles to the trap before falling to the seafloor is

calculated to be 40-116 cm/sec. These velocities are in excess of

those found even for the bottom current. Since the direction of

transport from upslope is virtually orthogonal to the bottom

current, this area as an immediate source is unlikely.

The crest of the East Katla Ridge is 32.4 km upslope. The

vertical relief change is 600 m. By similar calculations to those

above, the horizontal current velocities to transport the particles

from the ridge crest to the traps in one resuspension-deposition

cycle, would be 32-94 cm/sec, which as a cross-current is also

unlikely.

The shelf of Iceland is 110 km north of the sediment trap

mooring. Calculations reveal that a horizontal velocity averaging

40-120 cm/sec would be needed to resuspend material on the shelf and

transport it to the traps in one resuspension-deposition cycle.

These high currents are also unlikely.

The Iceland-Faroe Ridge is 250 km upstream from the traps.

Velocities of 100-292 cm/sec would be required to transport the

resuspended material from the ridge to the traps. Although high

velocities of the overflow water may occur at other times, the

measurements taken during this study do not even approach that

range. The largest size particles that could be transported from

the Iceland-Faroe Ridge assuming a constant horizontal velocity of 20 cm/sec (comparable to that measured during this study) are ones with maximum diameters of 100 μm for mineral grains and 140 μm for planktonic forams.

Particles smaller than 100 μm may be transported from the topographic highs as well as being resuspended locally. The high concentrations of SPM and high light-scattering values in mid-water suggest that for the small particles (< 20 μm) are carried quasi-conservatively by the water masses.

The above calculations indicate that virtually all the trapped coarse material > 125 μm which comprises 21-34% of the trap samples is locally (few kilometers) derived resuspended sediment.

CONCLUSIONS

1) Bottom currents cause local resuspension of material in the region south of Iceland.

2) Resuspension is shown by the presence of benthic, glacial assemblage, and iron-oxide coated forams caught at 10 mab and in some cases 100 and 500 mab in the sediment traps.

3) The maximum primary flux of material from the surface was measured to be far less than the Recent sedimentation rate, indicating substantial transport of material into the region by the bottom current.

4) The observed axis of the deep current system off Iceland (1400-1800 m) overlies coarse sediments, suggesting that the current

has been causing preferential erosion, and/or winnowing, of fine material and removal from the region.

5) The large flux of suspended material in the bottom current (approximately 100 kg/sec) may be responsible for the formation of the Gardar sediment drift to the southwest of the region.

6) Regional differences of clay mineralogy in the surface sediments suggest that the bottom current transports material from continental source rocks which are at least 500 km away, up current.

7) Regional differences in contents of organic carbon and carbonate in the box cores reflect preferential preservation in the cores from the channel versus those beneath the bottom current, or alternatively, preferential decomposition, dissolution, and/or erosion in the cores beneath the bottom current.

8) Presence of aragonitic tests and fragments in the traps at 10 mab but not in the surface sediments, is evidence of dissolution or mechanical destruction of this material at the seafloor and not in the water column.

9) Calculations for determining the distance of transport of the coarse, trapped material indicate that the greater than 125 μm size fraction, which comprises 21-34% of the trap samples, is locally (few kilometers) derived resuspended sediment.

CHAPTER V

SUMMARY AND CONCLUSIONS

Strong evidence for the transport and redistribution of large

volumes of deep-sea sediment over geologic time is the presence of

massive sediment drifts in the northern North Atlantic. As

demonstrated in this thesis, resuspension and redistribution of

deep-sea sediments also occurs in the present day on time scales of

days to weeks. Two approaches were used to investigate present-day

resuspension: 1) clear-water and nepheloid-layer suspended

particulate matter was examined to determine the differences between

the particles, and to determine the possible influence of

resuspended material, and 2) the composition of particles obtained

with sediment traps located from 500 mab to 10 mab was compared with

the surface sediments below.

The conclusions of the SPM clear-water and nepheloid-layer

studies are:

1) A correlation between light scattering and concentration of

suspended particulate matter in the Iceland Rise area using the

L-DGO nephelometer, demonstrates that there are differences between

particles in clear water and the nepheloid layer. Clear-water

samples show larger variations in concentration for a given change

in light scattering when compared with nepheloid-layer samples.

When the Iceland Rise regression equations for light scattering

versus concentration of suspended particulate matter are compared to

those of Biscaye and Ettreim (1974; 1977) on the Blake-Bahama Outer

Ridge, Hattaras Abyssal Plain and Lower Continental Rise, distinct

differences are observed. These studies indicate that correlations

of light scattering to concentration of suspended matter vary both

regionally and between clear water and the nepheloid layer.

However, in predicting concentrations from light scattering, the

correlations determined here are indistinguishable from those of

Biscaye and Eittreim. The 95% confidence limits for prediction of a

future observation in the Iceland Rise area encompasses the Biscaye

and Eittreim curves for log E/E_D values in excess of 0.5.

2) Particle size distributions of suspended particulate matter

show differences between clear-water and nepheloid-layer samples.

Clear-water samples have roughly equal volumes of material in

logarithmically increasing size grades between 1 and 20 μm.

Nepheloid-layer samples have lower variance distributions. These

differences are also reflected in the normalized differential volume

curves which show two-slope distributions being characteristic of

nepheloid layer samples, a feature previously observed only in

surface waters. The two-slope distribution is interpreted in this

study as being due to resuspension of material from the seafloor.

3) Differences in apparent density between suspended matter from

clear-water and nepheloid-layer samples are noted in the western

North Atlantic, but not in the Iceland Rise area. Compositional

differences between clear-water and nepheloid-layer particles in the

western North Atlantic are more extreme than in the Iceland Rise

area, and are regarded as a probable explanation of the differences
in apparent density. Apparent densities of nepheloid-layer samples
in the western North Atlantic study are greater than for clear-water
samples. The greater apparent densities correspond with large
increases in clays and mineral matter and a decrease in organic
matter between clear-water and nepheloid-layer samples.

4) Differences in the principal components of the suspended
particulate matter between clear-water and nepheloid-layer samples
are primarily an increase in clays and mineral matter and a decrease
in coccoliths. For the Iceland Rise study, this is interpreted as
being due to resuspension of material from the seafloor. In the
western North Atlantic, the decrease in coccoliths is due to
dissolution of carbonate at the seafloor and subsequent resuspension
of carbonate-poor sediments.

An examination and comparison of the sediment trap and surface
sediment samples support resuspension and redistribution of material
continuing in the present day. Conclusions are:

1) Coarse sediments underlie the bottom current axis from 1400
to 1800 m along the northern transect of stations with more
fine-grained sediment on either side of the axis suggesting
winnowing and preferential erosion in the current axis.

2) Surface sediments beneath the current axis contain an
assemblage of planktonic foraminifera representative of glacial
subpolar, or present-day polar conditions. The presence of these
forams is indicative of erosion or extensive advective transport.

3) Regional variations in clay mineralogy, organic carbon and carbonate contents indicate preferential preservation in cores from the channel or preferential decompostion, dissolution and/or erosion of the surface sediments beneath the bottom current.

4) A large horizontal flux of suspended material ($\sim$100 kg/sec) is transported across the northern transect of stations. The vertical flux of sediment calculated from sediment traps located at 500 mab was an order of magnitude less than Recent sediment accumulation rates. This suggests that a large fraction of the sediments in the region are brought into the area via the bottom current or turbidity currents from Iceland. The large horizontal flux of sediment may also contribute to the formation of Gardar sediment drift to the southwest.

5) An increase of greater than two orders of magnitude in material collected between 500 mab and 10 mab is indicative of present day resuspension and advection by the bottom current.

6) Resuspension of sediments is substantiated by the collection of particles whose source is clearly the seafloor in sediment traps located at 10, 100 and 500 mab. These resuspended components include benthic foraminifera, iron-oxide coated planktonic foraminifera, and the glacial, subpolar assemblage planktonic foraminifera (N. pachyderma (sinistral)).

7) The rapid settling velocity of the coarse (>125 μm), resuspended components indicate that they are locally derived (few kilometers) rather than horizontally advected from topographic highs. However, the smaller size fractions (<125 μm) may be transported from topographic highs as well as being locally resuspended.

REFERENCES

Adelseck, C.G. and W.H. Berger (1975). On the dissolution of planktonic foraminifera and associated microfossils during settling and on the sea floor. In: W.V. Sliter, A.W.H. Be and W.H. Berger (eds.), Dissolution of Deep-Sea Carbonates. Cushman Foundation Foram. Research Special Publication No. 13, pp. 70-81.

Armi, L. (1978). Some evidence for boundary mixing in the deep ocean. Journal of Geophysical Research 83: 1971-1979.

Bader, H. (1970). The hyperbolic distribution of particle sizes. Journal of Geophysical Research 75: 2822-2830.

Baker, E.T., R.A. Feely and K. Takahashi (1979). Chemical composition, size distribution and particle morphology of suspended particulate matter at DOMES sites A, B, and C: Relationships with local sediment composition. In: J.L. Bischoff and D.Z. Piper (eds.), Marine Geology and Oceanography of the Pacific Manganese Nodule Province. Plenum, New York, pp. 163-201.

Baker, E.T., R.W. Sternberg and D.A. McManus (1974). Continuous light-scattering profiles and suspended matter over Nitinat deep sea fan. In: R.J. Gibbs (ed.), Suspended Solids in Water. Plenum, New York, pp. 155-172.

Bartz, R., J.R.V. Zaneveld and H. Pak (1978). A transmissometer for profiling and moored observations in water. SPIE Vol. 160, Ocean Optics V: 102-108.

Be, A.W.H. (1977). An ecological, zoogeographic and taxonomic review of Recent planktonic foraminifera. In: A.T.S. Ramsay (ed.), Oceanic Micropaleontology. Academic Press, London, vol. 1, pp. 1-100.

Beardsley, G.F., H. Pak, K. Carder and B. Lundgren (1970). Light scattering and suspended particles in the eastern Equatorial Pacific Ocean. Journal of Geophysical Research 75: 2837-2845.

Berggren, W.A. and C.D. Hollister (1977). Plate tectonics and paleocirculation - commotion in the ocean. Tectonophysics 38: 11-48.

Berner, R.A. (1977). Sedimentation and dissolution of pteropods in the ocean. In: N.R. Anderson and A. Malahoff (eds.), The Fate of Fossil Fuel CO_2 in the Oceans. Plenum, New York, pp. 243-260.

Betzer, P.R. and M.E.Q. Pilson (1971). Particulate iron and the nepheloid layer in the western North Atlantic, Caribbean and Gulf of Mexico. Deep-Sea Research 18: 753-761.

Biscaye, P.E. (1965). Mineralogy and sedimentation of Recent deep-sea clay in the Atlantic Ocean and adjacent seas and oceans. Geological Society of America Bulletin 76: 803-832.

Biscaye, P.E. and S.L. Eittreim (1974). Variations in benthic boundary layer phenomena; nepheloid layers in the North American Basin. In: R. Gibbs (ed.), Suspended Solids in Water. Plenum, New York, pp. 227-260.

Biscaye, P.E. and S.L. Eittreim (1977). Suspended particulate loads and transports in the nepheloid layer of the abyssal Atlantic Ocean. Marine Geology 23: 155-172.

Bishop, J.K.B. (1977). The chemistry, biology and vertical flux of oceanic particulate matter. Ph.D. Thesis, M.I.T./W.H.O.I. Joint Program in Oceanography, 292 pp. (unpublished manuscript).

Bishop, J.K.B., J.M. Edmond, D.R. Ketten, M.P. Bacon and W.B. Silker (1977). The chemistry, biology, and vertical flux of particulate matter from the upper 400 m of the equatorial Atlantic Ocean. Deep-Sea Research 24: 511-548.

Bouma, A.H. (1969). Methods for the Study of Sedimentary Structures. John Wiley and Sons, New York, 458 pp.

Bouma, A.H. and T.K. Treadwell (1975). Deep-sea dune-like features. Marine Geology 19: M53-M59.

Brewer, P.G., D.W. Spencer, P.E. Biscaye, A. Hanley, P.L. Sachs, C.L. Smith, S. Kadar and J. Fredericks (1976). The distribution of particulate matter in the Atlantic Ocean. Earth and Planetary Science Letters 32: 393-403.

Broecker, W.S. and T. Takahashi (1978). The relationship between lysodine depth and in situ carbonate ion concentration. Deep-Sea Research 25: 65-95.

Brun-Cottan, J.-C. (1971). Étude de la granulometrie des particules marines mesures effectuees avec un compteur Coulter. Cahiers Océanographiques 23: 193-205.

Brun-Cottan, J.-C. (1976). Stokes settling and dissolution role model for marine particles as a function of size distribution. Journal of Geophysical Research 81: 1601-1606.

Burckle, L.H. and P.E. Biscaye (1971). Sediment transport by
    Antarctic Bottom Water through the eastern Rio Grande Rise.
    Geological Society of America Abstracts with Programs 3: 518-519.

Carder, K.L., G.F. Beardsley, Jr. and H. Pak (1971). Particle size
    distributions in the Eastern Equatorial Pacific. Journal of
    Geophysical Research 76: 5070-5077.

Carder, K.L., P.R. Betzer and D.W. Eggimann (1974). Physical,
    chemical and optical measures of suspended particulate
    concentrations: their intercomparison and application to the
    West African shelf. In: R.J. Gibbs (ed.), Suspended Solids in
    Water. Plenum, New York, pp. 173-193.

Crease, J. (1965). The flow of Norwegian Sea water through the
    Faroe Bank Channel. Deep-Sea Research 12: 143-150.

Crow, E.L., F.A. Davis and M.W. Maxfield (1960). Statistics Manual -
    with examples taken from ordnance development. Dover
    Publications, Inc., New York, 288 pp.

Davies, T.A. and A.S. Laughton (1972). Sedimentary processes in the
    North Atlantic Ocean. In: A.S. Laughton, W. Berggren et al.
    Initial Reports of the Deep Sea Drilling Project, XII. U.S.
    Government Printing Office, Washington, D.C., pp. 905-934.

Davies, T.A., O.E. Weser, B.P. Luyendyk and R.B. Kidd (1975).
    Unconformities in the sediments of the Indian Ocean. Nature
    253: 15-19.

Dietrich, G. (1967). The International "Overflow" Expedition (ICES)
    of the Iceland-Faroe Ridge, May-June 1960, A review. Rapports
    et Procès-verbaux des Réunions Conseil Permanent International
    pour l'Exploration de la Mer 157: 268-274.

Drake, D.E., R.L. Kolpak and P.J. Fischer (1972). Sediment transport
    on the Santa Barbara-Oxnard Shelf, Santa Barbara Channel,
    California. In: D.J.P. Swift, D.B. Duane and O.H. Pilkey
    (eds.), Shelf Sediment Transport. Dowden, Hutchinson and Ross,
    Stroudsburg, Pa., pp. 307-331.

Einstein, H.A. and R.B. Krone (1962). Experiments to determine
    modes of cohesive sediment transport in salt and water. Journal
    of Geophysical Research 67: 1451-1461.

Eittreim, S.L. and M. Ewing (1972). Suspended particulate matter in
    the deep waters of the North American Basin. In: A.L. Gordon
    (ed.), Studies in Physical Oceanography. Gordon and Breach,
    London, pp. 123-167.

Eittreim, S.L. and M. Ewing (1974). Turbidity distribution in the deep waters of the western Atlantic trough. In: R. Gibbs (ed.), Suspended Solids in Water. Plenum, New York, pp. 213-225.

Eittreim, S., A.L. Gordon, M. Ewing, E.M. Thorndike and P. Bruchhausen (1972). The nepheloid layer and observed bottom currents in the Indian-Pacific Antarctic Sea. In: A.L. Gordon (ed.), Studies in Physical Oceanography. Gordon and Breach, London, pp. 19-35.

Ellett, D.J. and D.G. Roberts (1973). The overflow of Norwegian Sea deep water across the Wyville-Thompson Ridge. Deep-Sea Research 20: 819-835.

Ericson, D.B., M. Ewing, G. Wollin and B.C. Heezen (1961). Atlantic deep-sea sediment cores. Geological Society of America Bulletin 72: 193-286.

Ewing, J.I. and C.D. Hollister (1972). Regional aspects of deep sea drilling in the western North Atlantic. In: C.D. Hollister, J.I. Ewing et al., Initial Reports of the Deep Sea Drilling Project, Volume XI. U.S. Government Printing Office, Washington, D.C., pp. 951-973.

Ewing, J., C. Windisch and M. Ewing (1970). Correlation of Horizon A with JOIDES bore-hole results. Journal of Geophysical Research 75: 5645-5653.

Ewing, M. and E.M. Thorndike (1965). Suspended matter in deep ocean water. Science 147: 1291-1294.

Feely, R.A. (1975). Major-element composition of the particulate matter in the near-bottom nepheloid layer of the Gulf of Mexico. Marine Chemistry 3: 121-156.

Feely, R.A. (1976). Evidence for aggregate formation in a nepheloid layer and its possible role in the sedimentation of particulate matter. Marine Geology 20: M7-M13.

Field, M.E. and O.H. Pilkey (1971). Deposition of deep-sea sands: comparison of two areas of the Carolina continental rise. Journal of Sedimentary Petrology 41: 526-536.

Flood, R.D. (1978). Studies of deep-sea sedimentary microtopography in the North Atlantic Ocean. Ph.D. Thesis, M.I.T./W.H.O.I. Joint Program in Oceanography, 395 pp. (unpublished manuscript).

Gardner, W.D. (1977a). Fluxes, dynamics and chemistry of
    particulates in the ocean. Ph.D. Thesis, M.I.T./W.H.O.I. Joint
    Program in Oceanography, 405 pp. (unpublished manuscript).

Gardner, W.D. (1977b). Incomplete extraction of rapidly settling
    particles from water samplers. Limnology and Oceanography 22:
    764-768.

Gardner, W.D. (1980). Field assessment of sediment traps. Journal
    of Marine Research 38: 41-52.

Garner, D.M. (1972). Flow through the Charlie-Gibbs Fracture Zone,
    Mid-Atlantic Ridge. Canadian Journal of Earth Science 9:
    116-121.

Hathaway, J.C. (1972). Regional clay mineral facies in estuaries
    and continental margin of the United States East Coast.
    Geological Society of America Memoirs 133: 293-315.

Heath, G.R., T.C. Moore and J.P. Dauphin (1977). Organic carbon in
    deep-sea sediments. In: N.R. Anderson and A. Malahoff (eds.),
    The Fate of Fossil Fuel CO_2 in the Oceans. Plenum, New
    York, pp. 605-626.

Heezen, B.C., C.D. Hollister and W.F. Ruddiman (1966). Shaping of
    the continental rise by deep geostrophic contour currents.
    Science 152: 502-508.

Hollister, C.D. (1967). Sediment distribution and deep circulation
    in the western North Atlantic. Ph.D. Thesis, Columbia
    University, New York, 471 pp. (Unpublished manuscript).

Hollister, C.D., R.D. Flood, D.A. Johnson, P.E. Lonsdale and J.B.
    Southard (1974). Abyssal furrows and hyperbolic echo traces on
    the Bahama Outer Ridge. Geology 2: 395-400.

Hollister, C.D., R. D. Flood and I.N. McCave (1978). Plastering and
    decorating in the North Atlantic. Oceanus 21: 5-13.

Hollister, C.D. and B.C. Heezen (1972). Geologic effects of ocean
    bottom currents, western North Atlantic. In: A.L. Gordon (ed.),
    Studies in Physical Oceanography. Gordon and Breach, London,
    pp. 37-66.

Honjo, S. (1976). Coccoliths: production, transportation and
    sedimentation. Marine Micropaleontology 1: 65-79.

Honjo, S. (1977). Biogenic carbonate particles in the ocean; Do
    they dissolve in the water column? In: N.R. Anderson and A.
    Malahoff (eds.), The Fate of Fossil Fuel CO_2 in the Oceans.
    Plenum, New York, pp. 269-294.

Honjo, S. (1978). Sedimentation of materials in the Sargasso Sea at a 5,367 m deep station. Journal of Marine Research 36: 469-492.

Honjo, S., K.O. Emery and S. Yamamato (1974). Non-combustible suspended matter in surface waters off eastern Asia. Sedimentology 21: 555-575.

Huang, T.C. and N.D. Watkins (1977). Contrasts between the Brunhes and Matuyama sedimentary records of bottom water activity in the South Pacific. Marine Geology 23: 113-132.

Jacobi, R.D., P.D. Rabinowitz and R.W. Embley (1975). Sediment waves on the Moroccan Continental Rise. Marine Geology 19: M61-M67.

Jerlov, N.G. (1968). Optical Oceanography. Elsevier Publ. Co., Amsterdam, 194 pp.

Johnson, D.A., M. Ledbetter and L.H. Burckle (1977). Vema channel paleo-oceanography: Pleistocene dissolution cycles and episodic bottom water flow. Marine Geology 23: 1-33.

Johnson, D.A. and A.N. Shor (1977). Initial cruise report ATLANTIS II-94, Leg I. W.H.O.I. Technical Report #77-70 (unpublished manuscript).

Johnson, G.L. and E.D. Schneider (1969). Depositional ridges in the North Atlantic. Earth and Planetary Science Letters 6: 416-422.

Jones, E.J.W., M. Ewing, J.I. Ewing and S.L. Eittreim (1970). Influence of Norwegian Sea overflow water on sedimentation in the northern North Atlantic and Labrador Sea. Journal of Geophysical Research 74: 1655-1680.

Kolla, V.R., L. Sullivan, S. Streeter and M. Langseth (1976). Spreading effects of Antarctic bottom water on the floor of the Indian Ocean inferred from bottom water potential temperature, turbidity, and sea-floor photography. Marine Geology 21: 171-189.

Krishnaswami, S. and M.M. Sarin (1976). Atlantic surface particulates: composition, settling rates and dissolution in the deep sea. Earth and Planetary Science Letters 32: 430-440.

Laine, E.P. and C.D. Hollister (1980). Geological effects of the Gulf Stream System on the Northern Bermuda Rise. Marine Geology (in press).

Ledbetter, M. and D.A. Johnson (1976). Increased transport of Antarctic Bottom Water in the Vema Channel during the last Ice Age. Science 194: 837-839.

Lee, A. and D. Ellett (1965). On the contribution of overflow water from the Norwegian Sea to the hydrographic structure of the North Atlantic Ocean. Deep-Sea Research 12: 129-142.

Lonsdale, P. and C.D. Hollister (1979). A near-bottom traverse of Rockall Trough: hydrographic and geologic inferences. Oceanologica Acta 2: 91-105.

Lonsdale, P. and J.B. Southard (1974). Experimental erosion of North Pacific red clay. Marine Geology 17: M51-M60.

Lonsdale, P. and F.N. Spiess (1977). Abyssal bedforms explored with a deeply towed instrument package. Marine Geology 23: 57-75.

Luyten, J.R. (1977). Scales of motion in the deep Gulf Stream and across the continental rise. Journal of Marine Research 35: 49-74.

Malmberg, S.-A. (1974). A note on the deep water south of Iceland -- "Overflow '73." ICES Reference C.M. 1974/C:32 (unpublished manuscript).

McCave, I.N. (1975). Vertical flux of particles in the ocean. Deep-Sea Research 22: 491-502.

McCave, I.N., P.F. Lonsdale, C.D. Hollister and W.D. Gardner (1980). Sediment transport over the Hatton and Gardar contourite drifts. Journal of Sedimentary Petrology (in press).

Meade, R.H. (1972). Transport and deposition of sediments in estuaries. Geological Society of America Memoirs 133: 91-120.

Moore, T.C. Jr. and G.R. Heath (1977). Survival of deep-sea sedimentary sections. Earth and Planetary Science Letters 37: 71-80.

Pak, H. and J.R.V. Zaneveld (1977). Bottom nepheloid layers and bottom mixed layers observed on the continental shelf off Oregon. Journal of Geophysical Research 82: 3921-3931.

Peterson, W.H. and G.G.H. Rooth (1976). Formation and exchange of deep water in the Greenland and Norwegian Seas. Deep-Sea Research 23: 273-283.

Pierce, J.W. (1976). Suspended sediment transport at the shelf break and over the outer margin. In: D.J. Stanley and D.J.P. Swift (eds.), Marine Sediment Transport and Environmental Management. John Wiley and Sons, New York, pp. 437-458.

Plank, W.S., H. Pak, and J.R.V. Zaneveld (1972). Light scattering and suspended matter in nepheloid layers. Journal of Geophysical Research 77: 1689-1694.

Richardson, P.L. (1977). On the crossover between the Gulf Stream and the Western Boundary Undercurrent. Deep-Sea Research 24: 139-159.

Rona, P.A. (1973). Worldwide unconformities in marine sediments related to eustatic changes of sea level. Nature Physical Science 244: 25-26.

Rowe, G.T. and W.D. Gardner (1979). Sedimentation rates in the slope water of the northwest Atlantic Ocean measured directly with sediment traps. Journal of Marine Research 37: 581-600.

Ruddiman, W.F. and A. McIntyre (1976). Northeast Atlantic Paleo-climatic changes over the past 600,000 years. Geological Society of America Memoirs 145: 111-146.

Schmitz, W.J., Jr. and N.G. Hogg (1978). Observations of energetic low frequency current fluctuations in the Charlie-Gibbs Fracture Zone. Journal of Marine Research 36: 725-734.

Sheldon, R.W. and T.R. Parson (1967). A practical manual on the use of the Coulter Counter in marine science. Coulter Electronics, Toronto, 66 pp.

Sheldon, R.W., A. Prakash and W.H. Sutcliffe, Jr. (1972). The size distribution of particles in the ocean. Limnology and Oceanography 17: 327-340.

Shor, A.N. (1978). Bottom currents on East Katla Ridge, NW Iceland Basin. ICES Reference C.M. 1978/C:60 (unpublished manuscript).

Shor, A.N. (1979). Bottom currents and abyssal sedimentation processes south of Iceland. Ph.D. Thesis, M.I.T./W.H.O.I. Joint Program in Oceanography, 246 pp. (unpublished manuscript).

Shor, A., P. Lonsdale, C.D. Hollister and D. Spencer (1980). Charlie-Gibbs Fracture Zone: bottom-water transport and its geological effects. Deep-Sea Research (in press).

Shor, A.N., D. Muller and D.A. Johnson (1977). Transport of Norwegian Sea Overflow -- preliminary results of ATLANTIS II cruise 94, June - July, 1977. ICES - CM 1977/C:44 Hydro. Comm. (unpublished manuscript).

Southard, J.B., R.A. Young and C.D. Hollister (1971). Experimental erosion of calcareous ooze. Journal of Geophysical Research 76: 5903-5909.

Spencer, D.W., P.G. Brewer, A. Fleer, S. Honjo, S. Krishnaswami and Y. Nozaki (1978). Chemical fluxes from a sediment trap experiment in the deep Sargasso Sea. Journal of Marine Research 36: 493-523.

Spencer, D.W., P.G. Brewer and P.L. Sachs (1972). Aspects of the distribution and trace element composition of suspended matter in the Black Sea. Geochimica et Cosmochimica Acta 36: 76-86.

Steele, J.H., J.R. Barrett and L.V. Worthington (1962). Deep currents south of Iceland. Deep-Sea Research 9: 465-474.

Sternberg, R.W., E.T.Baker, D.A. McManus, S. Smith and D.R. Morrison (1974). An integrating nephelometer for measuring suspended sediment concentrations in the deep sea. Deep-Sea Research 21: 887-892.

Stow, D.A.V. and J.P.B. Lovell (1979). Contourites: their recognition in modern and ancient sediments. Earth Science Reviews 14: 251-291.

Swift, J.H., K. Aagaard and S.-A. Malmberg (1980). The contribution of the Denmark Strait overflow to the deep North Atlantic. Deep-Sea Research 27: 29-42.

Takahashi, K. and S. Honjo (1980). Vertical flux of radiolaria: a taxon-quantitative sediment trap study from the western tropical Atlantic. Micropaleontology (in press).

Takahashi, T. (1975). Carbonate chemistry of sea water and the calcite compensation depth in the oceans. In: W.V. Sliter, A.W.H. Bé and W.H. Berger (eds.), Dissolution of Deep-Sea Carbonates. Cushman Foundation Foram. Research Special Publication No. 13, pp. 11-26.

Takahashi, T. and W.S. Broecker (1977). Mechanisms for calcite dissolution on the seafloor. In: N.R. Anderson and A. Malahoff (eds.), The Fate of Fossil Fuel CO_2 in the Oceans. Plenum, New York, pp. 455-478.

Thorndike, E.M. (1975). A deep-sea photographic nephelometer. Ocean Engineering 3: 1-15.

Tucholke, B.E. (1979). Relationships between acoustic stratigraphy and lithostratigraphy in the western North Atlantic Basin. In: B.E. Tucholke, P.R. Vogt et al. (eds.), Initial Reports of the Deep Sea Drilling Project Vol. XLIII. U.S. Government Printing Office, Washington, D.C., pp. 827-846.

Tucholke, B.E., W.R. Wright and C.D. Hollister (1973). Abyssal circulation over the Greater Antilles Outer Ridge. Deep-Sea Research 20: 973-995.

Watkins, N.P. and J.P. Kennett (1971). Antarctic Bottom Water: major change in velocity during the Late Cenozoic between Australia and Antarctica. Science 173: 813-818.

Worthington, L.V. (1969). An attempt to measure the volume transport of Norwegian Sea overflow water through the Denmark Strait. Deep-Sea Research 16: 421-432.

Worthington, L.V. (1970). The Norwegian Sea as a Mediterranean Basin. Deep-Sea Research 17: 77-84.

Worthington, L.V. (1976). On the North Atlantic circulation. The Johns Hopkins University Press, Baltimore, 110 pp.

Worthington, L.V. and G.H. Volkmann (1965). The volume transport of the Norwegian Sea overflow water in the North Atlantic. Deep-Sea Research 12: 667-676.

Young, R.N. and J.B. Southard (1978). Erosion of fine-grained marine sediments: sea-floor and laboratory experiments. Geological Society of America Bulletin 89: 663-672.

Zimmerman, H.B. (1971). Bottom currents on the New England continental rise. Journal of Geophysical Research 76: 5865-5876.

Zimmerman, H.B. (1972). Sediments of the New England Continental Rise. Geological Society of America Bulletin 83: 3709-3724.

BIOGRAPHICAL NOTE:

I, Mary Jo Richardson, was born on March 17, 1954, in Lynn, Massachusetts. I received my primary and secondary school education there and in nearby Salem. As an undergraduate I attended Smith College and Wesleyan University, graduating magna cum laude and phi beta kappa from the former with a bachelor's degree in geology in June, 1975. I began my graduate student career during the summer of 1975 when I entered the WHOI/MIT Joint Program in Oceanography. Research interests throughout these past five years have centered around suspended particulate matter studies in regions of dynamic current systems. I plan to continue doing research in this and related fields as a postdoctoral investigator at Lamont-Doherty Geological Observatory of Columbia University.